

IFAC



WARSZAWA 1969

INTERNATIONAL FEDERATION
OF AUTOMATIC CONTROL

Chemical and Allied General

Fourth Congress of the International
Federation of Automatic Control
Warszawa 16–21 June 1969

TECHNICAL
SESSION

46



Organized by
Naczelna Organizacja Techniczna w Polsce

INTERNATIONAL FEDERATION OF AUTOMATIC CONTROL

Chemical and Allied General

TECHNICAL SESSION No 46

**FOURTH CONGRESS OF THE INTERNATIONAL
FEDERATION OF AUTOMATIC CONTROL
WARSZAWA 16 – 21 JUNE 1969**



**Organized by
Naczelna Organizacja Techniczna w Polsce**



K-1315

Biblioteka
Politechniki Białostockiej



1181078

Contents

Paper No		Page
46.1	DK - S. Bay Jørgensen, M. Kümmel - Simulation of Distributed Systems in Chemical Engineering...	3
46.2	D - E. D. Gilles, B. Lübeck, M. Zeitz - Models and /GFR/ Simulation of Fixed-Bed Tubular Reactors.....	24
46.3	J - K. Izawa, H. Okamoto - Optimizing Control of Hydrogenation Process.....	41
46.4	CS - L. Šutek, B. Frankovič - The Design of a Control Algorithm for the Process of Urea Production.....	55
46.5	CS - Z. Burianec, J. Burianová, M. Hruška, A. Sichrovský - Theoretical Aspects for Optimal Control of Ammonia Synthesis Loop.....	69
46.6	SU - R. R. Tabast - Adaptive System Computer-Men for Chemical Process Control.....	87

Wydawnictwa Czasopism Technicznych NOT - Polska

Zakład Poligraficzny WCT NOT. Zam. 87/69.

SIMULATION OF DISTRIBUTED SYSTEMS IN CHEMICAL ENGINEERING

S. Bay Jørgensen and M. Kümmel

Chemical Engineering Department,
The Technical University of Denmark
Lyngby, Denmark

1. Introduction

In studies of the dynamic performance of critical units in chemical plants it is often necessary to make due regard to the distributed nature of these systems. This involves mathematical models of simultaneous partial differential equations or for staged systems a number of ordinary (or partial) differential equations, which must be solved for the relevant forcings. In the case of flowforcing which involves at least dynamically nonlinear models linearized models have been used most often.

Solution of linearized models in the frequency domain are straight forward and has been the most commonly used method. Solution in the time domain has mainly been accomplished by use of lumping techniques. This has particularly been done on digital computers which are rather slow and create stability problems which have limited the number of sections used in the spatial dimension. Analogue techniques have not been much in use¹⁻⁴ presumably because of the amount of nonlinear gears required for simulation of flow forcing. Many authors have been interested in the solution of these models by lumping techniques but very few have investigated the accuracy of the solution^{6,7}. Although there has been published studies of the dynamics of distributed chemical systems only a few papers^{8,9} discuss some general aspects of distributed systems.

In the present paper a broad terminology for chemical engineering systems is roughly stated and the mathematical models for a large group of systems are introduced. Simulation of these models is discussed and a special analog computer presented. The error of the simulation is investigated by means of the moments of the flow delay impulse responses and the deviations in the frequency characteristics are estimated.

2. System modelling

In the present paper is focused upon systems with two continuously flowing materials which only exchanges one quantity

physically and without chemical reaction. These limitations are imposed to simplify the following presentation. The concept can easily be generalized to systems with several changing quantities and/or materials.

In fig. 1 is shown a general model for a system where the physical transport is assumed to take place through the boundary 2 (numbers are shown on the figure) between the flowing materials 1 and 3. This boundary can be the boundary between two phases as in gas absorption or it can be more complex as a wall with two boundaries to the flowing materials as in conventional heat exchangers. The system model can be subdivided into the following elements: Flow element, which constitutes one flowing material. There are two of these in fig. 1 (1 and 3). Coupling element: Through which the quantity transport occurs. It has one boundary in common with flow element 1 and one with flow element 3. The quantity exchange on the boundary between a flow element and a coupling element is named the coupling process.

With this terminology it is simple to describe the system operation in a blocdiagram. Here each element constitutes a bloc, the vertical arrows symbolise the coupling processes and the in- and out-flows of material are shown by horizontal arrows. The flow directions in flow element 3 are shown to be either co- or counter-current, as in fig. 1. If we use a single pass counter current double pipe heat exchanger as an example, see fig. 3 for numbering, the operation principles are simply stated by means of the blocdiagram in fig. 2. If the capacity of the outer wall is significant then there also occurs heat transfer from flow element 3 to the passive coupling element 4. This is added in fig. 2. with dotted lines. This terminology has proved practical in connection with distributed and staged systems.

Formulation of mathematical models for specific cases follows directly from the balance for each element. The dynamic models are formulated from the assumption that the system is disturbed in a stationary state. This specifies the initial conditions.

The following systems have been studied. System I: The potential in one of the flow elements is assumed independent of the potential in the ^{other} flow element. An example is the condensing vapor-liquid heat exchanger. For the other systems

the potentials of both flow elements ^{are} assumed mutually dependent. This gives two situations: System II: Cocurrent flow and system III: Counter current flow. Examples are liquid-liquid heat exchangers (both II and III), gas liquid absorption (III) and gas liquid fluidized beds (II). Note system I is a limiting case for both II and III.

Mathematical models for the system elements.

The mathematical models for the coupling process, the coupling element and the flow element are formulated under the additional assumptions:

1. The coupling process is linear or linearized.
2. The transmission coefficients are independent of the potential and the flow velocity.
3. The physical properties of the materials are independent of the potential.
4. Axial molecular transport in the coupling elements is negligible.
5. The condition in the flow element is described by at most one space dimension.

With the coupling processes specified, the modelling problems for the flow elements are essentially hydrodynamic. In the present paper three different descriptions of the flow picture are discussed:

The plug flow model (PFM),

the axial dispersion model (ADM),

the staged model (STM), i.e. complete mixing and constant capacity on each stage and no flow delay between the stages.

The mathematical models are shown in fig. 4 together with models for the associated coupling element, when this has a finite capacity. The time constants τ_{ij} are defined on basis of film transmission coefficients. When the coupling element capacity is negligible, the dynamic model for this vanishes and τ_{ij} in the models for the flow elements are defined on basis of total transmission coefficients.

The inlet conditions for the flow elements are in all cases that the balance over the inlet is satisfied at all times. For ADM is used the inlet condition $U_1(\theta, 0^-) = U_1(\theta, 0^+)$ and the outlet condition $\frac{\partial U_1(\theta, 1)}{\partial \theta} = 0$. Fan and Ahn⁹ have shown that there are only minor differences in the frequency characteristics for dis-

turbances in inlet potential between these simple boundary conditions and more sophisticated ones when Pe is larger than 20.

When the models for the elements have been derived the models for the complete system are easily formulated by combination. The mathematical models for the three mentioned systems are shown in fig. 5 for PFM. The models for ADM and STM can be formulated by analogy. The results of the simulations will be compared to linearized frequency characteristics for PFM and STM. These have been computed from linearized modifications of the mathematical models.

3. The special analogue computer

The special analogue computer is designed to simulate STM with forcings in inlet potentials and flow velocity. The principle is described by Kümmel⁴. The hardware described has been improved. Especially the buffer amplifiers which now have 0.995 as mean voltage gain.

In preparing a simulation PFM and ADM models must be converted to the equivalent STM models by discretization of the continuous position variable. The derivatives are approximated for PFM by a backward first order difference quotient which introduces truncation errors $o(1/N)$. For ADM Costé, Rudd and Amundson¹⁰ have shown that by using central difference quotients it is possible to rearrange the model into an equation where the first derivative is approximated by a backward difference quotient. Here the coefficient to the second order difference quotient vanishes by the extra dispersion introduced when $N = Pe/2$. This model simulates ADM with a truncation error $o(1/N^2)$, which is much better than for PFM.

From the equivalent STM, the electrical model for the simulation and the system parameters are the analogue parameters determined when the maximum velocities, the ratio between the velocities and the timescale have been selected.

4. Error analysis

The use of this simulation for solution of other flow models than STM introduces the mentioned truncation errors. The nature and significance of these will be analysed on the basis of moments of the flow delay impulse responses for the three mentioned systems.

The investigations are carried out for all the systems trans-

port delay transfer functions. These are preferred because they are common to all distributed systems and determining for the system dynamics. Further the approximation in the simulation is caused by lumping of the continuous delays.

The i 'th moment is defined as:

$$M_i = \frac{\int_0^{\infty} \theta^i U(\theta, 1) d\theta}{\int_0^{\infty} U(\theta, 1) d\theta} = \frac{1}{M_0} \int_0^{\infty} \theta^i U(\theta, 1) d\theta \quad (1)$$

where M_0 is the zero'th moment. These can be computed from the transfer function $G(s)$ as shown by van der Laan¹¹. In the present connection the following moments are used:

The zero'th moment:

$$M_0 = G(0) = \int_0^{\infty} U(\theta) d\theta \quad (2)$$

The first moment about the origin:

$$\mu = - \frac{\dot{G}(0)}{G(0)} = \frac{\int_0^{\infty} \theta U(\theta) d\theta}{\int_0^{\infty} U(\theta) d\theta} \quad (3)$$

and the second moment about the mean:

$$\sigma^2 = \frac{\ddot{G}(0)}{G(0)} - \left[\frac{\dot{G}(0)}{G(0)} \right]^2 = \frac{\int_0^{\infty} (\theta - \mu)^2 U(\theta) d\theta}{\int_0^{\infty} U(\theta) d\theta} \quad (4)$$

The errors in the moments will for the static gain and the mean be computed as relative errors and given as percent:

$$E_I = \frac{I_{SIM} - I_{ORG}}{I_{ORG}} \cdot 100\%, \quad I = G, \mu, \sigma \quad (5)$$

The variance, however, is often close to zero for PFM, in these cases an absolute error is used

$$EA_I = I_{SIM} - I_{ORG} \quad (6)$$

These errors represent the deviations in the frequency characteristics for the various forcings. The relation for system I has been evaluated. For the complex systems have computations for system II shown ^{that} a similar relation apparently exists. The correspondence for system I between the moments and the flow delay transfer function is: E_G is equal to the error

in the static gain, E_{μ} is equal to the error in the time delay and E_{σ} corresponds to errors in the amplitude characteristics and to a smaller degree also in the phase characteristics, which occurs at medium and high frequencies.

The correspondence between the moments and the frequency characteristics for the distributed forcings is: A negative E_{σ} lifts both the amplitude and the phase curve and reduces the oscillations (see later) in both. A negative E_{μ} displaces the curves against higher frequencies. E_{σ} introduces small errors at medium frequencies and specially reduces ^{that} the amplitude in the oscillations in both curves. This means the medium value is almost correct. In designing the number of sections for a specific simulation it is in conclusion necessary to reduce firstly E_{σ} and E_{μ} and secondly E_{σ} . In this way the distributed transfer functions are simulated with nearly correct mean values, whereas oscillations are damped and the flow delay less accurate.

5. Results from computation of the moments and discussion

First the coupling element capacity in system I is neglected and the errors in simulating ADM as an equivalent STM and PFM as an equivalent STM investigated. Next the neglect of the coupling element capacity ^{is} analysed for the PFM-STM relation. Finally the coupling element capacity ^{is} neglected in the complex systems II and III and the errors in simulating PFM as equivalent STM analysed.

The neglect of the coupling element capacity simplifies the representation of each flow element to one dimensionless parameter c_t which is a modified Stanton number, where total transmission coefficients are used instead of film coefficients, multiplied by a geometrically dependent constant. This is for circular and square tubes $4 \cdot \frac{L}{d}$. The range for this number is apparently between 0 and 10, where zero represents a pure transmission system. However, for most operating equipment is c_t lower than 5.

5.1. System I.

The moments of ADM with the mentioned boundary conditions and the equivalent STM flow delay impulse responses are shown in fig. 6. In fig. 7 the relative errors are shown as a function of c_t/P_e . The static gain is here computed in dB and P_e assumed larger than 20. Note E_{σ} reaches a maximum and then decreases

rapidly, whereas E_G and E_μ are monotone functions.

The moments of PFM for systems with and without coupling element capacity are shown in fig. 6.

The errors in the gain and the mean for neglecting of the coupling element capacity are shown in fig. 8 for discrete values of N . For small c_t E_μ is rather small, but it becomes remarkable as $c_t > 1$, whereas E_G is very small for c_t less than 1 and increases much more rapidly for c_t larger than 1. The absolute differences in variance are shown in fig. 8 too. Note that the difference decreases by increasing c_t . As the variance of PFM in this case is zero the difference is completely determined by σ_{STM}^2 . This explains why the difference is always smaller than $1/N$.

The moments including the coupling element capacity are listed in fig. 6. This shows the mean is heavily influenced by the coupling element capacity whereas the static gain is independent. However, E_μ is independent of the capacity, because the two means are multiplied by the same factor $1 + y$. This shows that y represents the shift in the mean due to the capacity of the coupling element and the error of neglecting this in the simulation can easily be estimated from fig. 6. The difference between the absolute errors in the variance for the case with wall capacity (index cap) and for the case without is:

$$\Delta EA_\sigma = EA_{\sigma, \text{cap}} - EA_\sigma = (EA_\sigma) \cdot y(2 + y(1 - 2a(1 + \frac{c_t}{N}))) \quad (7)$$

This shows that ΔEA_σ is lower than or at the same order of magnitude as EA_σ for y less than 1. For small values of a ΔEA_σ is positive. For a larger than 0.5 ΔEA_σ can be negative in which case a conservative design is obtained when the wall capacity is neglected.

These considerations show that it is possible to neglect the coupling element capacity in dimensioning the number of sections when y is small. In cases of doubt the error can be estimated from eq.7. If the error is too big is it sufficient to include the wall capacity when computing the error in the variance. In this case it is often possible to use the relative error

$$E_{\sigma, \text{cap}} = E_\mu + \left(\frac{1+y}{y}\right)^2 \frac{c_t}{2a} \cdot (EA_\sigma)$$

5.2. The complex systems

For systems II and III the number of parameters will make

the interpretation of the results very tedious if the capacity of coupling elements is not neglected. Even then the analysis of the simulation errors is complicated by the number of parameters involved. These include the modified Stanton numbers for each flow element c_{t1} and c_{t3} , the residence time ratio κ and the number of sections N . The computations of the errors in the moments (E_G , E_u , EA_σ , (E_σ)) showed however that they are all nearly inverse proportional to N . This statement is rather crude especially at high c_{t1} , and low N . However, it is accurate within about 20% for between 5 and 200 lumps, which is assumed sufficient for the present purpose. The results are then presented for $N = 20$.

5.2.1. System II.

The errors in the static gain and the mean value are plotted in fig. 9. Note that the static gain E_G is independent on κ and E_u only is slightly dependent on κ . The maximum values are less than $(4/N)$ 100% and occur for $(c_{t1}, c_{t3}) = (4, 0.1)$. The absolute error in the variance for different κ values is plotted in fig. 10 a-e. Note that the absolute error is very large for $\kappa = 0.3$. For $\kappa = 0.3$ and 0.1 the relative error is applicable and is plotted in fig. 11 a and b. For large κ values the absolute error is approximately equal to the error for system I. For κ about 1 is EA_σ nearly equal to $1/N$ and for lower κ values the error increases with c_{t1} . For κ less than 0.3 the relative error varies heavily as shown with c_{t1} and c_{t3} .

5.2.2. System III.

The errors in the static gain are shown in fig. 12. At low c_{t3} values are these comparable to the errors for system I. E_u shown in fig. 13 is only weakly dependent on κ , and for large κ values very similar to system I, fig. 8. The error in the variance are plotted for the same κ values as for system II in fig. 14 a-e. For large κ and low c_{t3} the EA_σ is analogous to EA_σ for system I. At higher c_{t3} values a maximum occurs. This becomes more pronounced for κ lower than 1. At the very small κ values the relative error is the most convenient to use. This varies like system II rather much with the parameters.

6. Results from digital computed frequency responses

To illustrate the earlier considerations about the influence of the different errors on the distributed frequency responses a number of computations for system I have been performed. The

effect of increasing E_G is shown in fig. 16 a where U_1/U_3 are plotted for increasing numbers of sections. In 16 b an static error on 1% for each section is introduced. By comparing the two sets of curves we observe that accumulated static errors smaller than about +20% introduce large errors in the frequency responses. The effect of a big $|E_U|$ is shown in fig. 17 where the frequency characteristic for U_1/r_1 is shown for two c_{11} values. Note/for $E_U = -21\%$ is the resonance peak shifted strongly against higher frequencies. Finally is in fig. 18 the effect of absolute errors in the variance shown for U_1/r_1 frequency responses when the capacity of the coupling element is neglected. Note/that the deviations are concentrated on the peaks of the oscillations.

The results emphasize the earlier made conclusion about the necessity of obtaining small errors in the static gain and mean value before errors in the variance should be taken into account.

7. Results from analog simulations.

Several simulations have been performed on the special analogue computer with results which are in satisfactory agreement with the digital computed frequency responses. For the purpose of illustration are the frequency characteristics U_1/U_3 and U_1/r_3 for a simulated single pass shell and tube type counter flow heat exchanger shown in fig. 19 and 20, where digitally computed responses for the linearised version of the theoretical model (21 sections), the model with amplifier error and PFM also are shown. These show a satisfactory agreement between the analog and equivalent digital computations. For U_1/U_3 there is only minor differences between the models, whereas in the flowforced case specially the phase curve differs. Note that PFM has a rapidly increasing phase whereas STM is limited. This is due to the error in the variance. If 51 sections are used the frequency characteristics are almost equivalent to about $\Omega \approx 1$.

As an example of system II has ADM for a gas-liquid fluidized bed with mass transfer between the gas and the liquid been simulated. The purpose of the original experiment ¹² was to obtain residence time distributions for the gasphase by tracer techniques. The present simulation was carried out to investigate the tailing effect. Fig. 21.

8. Conclusion.

With the presented curves is it possible to estimate the accuracy of a specific simulation and the number of lumps.

The results show that for constant N has system I unlimited E_G and E_μ at high values of c_{t1} . In contrast is EA_σ limited to $1/N$. For system III is E_G and E_μ also unlimited and EA_σ is at least for χ larger than 1 limited too. For practical purposes is EA_σ unlimited at low χ values, where it often is feasible to use the relative error as a basis for the design. For system II is it remarkable that both E_G and E_μ are limited in the region under consideration. For χ larger than 1 is EA_σ limited too, but for low χ values are EA_σ unlimited at high c_{t1} values. Here it is feasible just/as for system III to use the relative error in the variance. However, the situations with unlimited errors occur only for high c_{t1} values which is unusual. That system III has simulation errors which for large χ and small c_{t3} is comparable to those for system I is not surprising because at these parameter values system I is the limiting case for system III. This limiting case was indicated by Machubuci¹³ to be a good one any time χ is larger than 3 which is in good agreement with the present results except for very large c_{t3} .

These considerations show that it is possible to simulate systems of the mentioned types in a wide region of the parameters, with satisfactory approximation to the distributed frequency characteristics.

The results obtained with the special analog show satisfactory agreement with the digital computed frequency responses and show/that it is possible to perform accurate simulations of practical chemical processing systems with medium number of sections.

References

1. Fricke, L.H., H.J. Morris, R.E. Otto and T.J. Williams. Chem.Engng. Progr. Symposium Series No. 31, 56 (1960) 8.
2. Privott, Ir., W.J. Ph.D. thesis North Carolina University 1965.
3. Barabaschi, S., M. Conti, L. Gentilini and A. Mathis. Automatica 2 (1964) 1.
4. Kummel, M., To be published.
5. Wiig, K.N.. Paper presented at 8.SAMS meeting J nk ping, Sweden. 25. and 26.April 1963.
6. Mathis A. and P. Giordano. Annales de l'Assoc.Intern. pour le Calcul Analogique 6 (1964) 9.

7. Takahaski, Y. Automatic and Manual Control, A. Rustin, ed. Butterworth, London 1952. p.235.
8. Hsu I.P. and N. Gilbert. A.I.Ch.E. Journal 8 (1962) 593.
9. Fan, L.-T. and Y.-K. Ahn. Chem.Engng.Progr.Symposium Series No 46, 59 (1963) 91.
10. Coste, I., D. Rudd and N. R. Amundson. The Canadian Journal of Chem.Engng. (1961) 149.
11. van der Laan, E.Th. Chem.Engng.Science 7 (1958) 187.
12. Østergaard, K. and M.L. Michelsen. To be published in Canadian Journ. of Chem. Engng.
13. Masubuchi, M. Trans.Japan Soc. Mechanical Eng. 24 (1958) 209.

Nomenclature

- a. ratio between outer and inner quantity transmission pr unit length, time and potential for a coupling element (e.g. $a = \frac{\tau_{21}}{\tau_{23}}$)
- b. ratio between the capacitance pr unit length in a flow element and an associated coupling element. (e.g. $b_1 = \frac{\tau_{12}}{\tau_{21}}$)
- c. Stanton number multiplied by a geometrically dependent constant (e.g. $c_2 = \frac{1}{\tau_{12}}$)
- c_t As c but with total transmission coefficients (e.g. $c_{t1} = \frac{\tau_1}{\tau_{23}}$)
- d tube diameter
- D Axial dispersion coefficient
- E_I relative error see eq. (5)
- EA_I absolute error see eq. (6)
- $G(s)$ Transfer function
- L System length
- M_i i'th moment of a distribution see eq. (1)
- N Number of sections
- Pe axial Peclet number ($\frac{VL}{D}$)
- r Relative flow perturbation
- s Laplace variable
- St Stanton number
- t Time coordinate
- U Potential
- V Linear flow velocity
- x Length coordinate
- y $= 1/(b(1+a)^2)$

θ	dimensionless time (t/τ_p)
x	τ_1/τ_3
u	mean value of a distribution eq. (3)
ξ	dimensionless length. (x/L)
σ^2	variance of a distribution eq. (4)
τ	time constant
τ_{ij}	quantity transmission pr. unit length, time and potential through the boundary ij divided by quantity capacity pr. unit length and potential.
τ_p	residence time
Ω	dimensionless frequency



Fig. 1. General
system model

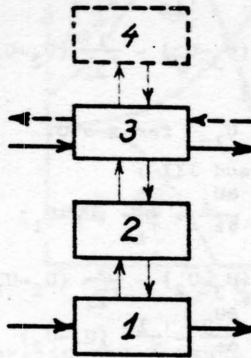


Fig. 2. System
blocdiagram

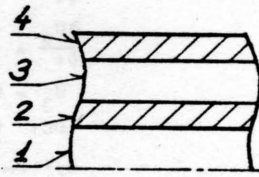


Fig. 3. Axial cut
through a half
double pipe.

Coupling process: Convection

$$f(U_i, U_j) = \frac{1}{\tau_{ji}} (U_i - U_j)$$

Coupling element:

$$\frac{\partial U_2}{\partial t} = f(U_3, U_2) - f(U_1, U_2)$$

Flow elements: (see text for BC)

$$\text{PFM} \quad \frac{\partial U_1}{\partial t} = -V_1 \frac{\partial U_1}{\partial x} + f(U_2, U_1)$$

$$\text{ADM} \quad \frac{\partial U_1}{\partial t} = -V_1 \frac{\partial U_1}{\partial x} + D_1 \frac{\partial^2 U_1}{\partial x^2} + f(U_2, U_1)$$

$$\text{STM} \quad \frac{dU_{1,i}}{dt} = -\frac{V_1}{\Delta x} (U_{1,i} - U_{1,i-1}) + f(U_{2,i}, U_{1,i})$$

$$i = 1, 2, \dots, N$$

Fig. 4. Models for the elements (table)



System I

$$\frac{\partial U_1}{\partial t} = v_1 \frac{\partial U_1}{\partial x} + \frac{1}{\tau_{12}} (U_2 - U_1)$$

$$\frac{\partial U_2}{\partial t} = \frac{1}{\tau_{23}} (U_3 - U_2) - \frac{1}{\tau_{21}} (U_2 - U_1)$$

$$U_3 = U_3(t)$$

$$\text{BC: } U_1 = U_{10} \text{ for } x = 0.$$

System II and III :

$$\frac{\partial U_1}{\partial t} = -v_1 \frac{\partial U_1}{\partial t} + \frac{1}{\tau_{12}} (U_2 - U_1)$$

$$\frac{\partial U_2}{\partial t} = \frac{1}{\tau_{23}} (U_3 - U_2) - \frac{1}{\tau_{21}} (U_2 - U_1)$$

$$\frac{\partial U_3}{\partial t} = \mp v_3 \frac{\partial U_3}{\partial t} - \frac{1}{\tau_{32}} (U_3 - U_2)$$

(-) for system II and (+) for system III

BC: System II

$$U_2 = U_{10} \quad x = 0$$

$$U_3 = U_{30} \quad x = 0$$

System III

$$U_1 = U_{10} \quad x = 0$$

$$U_3 = U_{3L} \quad x = L$$

Fig. 5. Plug flow models for the three systems (table)

ADM		STM		PFM	
N = Pe/2		Coupling element capacity		without	with
		without	with		
$U(0)$	$\frac{Pe}{e} (1 - \sqrt{1 + \frac{4c_t}{Pe}})$	$(1 + \frac{c_t}{N})^{-N}$	$(1 + \frac{c_t}{N})^{-N}$	e^{-c_t}	e^{-c_t}
U	$\frac{1}{\sqrt{1 + \frac{4c_t}{Pe}}}$	$(1 + \frac{c_t}{N})^{-1}$	$(1+y)(1 + \frac{c_t}{N})^{-1}$	1	1+y
σ^2	$\frac{2}{Pe(1 + \frac{c_t}{Pe})^{3/2}}$	$\frac{1}{N}(1 + \frac{c_t}{N})^{-2}$	$\frac{2a}{c_t} y^2 (1 + \frac{c_t}{N})^{-1} + (1+y)^2 (1 + \frac{c_t}{N})^{-2} \frac{1}{N}$	0	$\frac{2a}{c_t} \cdot y^2$

Fig. 6. Moments for system I

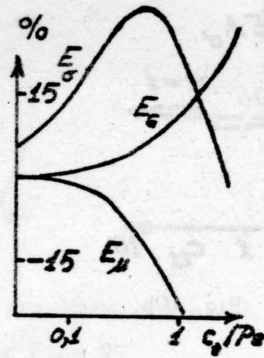


Fig. 7. Errors in the moments for system I (ADM)

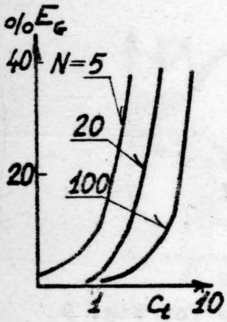


Fig. 8a

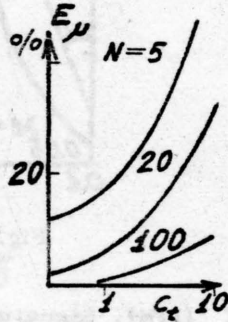


Fig. 8b

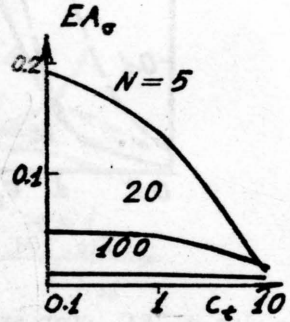


Fig. 8c

Fig. 8a-c. Errors in the moments for system I (PFM)



Fig. 9. E_G and E_u for system II (PFM). Signature:
 --- $c_{t3} = 10$, -- $c_{t3} = 1$ and -.- $c_{t3} = 0.1$

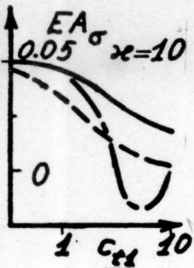


Fig. 10a.

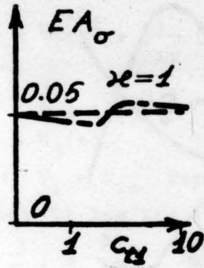


Fig. 10b.

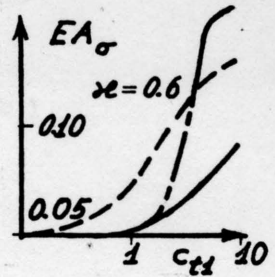


Fig. 10c.

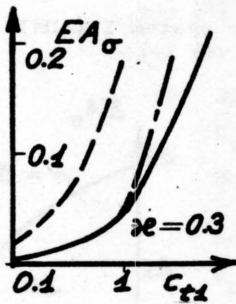


Fig. 10d.

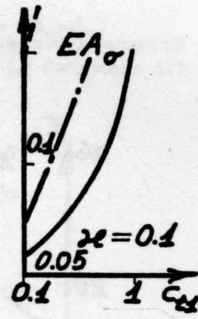


Fig. 10e.

Fig. 10a-e. EA_σ for system II (PFM). Signature, as for Fig. 9

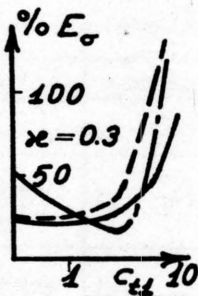


Fig. 11a.

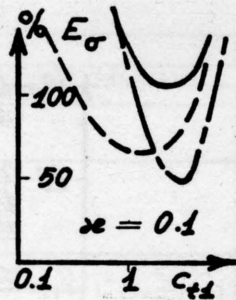


Fig. 11b.

Fig. 11a-b. E_σ for system II (PFM). Signature, as for Fig. 9

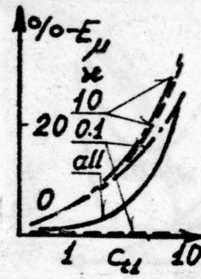
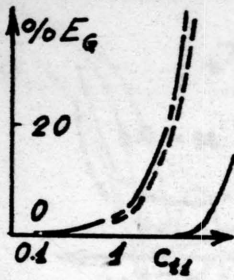


Fig. 12. E_G for system III (PFM). Fig. 13. E_{μ} for system III (PFM).
Signature, as for Fig. 9 Signature, as for Fig. 9

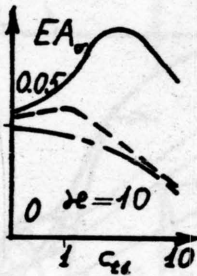


Fig. 14a

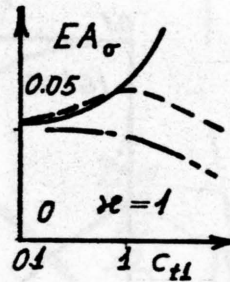


Fig. 14b

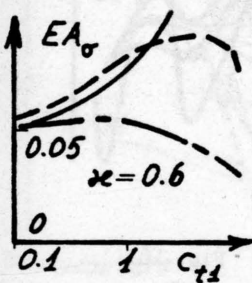


Fig. 14c

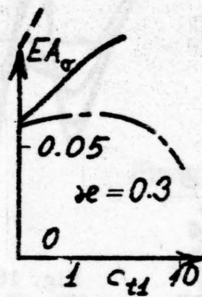


Fig. 14d

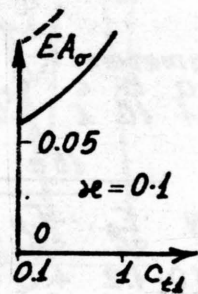


Fig. 14e

Fig. 14a-e. EA_{σ} for system III (PFM). Signature, as for Fig. 9

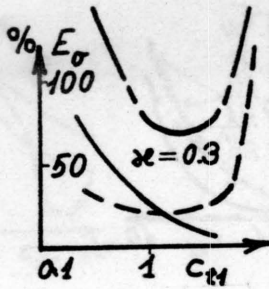


Fig. 15a

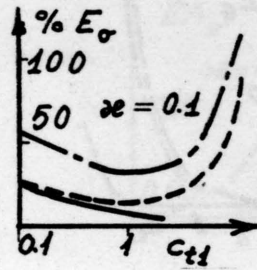


Fig. 15b

Fig. 15a-b. E_σ for system III (PFM). Signature, as for Fig. 9

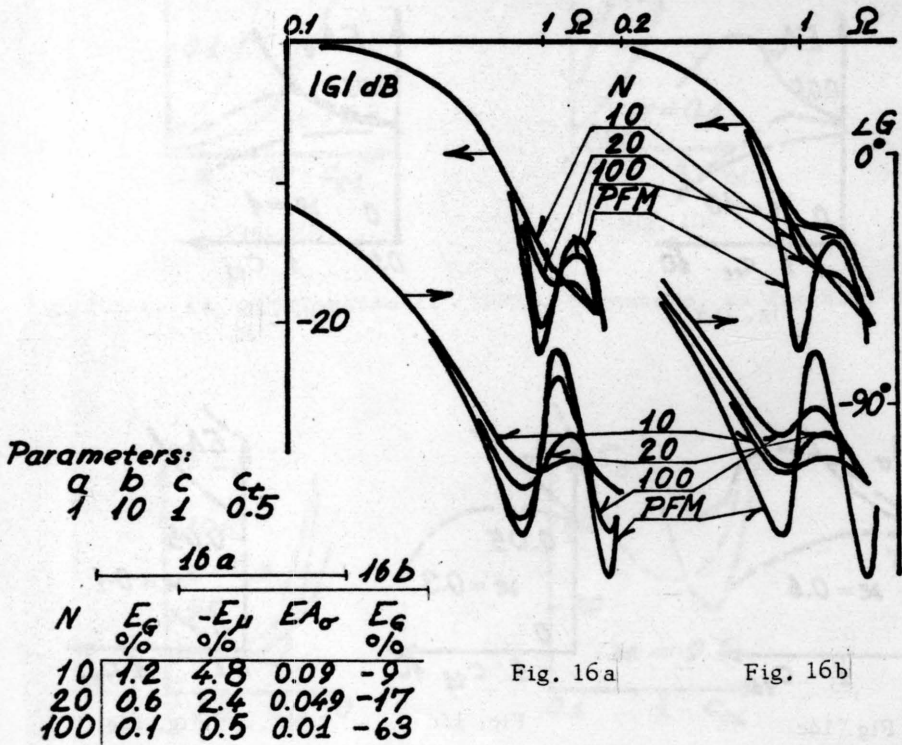
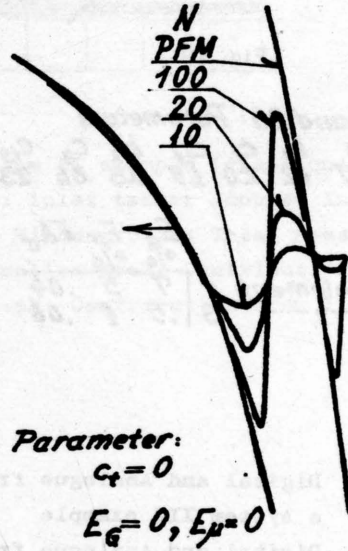
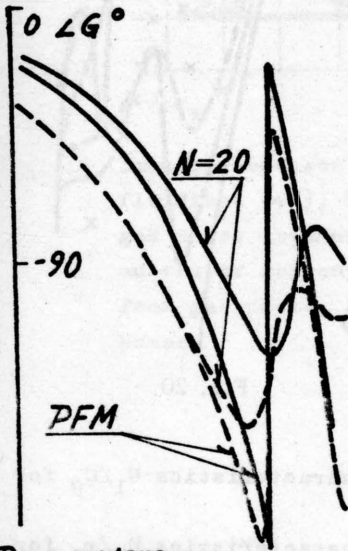
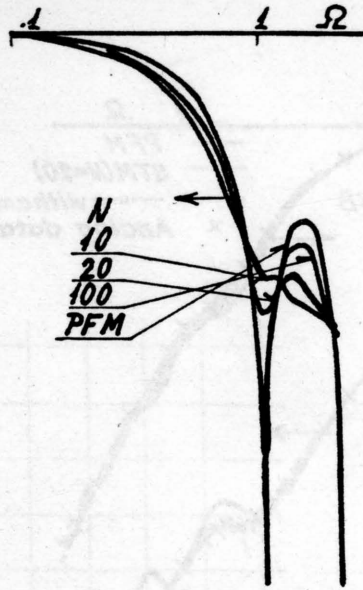
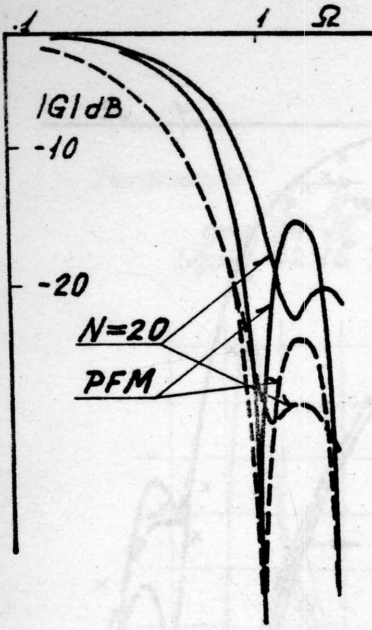


Fig. 16a

Fig. 16b

Fig. 16. Effect of E_G on frequency response for system I



Parameter:

$$c_t = 0$$

$$E_G = 0, E_\mu = 0$$

$$\begin{array}{c|ccc} N & 10 & 20 & 100 \\ \hline EA_\sigma & .1 & .05 & .01 \end{array}$$

Parameters:

case	sgn.	a	b	c	c_t	E_G %	$-E_\mu$ %	EA_σ
1	--	1	10	.1	.05	~0	.5	.05
2	—	1	10	10	5	65	21	.03

Fig. 17. Effect of E_μ on frequency response for system I

Fig. 18. Effect of EA_σ on frequency response for system I

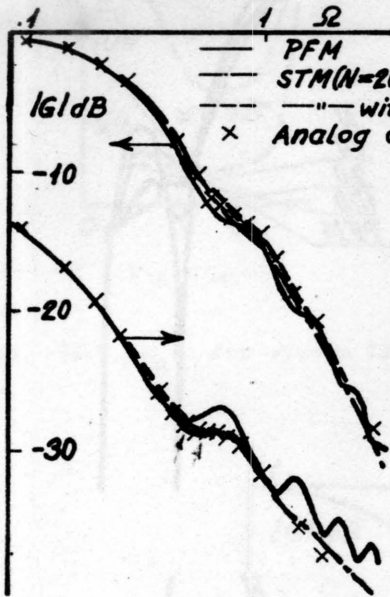


Fig. 19.

Fig. 19 and 20: Parameters

x	a	b_1	c_1	c_2	b_3	c_3	c_{23}
2.0	2.7	1.2	2.0	1.5	3.8	.85	.23

Flowelement		E		EA_σ
		ξ %	μ %	
1	3	.7	.5	.04
	3	.5	.1	.06

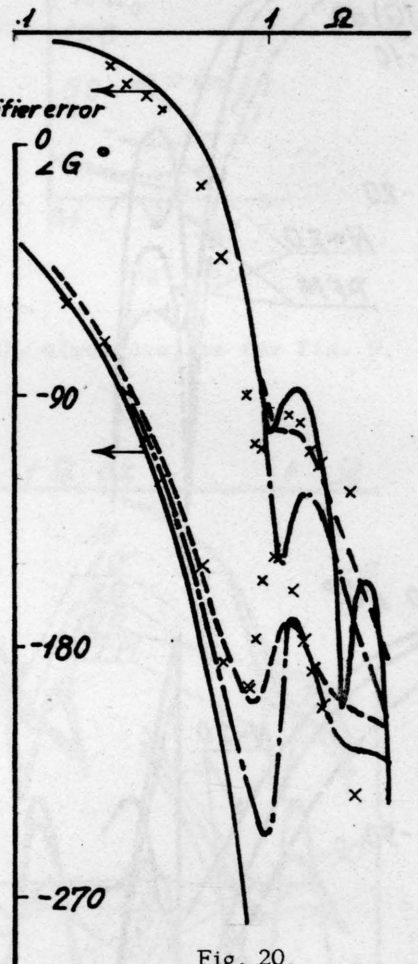


Fig. 20

Fig. 19, Digital and Analogue frequency characteristics U_1/U_3 for a system III example

Fig. 20, Digital and Analogue frequency characteristics U_1/r_3 for a system III example

Parameters:

	P_0	N	C_t
gas	24	12	.12
liquid	32	16	.74

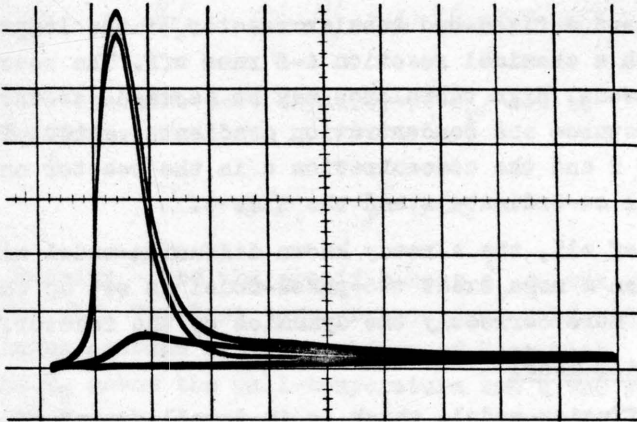


Fig. 21. Impulseresponses for a system II example (gas-liquid fluidized bed), Left trace: inlet tracer impulse into gas phase attenuated 1:5. Highest peak: Total measured tracer concentration, Smaller peak: Contribution from gas phase. Smallest peak: Contribution from liquid phase.

MODELS AND SIMULATION OF FIXED-BED TUBULAR REAKTORS

E.D.Gilles, B.Lübeck, M.Zeitz

Institute of Chem. Technologie, Techn.Hochschule Darmstadt
Darmstadt, Western-Germany

1. Constitution of the model

We regard a fixed-bed tubular reactor of the length 1 /fig. 1/, in which a chemical reaction A-B runs off. The reaction mixture be gaseous. High turbulence may be assumed, so that no radial temperature- and concentration gradients, exist. Thus the temperature T and the concentration c in the reactor only depend on the axial co-ordinate z and the time t.

First of all, the already known diffusion-model will be discussed. Then a more exact two-phase-model is set up which allows to describe more correctly the dynamics of the reactor.

1.1. Diffusion-model

The diffusion-model, which is in detail explained in¹, comprises two balances, a balance of mass for the concentration c of the disappearing substance A and a balance of energy to determine the temperature T. This model assumes, that the temperature of catalyst and the temperature of gas are equal. If r is the individual reaction rate of the substance A referred to the catalyst-volume V_K , D_z eff the coefficient of axial back-mixing and v_z the axial flow-rate, we get the balance of mass:

$$\frac{\partial c}{\partial t} = D_{z \text{ eff}} \frac{\partial^2 c}{\partial z^2} - v_z \frac{\partial c}{\partial z} + \frac{1-\epsilon}{\epsilon} r(c, T)$$

/1/

The relative porosity ϵ is the ratio between that part of the cross-section F_G , which is occupied by the gas flow, and the whole sectional area F of the reactor. The boundary conditions are obtained by regarding the balances at the bounds $z = 0$ and $z = 1$. If c_0 is the inlet concentration and T_0 the inlet temperature of the gas, we get by consideration of the law for ideal gas:

$$c_0(t) \approx c_0(t) \frac{T_0(t)}{T(t)} = c_0(t) - \frac{D_{z \text{ eff}}}{v_z} \left(\frac{\partial c}{\partial z} \right)_{z=0}$$

/2/

For the bound $z = 1$ follows:

$$\left(\frac{\partial c}{\partial z}\right)_{z=1} = 0 \quad /3/$$

With the equivalent rate r_0 , the reaction enthalpy ΔH_R and the effective thermal conductivity $\lambda_{z \text{ eff}}$ follows for the balance of energy:

$$(\rho \hat{c}_p) \frac{\partial T}{\partial t} = \lambda_{z \text{ eff}} \frac{\partial^2 T}{\partial z^2} - v_z (\rho \hat{c}_p)_G \frac{\partial T}{\partial z} + (-\Delta H_R) \frac{1-\epsilon}{\epsilon} r_0(c, T) - a(T - T_w) \quad /4/$$

The effective specific heat capacity $\rho \hat{c}_p$ can be calculated with the equation:

$$(\rho \hat{c}_p) = (\rho \hat{c}_p)_G + \frac{1-\epsilon}{\epsilon} (\rho \hat{c}_p)_K \quad /5/$$

with the density and the specific heat \hat{c}_p of the gas /G/ and the catalyst /K/. The last term on the right hand side of equation /4/ takes account of the exchange of heat with the tube wall, where T_w means the wall-temperature and a the coefficient of exchange. For the temperature there exist similar boundary conditions as for the concentration:

$$T_0(t) = T(a, t) = \frac{\lambda_{z \text{ eff}}}{v_z (\rho \hat{c}_p)_G} \left(\frac{\partial T}{\partial z}\right)_{z=0} \quad /6/$$

$$\left(\frac{\partial T}{\partial z}\right)_{z=1} = 0 \quad /7/$$

The lack of this diffusion model is obvious. This quasi-homogeneous model does not consider the normally existing temperature differences between the two phases which take part in the reaction. This lack is especially important by describing dynamic processes. The main influence on the reaction rate has the temperature of the catalyst, on which changes of the gas temperature take a very delayed effect. We find similar conditions with regards to the concentration of the reactand A especially in diffusion controlled reactions. Here the time delays should be considered which exist between the concentration in the gas flow and the concentration in the active centers of the catalyst. As the diffusion model cannot accomplish those demands, we develop-

ped a new two phase-model especially for the description of dynamic processes.

1.2. Two phase-model

The free sectional area F_G of the reactor, which is not filled up with contact-material is splitted in two parts as shown in fig. 1. In the "fixed" part /R/ with the area F_R the heat- and mass transport be effected only by means of diffusion and thermal conduction. The remaining free sectional area F_S be a pure plug-form-flow. The chemical reaction along the catalyst is included into the part /R/ which is exchanging heat and mass with the part /S/. The concentration in /R/ should be equal to the concentration c_K at the surface of the catalyst. According to this, it is assumed that there is no difference between the temperature in this part and the catalyst temperature T_K . If we regard the reaction rate with relation to the contact-volume as done before we come with $\xi' = \frac{F_R}{F_R + F_K}$ to the following balance equations:

$$\frac{\partial c_K}{\partial t} - D'_{z \text{ eff}} \frac{\partial^2 c_K}{\partial z^2} + \frac{1-\xi'}{\xi'} \tau_o(T_K, c_K) - b_1(c_K - c_G) \quad /8/$$

$$(\overline{\rho \hat{c}_p}) \frac{\partial T_K}{\partial t} - \lambda'_{z \text{ eff}} \frac{\partial^2 T_K}{\partial z^2} + (-\Delta H_K) \frac{1-\xi'}{\xi'} \tau_o(T_K, c_K) - a_1(T_K - T_G) - a_2(T_K - T_w) \quad /9/$$

The effective specific heat-capacity accomplishes equation /5/, if we replace ϵ by ξ' . The quantities a_1 and b_1 are coefficients for the heat- resp. mass-transfer. The boundary conditions of /R/ have a rather simple form, as it is allowed to assume, that the axial heat- and mass flow disappears identically on the bounds $z = 0$ and $z = 1$. Thus follows:

$$\left(\frac{\partial c_K}{\partial z} \right)_{z=0,1} = 0 \quad \left(\frac{\partial T_K}{\partial z} \right)_{z=0,1} = 0 \quad /10/$$

To determinate the concentration c_G and the temperature T_G in part /S/ we receive with $\lambda = \frac{F_R}{F_S}$ the following balance equations:

$$\frac{\partial c_G}{\partial t} = -v_z' \frac{\partial c_G}{\partial z} - \lambda b_1(c_G - c_K) \quad /11/$$

$$\left[\frac{dT_G}{dt} \cdot (\rho \hat{C}_p)_G - v_z' (\rho \hat{C}_p)_G \frac{\partial T_G}{\partial z} - \alpha a_r (T_G - T_K) - a_3 (T_G - T_w) \right] \quad /12/$$

The boundary conditions are:

$$c_G(0,t) = c_0(t) \quad T_G(0,t) = T_0(t) \quad /13/$$

1.3. The diffusion-model as a special case of the two phase-model

If the mass- and heat transfer between the two parts /R/ and /S/ is so intensive, that the temperatures T_G and T_K as well as the concentrations c_G and c_K correspond, the two phase-model passes to the diffusion-model. In order to achieve this, we substitute in the balance-equations /8/ and /9/ by means of the equations /11/ and /12/ the terms, which describe the heat- and mass-transfer between /R/ and /S/. Thus we receive the following relations between the coefficients of those two models:

$$\frac{D_{z\text{eff}}}{D_{z\text{eff}}} = \frac{\lambda_{z\text{eff}}}{\lambda_{z\text{eff}}} = \frac{F_R}{F_R} \quad /14/$$

$$v_z' F_S = v_z F_G \quad /15/$$

$$\alpha F_G = \alpha_2 F_R + \alpha_3 F_S \quad /16/$$

In the particular case of an extremely quick heat- and mass-transfer between /R/ and /S/ the boundary conditions of the two phase-model pass to those of the diffusion-model too. This can be shown by simple balances at the bounds $z = 0$ and $z = 1$ of the reactor. We get at the bound $z = 0$ for the concentration:

$$c_0(t) = c_G(0,t) = \frac{D_{z\text{eff}}}{v_z} \left(\frac{dc_K}{dz} \right)_{z=0} \frac{F_R}{F_S} \quad /17/$$

With $c_G = c_K$ and the equations /14/ and /15/ we receive the boundary conditions /2/ of the diffusion-model. Only in case of an extremely intensive heat- and mass transfer between /R/ and /S/ the diffusion-model can describe the dynamic processes in a fixed-bed reactor.

2. Simulation of fixed-bed tubular reactor

On principle there are three possibilities for the analog computer simulation of systems with locally distributed parameters, which are described by partial differential equations: the method of differences, the method of characteristics and the model simulation¹. - The last method is the most suitable for the simulation of fixed-bed tubular reactors, which represent boundary-value-problems and as consequence of chemical-reactions include non-linear sources of heat and mass. This method bases essentially on an integral transformation by the means of eigenfunctions². For the general two phase-model a simulation diagram is derived. Then the results of a special case are discussed.

2.1. Simulation plan for the two phase-model

In the considered equation-system /8/, /9/, /11/, /12/ we put all differential terms to the left and short the right side of the differential equations by ϕ_1 /1 = 1,2,3,4/:

$$\phi_1 = b_r (c_G - c_K) + \frac{1-\varepsilon'}{\varepsilon'} + (c_K, T_K) \quad /18/$$

$$\phi_2 = \frac{1}{(\rho c_p)_G} \{ a_1 (T_G - T_K) + a_2 (T_W - T_K) + (-\Delta H_R) \frac{1-\varepsilon'}{\varepsilon'} + c_0 (c_K, T_K) \} \quad /19/$$

$$\phi_3 = \frac{b_r \alpha}{V_2} (c_K - c_G) \quad /20/$$

$$\phi_4 = \frac{1}{V_2 (\rho c_p)_G} \{ \alpha a_1 (T_K - T_G) + a_2 (T_W - T_G) \} \quad /21/$$

These new functions depend on the variables of state resp. the input quantities of the reactor and can be regarded as sources of the system. After these abbreviations the two phase-model of the reactor is expressed as follows:

$$\frac{\partial C_k}{\partial t} - D_{z,eff} \frac{\partial^2 C_k}{\partial z^2} = \phi_1(C_k, T_k, C_G) \quad /22/$$

$$\frac{\partial T_k}{\partial t} - \frac{\lambda_{z,eff}}{(s c_p)} \frac{\partial^2 T_k}{\partial z^2} = \phi_2(C_k, T_k, C_G) \quad /23/$$

$$\frac{1}{V_G} \frac{\partial C_G}{\partial t} + \frac{\partial C_G}{\partial z} = \phi_3(C_k, C_G) \quad /24/$$

$$\frac{1}{V_L} \frac{\partial T_G}{\partial t} + \frac{\partial T_G}{\partial z} = \phi_4(T_k, T_W, T_G) \quad /25/$$

Simplifying the initial conditions of the reactor are supposed to be Null:

$$C_k(z, 0) = T_k(z, 0) = T_G(z, 0) = C_G(z, 0) = 0 \quad /26/$$

It is now provided, that the time behaviour of the reactor is dominantly determined by the time delays of the system on account of the heat capacity of the fixed bed. The dynamic processes, caused by the gas-flow are normally so quick, that they can be regarded as quasi-stationary. That means, we can neglect the differential quotient with respect to time in the balance-equations of the streaming phase without making a considerable mistake. After being simplified in this way the two differential equations /24/ and /25/ can be integrated by help of an analog computer without any difficulties.

The substantial idea of the model simulation is to pass the partial differential equations with consideration of the boundary conditions to normal differential equations by using a suitable integral transformation. The integration of those only time-controlled equations leads to the transformed system-quantities, f.i.:

$$c_{x,y}^*(t) = \int_0^l \varphi_p(z) c_x(t, z) dz \quad /27/$$

The kernels $\varphi_p(z)$ of this so-called model transformation are exactly the eigenfunctions of the system, which are defined by the following differential equation and boundary condition:

$$\frac{d^2 \varphi_p}{dz^2} = -\kappa_p^2 \varphi_p, \quad \left(\frac{d\varphi_p}{dz} \right)_{z=0, l} = 0 \quad /28/$$

As solution of this eigenvalue problem we find the trigonometrical cosine functions, which we will normalize:

$$\varphi_p(z) = \sqrt{\frac{2}{l}} \cos \kappa_p z \quad /29/$$

The eigenvalues κ_p are the zeros of the equation:

$$\sin \kappa_p l = 0 \quad \rightarrow \quad \kappa_p = \frac{\nu \pi}{l} \quad \nu = 1, 2, \dots, \infty \quad /30/$$

By means of the model transformation we pass the partial differential equations to an infinite system of ordinary differential equations:

$$\frac{dc_{x,y}^*}{dt} + D_{zeff} \left(\frac{\nu \pi}{l} \right)^2 c_{x,y}^* = \phi_{1,\nu}^* \quad \nu = 1, 2, \dots, \infty \quad /31/$$

Those equations are uncoupled and each equation can be integrated on the analog computer dependent from the transformed source-function:

$$\phi_{1,\nu}^*(t) = \int_0^l \varphi_p(z) \phi_1(t, z) dz \quad /32/$$

We characterize the homogeneous part of the differential equation by means of the transfer functions:

$$\bar{g}_{1,\nu}(s) = \frac{1}{s + D_{zeff} \left(\frac{\nu \pi}{l} \right)^2} \quad /33/$$

To allow the inverse transformation we expand the quantity $c_K(t, z)$ into a series after the eigenfunction and receive with consideration of the orthogonal relation:

$$\int_0^l \varphi_m(z) \varphi_n(z) dz = \begin{cases} 0 & n \neq m \\ 1 & n = m \end{cases} \quad /34/$$

the transformed input-quantities as coefficients of the expansion.

$$C_K(t, z) = \sum_{p=0}^{\infty} C_{Kp}^*(t) \varphi_p(z)$$

/35/

Thus the given boundary-value-problem is decomposed into the following partial problems, which can be solved by means of the analog computer corresponding to the simulation plan, shown in fig. 2:

- 1/ Fourier analysis /FA/ of the source-function
- 2/ Intergration of the time-differential-equation
- 3/ Fourier synthesis /FS/
- 4/ Non-linear recycling

Thus the electronical simulation of an onedimensional system requires the integration of ordinary differential equations after time and space and the execution of a finite integral with the Fourieranalysis. The fact, that on an analog computer the machine time is the only available quantity - what normally leads to difficulties- can be avoided. It is necessary to perform continuously the integration after the time and to integrate after the space by means of a fast-speed repetitive computation. The technical performance of the model simulation is realized in the following way:

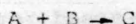
In the middle part of the simulation diagram of fig. 2 the computation is performed continuously. In this part the Fourier-coefficients of the output quantities are determined by developing them from the coefficients of the sourcefunction. By help of a fast-speed repetitive computation the profile of the output quantity is derived from the time-variable amplitudes in a Fourier synthesis. It is necessary to multiply the Fourier coefficients with the corresponding eigenfunctions and sum up after that. The local profile of the output quantity $c_K / t, z /$ traverses the non-linearity and leads, connected with the functions c_G and T_K , to the source function $\phi_1 / c_G, c_K, T_K /$. The Fourier analysis of the source function is also performed by a repetitive operation ϕ , is multiplied with the various eigenfunctions and sequently integrated between the limits 0 and 1 over the time coordinate, which correspond to the space. These results are the

Fourier coefficients of the source function. They are feeded to the storing elements by a short shut of the switches. The great advantage of this method of simulation is, that normally with only few eigenfunctions a high degree of accuracy can be achieved. In contradistinction to other methods the output quantity in this case is a continuous function and can easily be observed by an oscillograph.

After these detailed remarks referring to the modal simulation of the quantity c_K the whole simulation diagram of a fixed-bed tubular reactor in fig. 3 is easily to understand. The model simulation is there applied to the differential equations /22/ and /23/. The simplified equations /24/ and /25/ are to be integrated only after space. The source functions ϕ_i / $i = 1, 2, 3, 4$ / are formed out of the simulated terms c_G , c_K , T_G and T_K by recycling. In order to simplify the simulation diagram the flow rate v_z is assumed to be constant.

2.2. Results of a reactor simulation

The simulation of the fixed-bed reactor is carried out for a diffusion controlled exotherm reaction



/36/

This could be f.i. a hydration. The reaction rate shall be expressed with the equation:

$$r_0 = -r_A = k_0 e^{-E/RT_K} c_A c_B$$

/37/

The temperature T_K of the catalyst appears in the Arrhenius-Term. If the mass transfer between /R/ and /S/ is very intensive, follows $c_{AK} = c_{AG} = c_A$. Neglecting the axial diffusion we find for the concentration c_A

$$\frac{dc_A}{dz} = \frac{1}{L} \cdot \frac{1-E}{E} T_A(c_A, T_K)$$

/38/

The component B is assumed to be surplus. The energy balances for /R/ and /S/ shall accomplish the equations /9/ and /12/ of the twophase modal. The modal simulation of this equation system leads to the following results:

Fig. 4 shows a stationary state of the reactor. The gas enters the reactor with the inlet temperature T_0 and the inlet concentration c_{A0} . Along the whole length of the reactor the catalyst temperature exceeds the gas temperature, because of the fact, that the heat, which originates in the fixed-bed by reaction, can be led away only by the streaming gas. Compared to homogeneous tube-reactors we constate a remarkable difference in the performance of the reaction. Instead of an exponential increase of temperature, which we found in homogeneous reactors, the gas temperature shows here already in the beginning a very sharp rise. The heat transfer between the two phases has obviously an equalizing effect on the gas temperature profile. Similar to a stirred tank reactor also a fixed-bed reactor can have three stationary states. Fig. 5a shows a stable, singular state in a low temperature range; fig. 5b shows it in a high temperature range. We must pay attention to the fact, that in the critical case b the maximum temperature exists at the beginning of the reactor.

Fig. 6a shows in a oscillogram series how the two temperature profiles and the concentration profile in the reactor follow a sudden variation of inlet concentration with respect to time. Raising the inlet concentration leads to a higher temperature range for the reaction. The accordingly increased reaction rate effect a reduced concentration of the substance A at the end of the reactor. Corresponding effects shows a sudden variation of the inlet concentration /s.fig. 6b./. Fig. 6c shows the effect on the reaction caused by a slow reduction of the transfer coefficient a_1 . The maximum temperature in the reactor increases and passes further on in flow direction, when a_1 is reduced. Therefore we can suppose, that a fixed-bed reactor operating with non diffusion controlled reaction has a tendency to "run away" in the front part.

Frequently fixed-bed tubular reactors, f.i. hydrogenizing plants, are operated in recycle process /s.fig. 7a/. The not consumed substances A and B are separated from the product C in a special material separating device, recooled and brought again to the entrance. Simulating this recycle process the influence of the separating device is taken into consideration by various first-order delay components. Besides it is provided that the

inlet temperature of the reactor is kept constant by an automatic control system. Thus the dynamical feed-back is effected only by the concentration of the component A in the recycled mass stream. The substance B, f.i. hydration-gass, be surplus. By recycling the concentration of the substance A at the inlet increases and the reaction-zone shifts towards the front part of the reactor. This has as effect, that at the reactor outlet the amount of the substance A, which can be recycled, is diminished. Thus the reaction zone is shifted towards the opposite direction and the recycle process may become dynamically unstable. This is shown in fig. 7b of the oscillogram series and is also constated in practical operations.

3. Stability of fixed-bed reactors

A fixed-bed tubular reactor with exothermic reactions has all structural qualities which may lead to dynamic instabilities. The amount of heat produced by the reaction represents the source of energy for the system. The internal feedbacks appear as backmixing, diffusion and heat transfer. It shall be analysed, which are the conditions for the existence of instabilities of an autonom reactor. We restrict to the case of a very intensive mass- and heat transfer between both phases and start from the diffusion model, equation /1/ and /4/, which we linearize for a given stationary temperature- and concentration profile $T_S /z/$ and $c_S /z/$. If η and ζ are defined as small variations of temperature and concentration, we can write:

$$\eta = \eta_1 e^{\alpha z} ; \zeta = \zeta_1 e^{\alpha z} ; \eta_w = \frac{1}{a} \eta_1 e^{\alpha z} \quad /39/$$

where

$$\alpha = \frac{V_2}{2 D_{\text{eff}}} - \frac{V_2 (P_2)_0}{2 \lambda_{\text{eff}}} \quad /40/$$

This assumption is allowed, if we provide, that the compensation of temperature and concentration bases upon the same transport mechanism. Simplifying we regard $v_z = \text{const.}$ The small variations of the reaction rate can be expressed in the following way:

$$r - r_S = \frac{\varepsilon}{1 - \varepsilon} \phi = \frac{\varepsilon}{1 - \varepsilon} \{ h_r(z) \eta_1 - h_c(z) \zeta_1 \} \quad /41/$$

Now we get for the linearized differential equations of the reactor:

$$(\mathcal{L}_P) \frac{\partial X_1}{\partial t} - \lambda_{\text{eff}} \frac{\partial^2 X_1}{\partial z^2} + \beta_0 X_1 = (-\Delta H_R) \phi + Y \quad /42/$$

$$\frac{\partial X_2}{\partial t} - D_{\text{eff}} \frac{\partial^2 X_2}{\partial z^2} + \beta_0 X_2 = -\phi \quad /43/$$

The boundary conditions of the quantities $X_{1/2}$ have the form

$$\left\{ \frac{\partial X_{1/2}}{\partial z} - \alpha X_{1/2} \right\}_{z=0} = X_{1/2} \quad /44/$$

$$\left\{ \frac{\partial X_{1/2}}{\partial z} + \alpha X_{1/2} \right\}_{z=L} = 0 \quad /45/$$

Now we determine the Green's functions $G_{1/2}$ corresponding to the differential operators on the left sides of the differential equations /42/ and /43/. With s as complex variable we get in the Laplace-space:

$$G_{1/2}(z, \mathcal{L}, s) = \sum_n^{\infty} g_{1/2n}(s) f_n(z) f_n(\mathcal{L}) \quad /46/$$

are the eigenfunctions. With the eigenvalues the transfer functions $g_{1/2n}$ accomplish the following differential equations:

$$g_{1n}(s) = (\mathcal{L}_P) s + \lambda_{\text{eff}} (\alpha^2 + 2\gamma_n^2) + a \quad /47/$$

$$g_{2n}(s) = s + D_{\text{eff}} (\alpha^2 + 2\gamma_n^2) \quad /48/$$

If all inlet quantities disappear, we receive for ϕ :

$$\phi(z) = \int_0^L \{ (-\Delta H_R) h_r(z) G_r(z, \mathcal{L}) + h_p(z) G_p(z, \mathcal{L}) \} \phi(\mathcal{L}) d\mathcal{L} \quad /49/$$

It is possible, to expand $h_{1/2}/z/$ in series of orthogonal cosine functions. Considering the constant term $h_{1/2m}$ of these series, we find as first approximation uncoupled characteristic equations for the various eigenfunctions. For the eigenfunction

number n we get the following algebraical equation:

$$1 - (-\Delta/k) h_{1n} g_n(s) + h_{2n} g_{2n}(s)$$

/50/

If also the high order terms of the series for $h_{1/2}/z/$ are considered, then the characteristic equations of the eigenfunction are coupled between each other.

In a similar way an analysis of stability can be performed for the twophase-model. Because of the fact, that in this case the characteristic equations of the various eigenfunctions are coupled between each other too, the results can only be got numerically by means of a digital computer.

Literature:

- | | | |
|---|-------------------------|---|
| 1 | E.D. Gilles | Neuere Methoden der Prozeßanalyse und Prozeßregelung
Fachseminar Frühjahr 1968 Technische Universität Berlin |
| 2 | E.D. Gilles
M. Zeitz | Modales Simulationsverfahren für Systeme mit örtlich verteilten Parametern
Regelungstechnik 17 /1969/ |

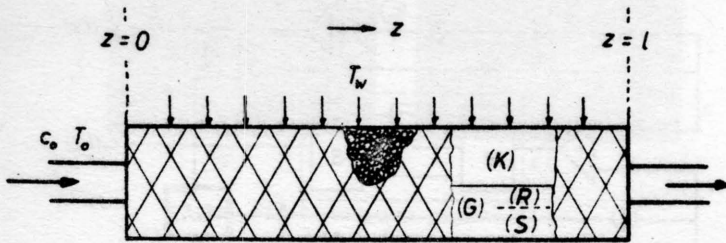
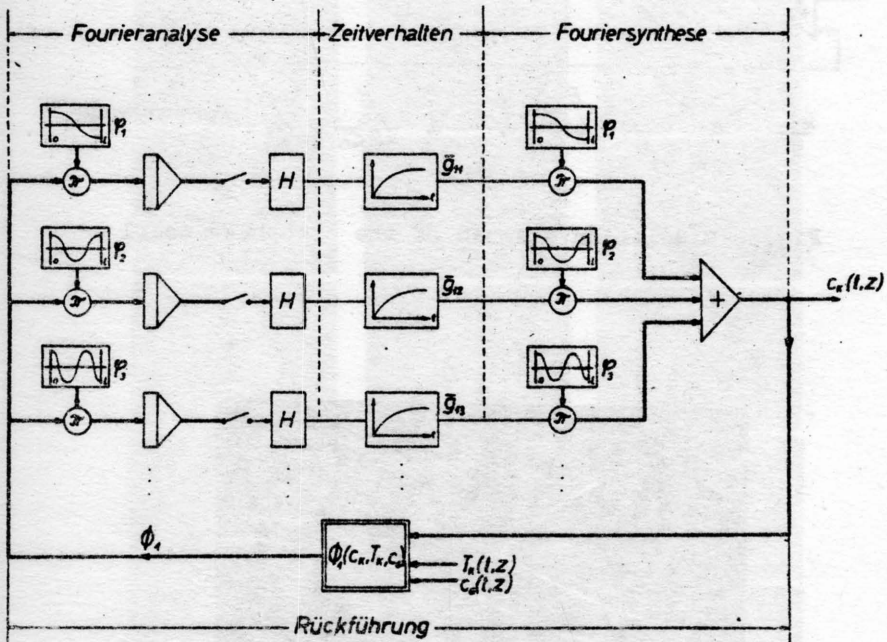


Fig. 1. Fixed-bed tubular reactor

Fig. 2. Model simulation of the function c_K

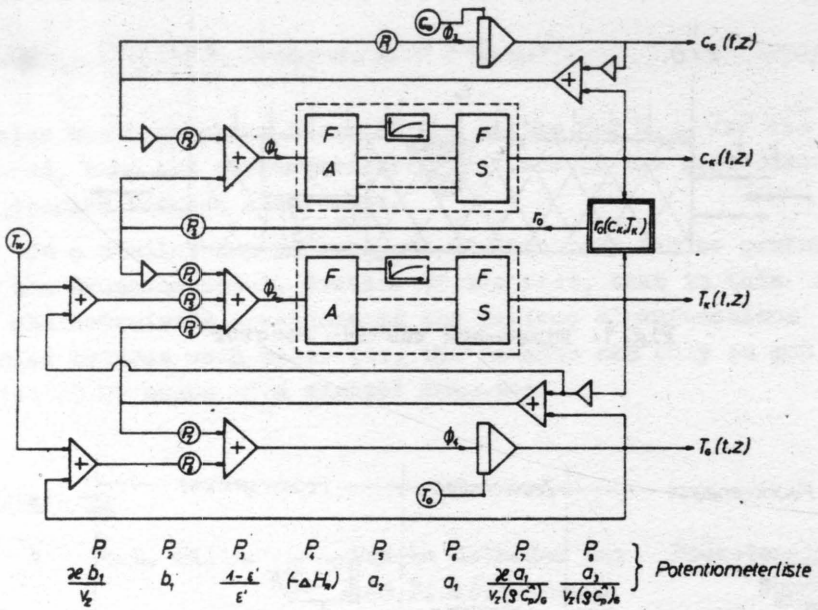


Fig.3. Simulation diagram of the two-phase model

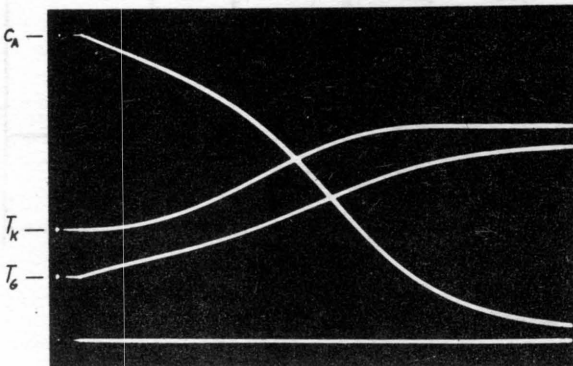


Fig.4. Stationary reaction-profiles

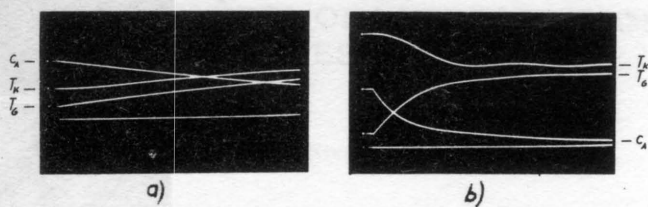


Fig.5. Singular profiles

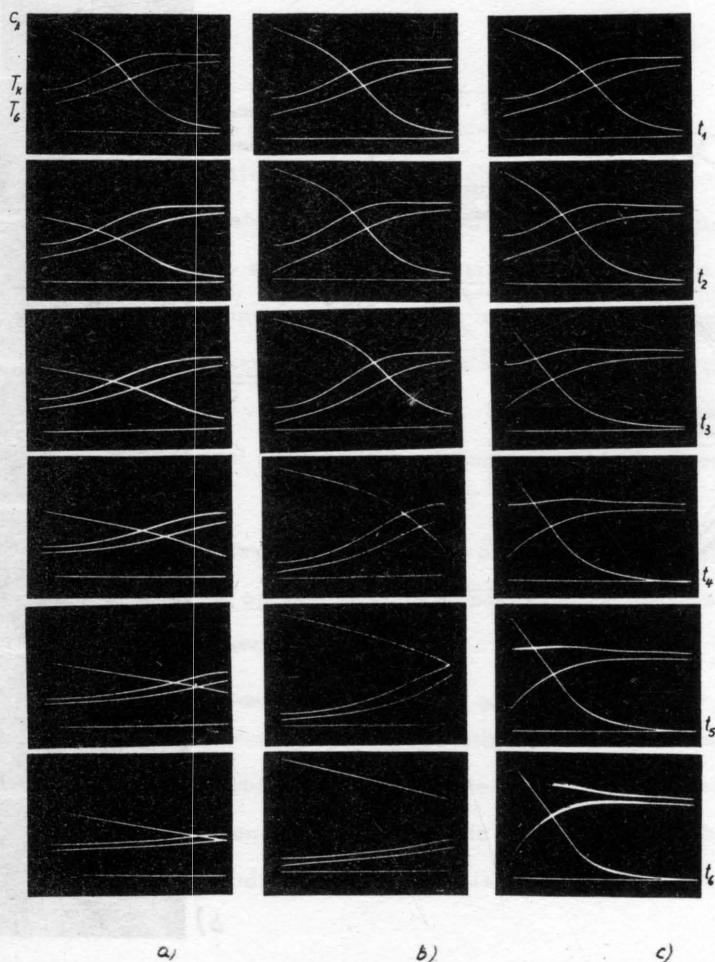


Fig.6. Reaction-profiles

- a/ after jump variation of the inlet concentration
- b/ after jump variation of the inlet-temperature
- c/ by reducing the heat-transfer coefficient a_1

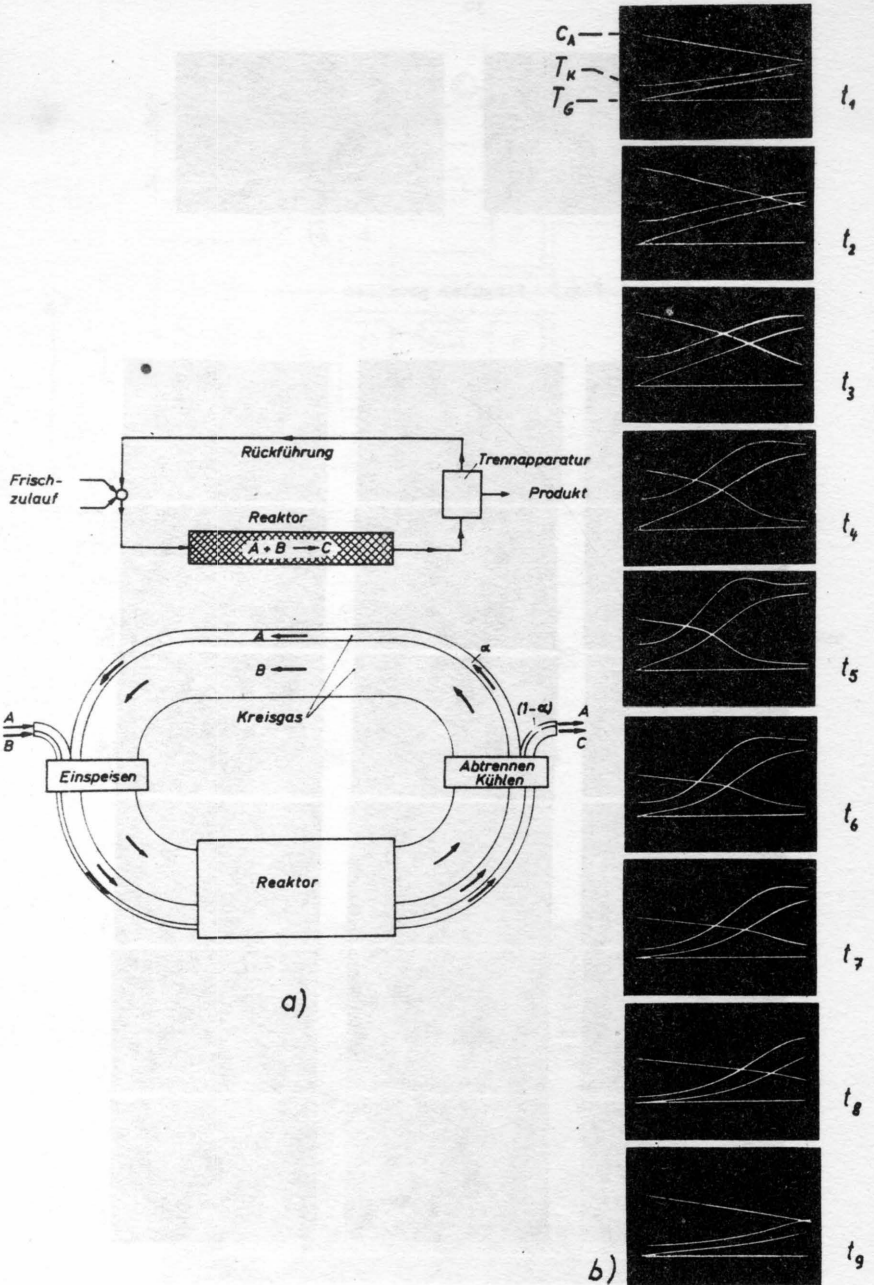


Fig.7. Reactor in recycling process

a/ recycling process and massflow diagram

b/ marginal vibration

OPTIMIZING CONTROL OF HYDROGENATION PROCESS

Keisuke Izawa and Hiroshi Okamoto

Department of Control Engineering

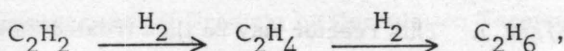
Tokyo Institute of Technology

Meguro-ku, Tokyo, Japan

1. Description of Optimizing Control System

Frequently the best operating conditions for chemical processes are disturbed by some uncontrollable and/or unmeasurable variables such as catalyst activity which varies in somewhat uncertain ways. In such a process, an approach of optimizing control becomes important and the typical objective functions of such chemical process would be the yield of products, the conversion rate, the purity of products, etc. It is the most important problem for optimizing control to locate the maximum point of the objective function.

The pilot equipment of hydrogenation process of acetylene is constructed in order to investigate the optimizing control method (Fig. 1). In the reaction process under the investigation;



the mole fraction of the intermediate product or ethylene is considered as the objective function and is observed to have a maximum point against the flow rate of mixture of acetylene and hydrogen into the reactor, as shown in Fig. 2. The reactor is fluidized bed type and is controlled at a constant temperature.

In optimizing control system it is necessary to perturb the input of the process for finding out the maximum point of the objective function experimentally. In the method here discussed, the gradient of the objective

function is calculated from the input and output data of the reactor and is utilized to complete the feedback loop for optimization. In order to determine the gradient of the objective function, it is usually required to calculate the cross-correlation function of the input and output of the process. Sinusoidal signal or pseudo-random signal is utilized as the input signal.⁽¹⁾ In this paper, M-sequence (Maximum length null sequence) signal is used as the perturbation signal of the inlet flow to the reactor.

The awkward calculation of the gradient of mole fraction or of the objective function is by-passed by the following approximation. In order to calculate the gradient, it is necessary to integrate the impulse response curve or the correlation function during one period of the input signal. And this requires so many memory elements. Since the impulse response of the process to be discussed is not oscillatory and is rather fixed, it may be possible to approximate the magnitude of the gradient by the peak height of the cross correlation function in stead of the peak area. This enables to simplify the whole optimizing control equipments.

2. Mathematical Model of the System

In the process shown by Fig. 1 the mixing ratio of the reactant is chosen as $C_2H_2 : H_2 = 1:8$ and the flow rate of the reactant is so selected that its linear velocity is within 5 to 20 times of the minimum fluidizing velocity of the reactor (0.34cm/sec.). This reactor may be then treated as an ideally stirred system with first order reaction.

Simultaneous differential equations of the ideally stirred first order reaction system shown by Fig.3 are

$$\frac{dn_1}{dt} = z(1 - n_1) - k_1 n_1 \quad (1)$$

$$\frac{dn_2}{dt} = k_1 n_1 - (k_2 + z) n_2 \quad (2)$$

$$\frac{dn_3}{dt} = k_2 n_2 - z n_3 \quad (3)$$

where $\frac{x}{V} = z(\text{min})^{-1}$ is the space velocity, k_1 and k_2 are reaction constants and n_1 , n_2 and n_3 are the concentration (mole per liter) of acetylene, ethylene and ethane respectively. The input and output of the process under investigation are x and n_2 . Assuming the process is always very close to steady state and observing the small deviation of each process variable from the steady state, the transfer function $G_e(s)$ from the small change of x from its steady state \bar{x} to the change of n_2 from its steady state \bar{n}_2 is expressed as⁽²⁾

$$G_e(s) = \frac{k_1(1 - \bar{n}_1) - \bar{n}_2(k_1 + \bar{z}) - \bar{n}_2 s}{(s + \bar{z} + k_1)(s + \bar{z} + k_2)} \quad (4)$$

where $\bar{z} = \frac{\bar{x}}{V}$.

Since the dynamic characteristics of this reaction system is almost fixed and considered as linear and the mole fraction of ethylene has a maximum point against the flow rate of the reactant, this reaction process is characterized by the model of Fig. 4, where the linear dynamic component $G_0(s)$ and the non-linear component $f(\bar{x})$ are connected in series. The latter defines the objective function in this optimizing process. From the equations (1), (2) and (4) the followings are obtained.

$$f(\bar{x}) = \frac{k_1 \bar{z}}{(k_1 + \bar{z})(k_2 + \bar{z})} \quad (5)$$

$$G_0(s) = \frac{(k_1 + \bar{z})(k_2 + \bar{z})}{k_1 k_2 - \bar{z}^2} \cdot \frac{k_1 k_2 - \bar{z}^2 - \bar{z} s}{(s + k_1 + \bar{z})(s + k_2 + \bar{z})} \quad (6)$$

3. Measurement of Gradient by Correlation Technique⁽³⁾

Linearizing the non-linear component $f(\bar{x})$ in the neighbourhood of \bar{x} the transfer function $G(s, \bar{x})$ of the process in Fig. 4 is represented as

$$G(s, \bar{x}) = \left. \frac{\partial f(x)}{\partial x} \right|_{x=\bar{x}} \cdot G_0(s) \quad (7)$$

In addition to the input signal $\bar{x}(t)$ of the process, M-sequence signal $\hat{x}(t)$

is applied as the perturbation signal which has two levels of α and $-\alpha$.

Then the output $y(t)$ of the process is described by the convolution integral:

$$y(t) = \int_0^{\infty} g(\alpha, \bar{x}) \{ \bar{x} + \hat{x}(t - \alpha) \} d\alpha, \quad (8)$$

where $g(t, x)$ is the weighting function of the process at the instant t for the input \bar{x} . Taking cross correlation between $y(t)$ of the equation (8) and an M-sequence signal $x^*(t)$, the value of which is 0 or 1, we obtain

$$\int_0^{\infty} g(\alpha, \bar{x}) \Phi_{x^*x}(\tau - \alpha) d\alpha = \Phi_{x^*y}(\tau) - \Phi_{x^*\bar{y}} \quad (9)$$

$$\text{where} \quad \bar{y} = \int_0^{\infty} g(\alpha, \bar{x}) \bar{x} d\alpha \quad (10)$$

$$\Phi_{x^*x}(\tau) = \frac{1}{N\Delta} \int_0^{N\Delta} x^*(t - \tau) \hat{x}(t) dt \quad (11)$$

$$\Phi_{x^*y}(\tau) = \frac{1}{N\Delta} \int_0^{N\Delta} x^*(t - \tau) y(t) dt \quad (12)$$

$$\text{and} \quad \Phi_{x^*\bar{y}} = \frac{1}{N\Delta} \int_0^{N\Delta} x^*(t - \tau) \bar{y} dt \quad (13)$$

We denote the power spectrum density of $\Phi_{x^*x}(\tau)$, shown in Fig. 5, by $\Phi_{x^*x}(\omega)$.

For very small ω ⁽⁴⁾,

$$\Phi_{x^*x}(\omega) \doteq \Phi_{x^*x}(0) \quad (14)$$

and the latter will be calculated as:

$$\Phi_{x^*x}(0) = \int_0^{N\Delta} \Phi_{x^*x}(\tau) d\tau = \frac{N+1}{2N} \alpha \Delta \quad (15)$$

From equations (9), (14) and (15), the approximate form of $g(\tau, \bar{x})$ is obtained as

$$g(\tau, \bar{x}) \doteq \frac{2N}{(N+1)\alpha\Delta} \{ \Phi_{x^*y}(\tau) - \Phi_{x^*\bar{y}} \} \quad (16)$$

Although it is difficult to separate \bar{y} from y , the estimation of ϕ_{xy} is successfully made as follows. Choosing $N\Delta$ large enough to satisfy equation (17) for such τ' as close to $N\Delta$ but smaller, it is possible to replace $\phi_{x^0\bar{y}}$ by $\phi_{xy}(\tau')$.

$$\phi_{xy}(\tau') \doteq \phi_{x^0\bar{y}} \quad (17)$$

From the equations (16) and (17)

$$g(\tau, \bar{x}) \doteq \frac{2N}{(N+1)\alpha\Delta} \{ \phi_{xy}(\tau) - \phi_{xy}(\tau') \} \quad (18)$$

At steady state the process gain $G(0, \bar{x}) = \frac{\partial f(\bar{x})}{\partial \bar{x}}$ becomes simply as

$$G(0, \bar{x}) = \int_0^\infty g(\tau, \bar{x}) d\tau \quad (19)$$

From the equations (7), (18) and (19), the local slope of the objective function is obtained as follows

$$\begin{aligned} f'(\bar{x}) &= \left. \frac{\partial f(x)}{\partial x} \right|_{x=\bar{x}} = \int_0^\infty g(\tau, \bar{x}) d\tau \\ &= \frac{2N}{(N+1)\alpha\Delta} \int_0^\infty \{ \phi_{xy}(\tau) - \phi_{xy}(\tau') \} d\tau \end{aligned} \quad (20)$$

3-1 Equipment for the Experiment

Fig. 1 shows the equipment for the experiment. The mixture of hydrogen and acetylene at constant ratio ($C_2H_2: H_2 = 1:8$) is fed into a fluidized bed reactor and the small portion of the total inlet flow to the reactor is perturbed by means of a solenoid valve which is controlled by an 'M'-sequence signal. The reactor holds about 8 grams of the catalyst (palladium-coated silica alumina particles with about 150μ of diameter). The temperature of the reactor is kept at about $40^\circ C$.

A small portion of the outlet flow of the reactor is fed with constant flow rate (0.8 cm/sec) into a tube packed with silica gel. This packed

tube acts as a gas chromatograph column. A thermal conductivity detector of hot wire type is attached to the outlet of the packed tube. When the reactor inlet flow is perturbed by M-sequence signal, then the each component of the outlet gas of the reactor has the different retention time or the delay through the packed column.

The value of the cross correlation function between the output signal from the detector and the M-sequence signal at a certain delay time gives a continuous information about the local slope of the yield curve.

3-2 Experiment

Several experimental runs are tried with different values of \bar{x} and \hat{x} (see Fig. 2), using the same M-sequence signal with $\Delta = 1 \text{ min}$ and $N = 31$. Fig. 6 is an example of thus obtained $\Phi_{xy}(\tau)$ and shows the peak of ethylene appears at $\tau = 15\Delta$. This case is almost same as the Run No. 2 in Fig. 2, when the local slope is negative, and so is the peak value of $\Phi_{xy}(\tau)$.

The area under the curve $\Phi_{xy}(\tau)$ for ethylene peak is actually proportional to the local slope of the ethylene yield curve. But it is very awkward to measure the area. The simplified answer to this is as follows:

Instead of ethylene peak area, the peak height is measured. The relationship between the local slope of the yield curve of ethylene against the inlet flow and the peak height is shown in Fig. 7.

Fig. 7 may assure that the peak height would be used as the measure of the local slope.

3-3 Continuous Measurement of Cross-correlation Function

Reconsidering correlation function $\Phi_{xy}(\tau)$ of equation (12), as an example, the integral operation upon t is only possible to x^* and y between $t - N\Delta$

and the present instant t . Thus $\Phi_{x^0 y}(\tau)$ should be rewritten as

$$\Phi_{x^0 y}(\tau, t) = \frac{1}{N\Delta} \int_{t-N\Delta}^t y(\alpha) x^0(\alpha - \tau) d\alpha \quad (21)$$

Considering equation (21), equation (20) is shown as

$$f'(\bar{x}, t) = \frac{2}{(N+1)\Delta^2} \int_0^\infty \left[\int_{t-N\Delta}^t y(\alpha) x^0(\alpha - \tau) d\alpha - \int_{t-N\Delta}^t y(\beta) x^0(\beta - \tau') d\beta \right] d\tau \quad (22)$$

Introducing $y'(t)$:

$$y'(t) = \begin{cases} y(t - N\Delta) & : t \geq N\Delta \\ 0 & : 0 \leq t < N\Delta \end{cases} \quad (23)$$

equation (21) becomes,

$$\Phi_{x^0 y}(\tau, t) = \frac{1}{N\Delta} \int_0^t \{y(\alpha) - y'(\alpha)\} x^0(\alpha - \tau) d\alpha \quad (24)$$

The continuous correlator in Fig. 1 is constructed to obtain $U(t)$ shown by the equation (25).

$$\begin{aligned} U(t) &= \int_0^t w(t) dt \\ &= \int_0^t \{y(t) - y'(t)\} \{x^0(t - \tau) - x^0(t - \tau')\} d\tau \end{aligned} \quad (25)$$

The value of $U(t)$ corresponds to a height of $g(\tau, \bar{x})$ at the instant t . Referring the experimental result of Fig. 7, $U(t)$ may be used as the measure of $f'(\bar{x}, t)$ of equation (22). In equation (25) $x^0(t - \tau) - x^0(t - \tau')$ is the 3-level signal (+1, 0 and -1), and $y'(t)$ can easily be obtained by some delay element such as a tape recorder.

From the result shown in Fig. 6, $\tau = 15\Delta$ and $\tau' = 13\Delta$ are used in equation (25).

Fig. 8-(a) and (b) show experimental results of thus obtained continuous cross-correlation for 2 cases of Run No.1 and Run No. 2 of Fig. 2 respectively.

From the Fig. 8-(a) and (b), it is observed that the signal $U(t)$ is completed after elapsing $N \Delta$ or the one period of the M -sequence input signal and thereafter $U(t)$ changes very little if the process is at the steady state showing a fixed value of $f(\bar{x}, \tau)$. The output of the correlator $U(t)$ is positive and negative for the Run No. 1 and Run No. 2 respectively. The signal $U(t)$ is used as an actuating signal for corrective action of \bar{x} .

4 Conclusion

In optimizing control system, it is the most important problem to measure the gradient or the slope of the objective function. This paper proposes an approximate method of optimization based upon correlation technique.

Experimental results with a pilot equipment of hydrogenation of acetylene assure that the output of the here proposed correlator can be used as an effective estimating device of the gradient of the objective function for optimizing control.

Acknowledgement

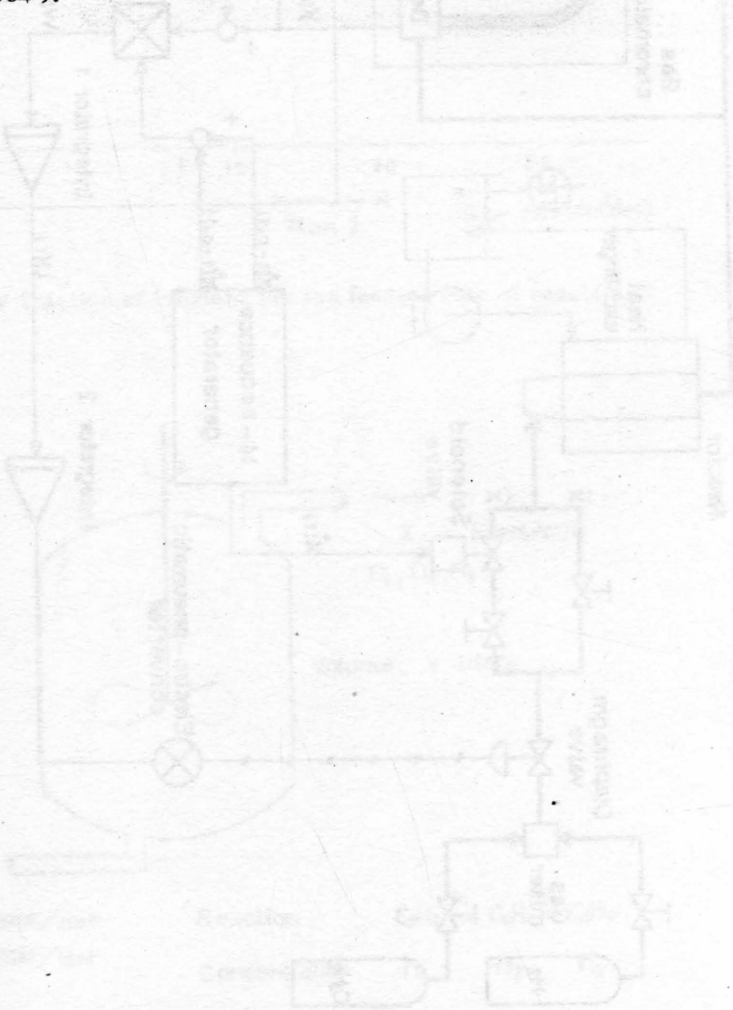
The authors appreciate the help of Kazuhisa Takeuchi and Akira Nakajima for constructing the here proposed correlator and thank Toshiji Hirose for fundamental experiments which suggests the theoretical model.

References

- (1) Van der Grinten, P.M.E.M, "The Application of Random Test Signals in Process Optimization" , Proc. 2nd Congress IFAC(Basle) Theory, 551-555, (1963).
- (2) Box, G.E.P. and J. Chanmugam, "Adaptive Optimization of Contin-

uous Processes" , I & EC Fund. Vol. 1, No. 1, 2-16, (1962).

- (3) Ohchi, S, Furuta, K and Izawa, K, "Optimizing Control Using M-sequences" , Trans. Soc. Instrument and Control Engineers, Vol.2, No. 4, 276-282, (1966).
- (4) Izawa, K and Furuta, K, "A Method of Determining Process Dynamics" , Proc. Instrument and Measurement on Auto. Cont. (Stockholm), 7-18, (1964).



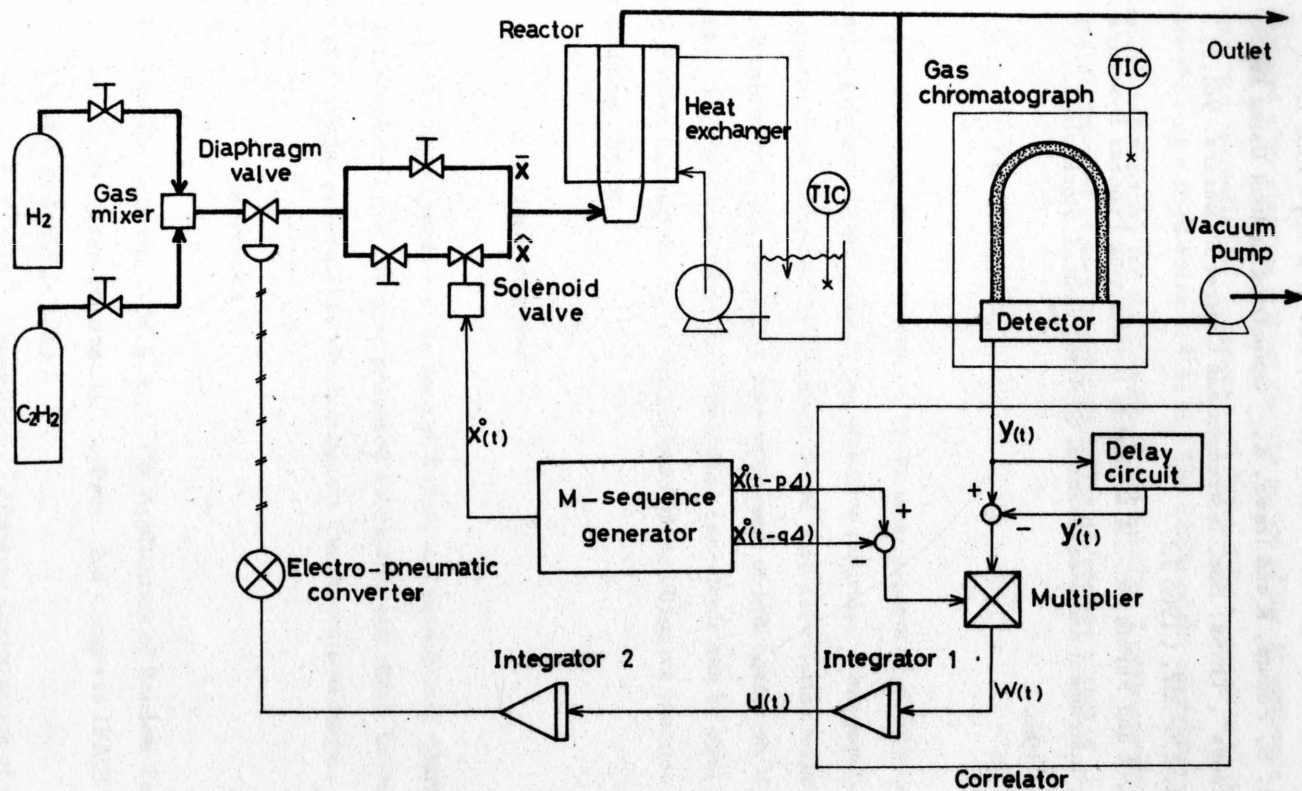


Fig. 1. Schematic diagram of optimizing control system.

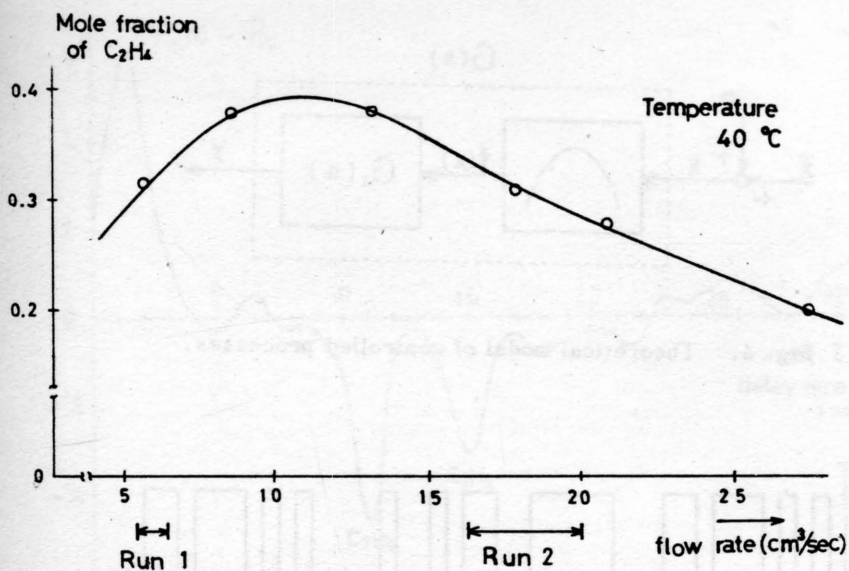


Fig. 2. Mole fraction of ethylene versus feeding rate of reactant.

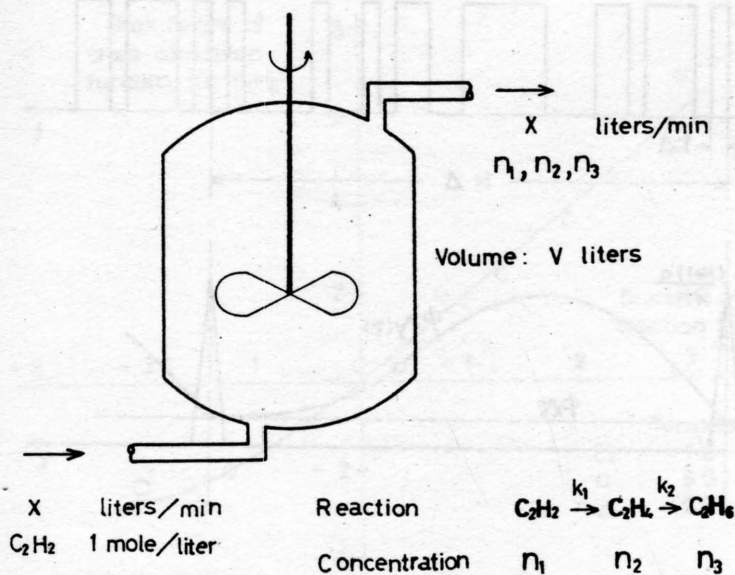


Fig. 3. Ideally stirred continuous flow reactor.

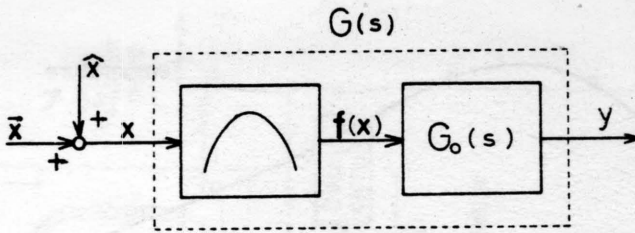


Fig. 4. Theoretical model of controlled processes.

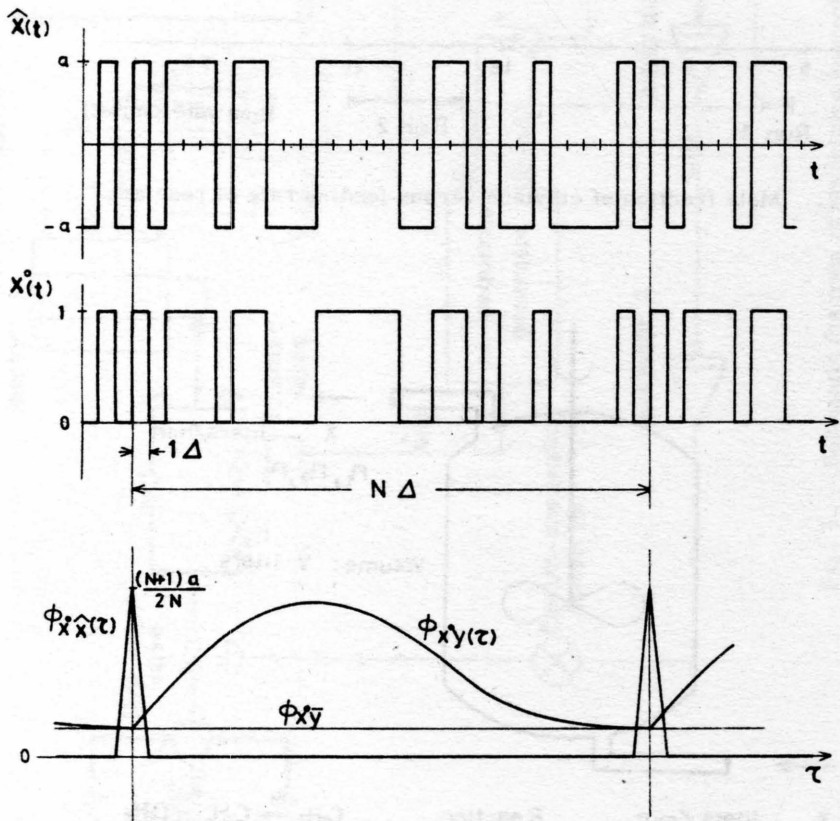


Fig. 5. M-sequence signals and correlation functions.

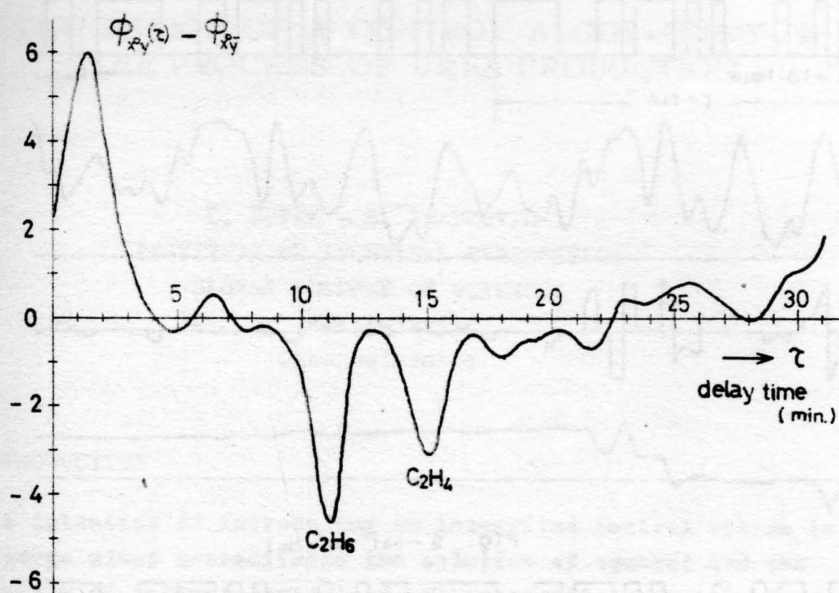


Fig. 6. An example of cross-correlation function between delayed M-sequence signal and output signal of the process.

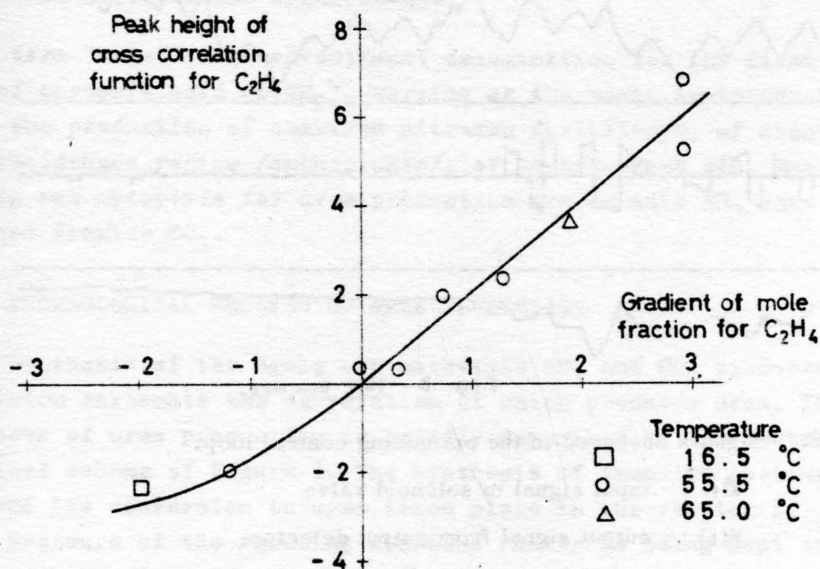


Fig. 7. Peak height of cross-correlation function versus gradient of mole fraction for ethylene.

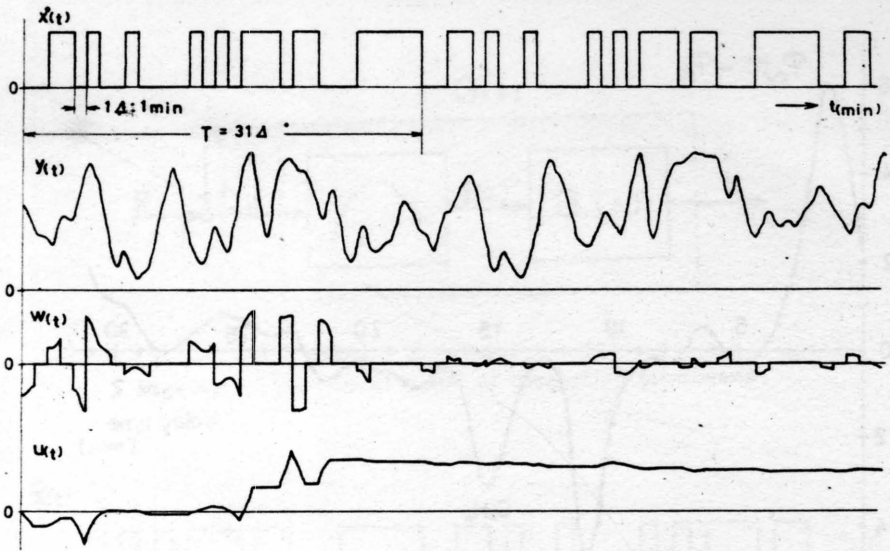


Fig. 8 - (a) Run No 1

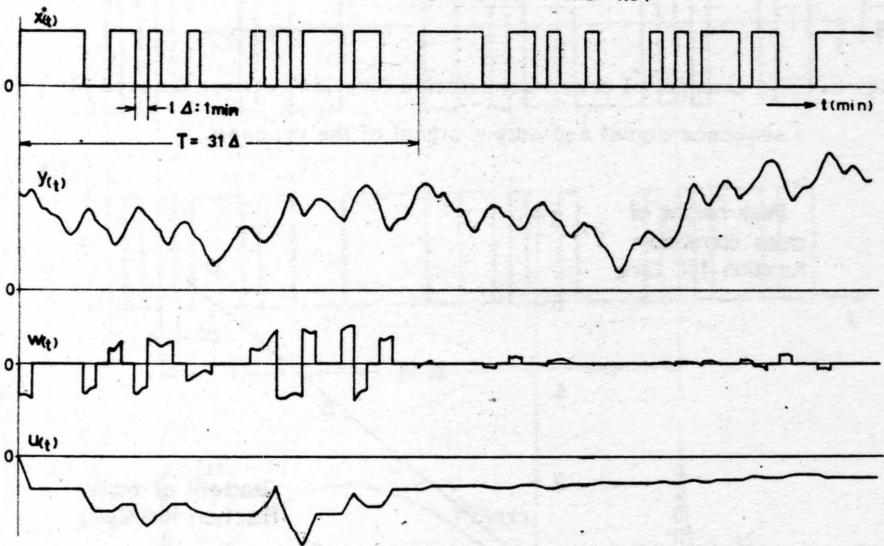


Fig. 8 - (b) Run No 2

Fig. 8. Signals observed in the optimizing control loop.

$x(t)$: input signal to solenoid valve

$y(t)$: output signal from output detector

$w(t)$: input to integrator 1

$u(t)$: output of integrator 1 (approximately proportional to the gradient of mole fraction of ethylene).

THE DESIGN OF A CONTROL ALGORITHM FOR THE PROCESS OF UREA PRODUCTION

L. ŠUTEK - B. FRANKOVIČ
INSTITUTE OF TECHNICAL CYBERNETICS
SLOVAK ACADEMY OF SCIENCES
Bratislava
Czechoslovakia

INTRODUCTION

The intention of introducing an integrated control system in a large plant necessitated the solution of control and the problem of optimal control of all important production processes and production lines. In the plant the production of granulated urea figures among the production processes of paramount importance because of the amount of the manufactured product and its economic significance.

The term "urea" is a conventional denomination for the diamide of carbonic acid $\text{CO}(\text{NH}_2)_2$ serving as the basic semiproduct for the production of combined nitrogen fertilizers, of urea-formaldehyde resins /aminoplasts/, of barbiturates etc. The basic raw materials for urea production are ammonia NH_3 and carbon dioxide CO_2 .

THE TECHNOLOGICAL PROCESS OF UREA PRODUCTION

The synthesis of the basic raw materials NH_3 and CO_2 produces ammonium carbamate the dehydration of which produces urea. The process of urea production is briefly described in the technological scheme of Figure 1. The synthesis of ammonium carbamate and its conversion to urea takes place in the reactor 1. The pressure of the reacting compound /melt/ is being kept at a constant value of approximately 200 atp by a reduction valve 2. Through an expansion behind the reduction valve /pressure 20 atp./ a part of ammonia is released from the reacting com-

pound and the unconverted carbamate, thus lowering the temperature of the compound. A further release of ammonia occurs in the decomposing exchanger 3, heated by steam where the decomposition of the larger part of the carbamate takes place. The mixture of the gaseous phase /ammonia, carbon dioxide, steam/ is separated from the liquid phase in separator 4, from where it is led into the absorption column 5 for absorbing the carbon dioxide in a solution of ammonia. The influx of the ammonia solution comes from the ammonia condenser 6 in which it is developed from gaseous ammonia, steam and added vapour condensates. The inert gases with a certain content of gaseous NH_3 are being let through by a pressure control device into the pipeline of terminal gases. The recycling solution generated in the absorption column is being batched into the reactor by pumps 7. In the second phase of the expansion /valve 8/ the decomposition is finished /decomposing exchanger 9/ and in separator 10 the separated urea flows into the supply tank while the gases flow off either directly into the terminal gas pipelines or into the combined absorbing condenser under condensate addition. The solution obtained therein is being pumped after degasification into absorption column 5 thus completing the system of total recycling.

The first stage of urea thickening is being carried out in fully automated vacuum evaporators 11. A very high stage of thickening is attained in the surface evaporating device LUWA 12 through evaporation under atmospheric pressure. A high rate of urea thickening is a condition of successful urea granulation in the granulating tower 13. A slow surface thickening or granulation allow for the decomposition of urea thus lowering its concentration in the resulting product. It is not advantageous to increase the speed of evaporation by raising the heat level over 140° since this involves an intense development of biuret - an undesired component.

THE CONCEPTION OF UREA PRODUCTION CONTROL

From the viewpoint of controlling the urea production process it is interesting to observe that part of the process in which

the synthesis of urea takes place, i.e. the reactor with the decomposing exchangers and with the circuits producing the recycling solutions. This part of the process inclined to be unstable especially under the influence of setting up the partial or total cycling course. The feature of these instabilities is an integrated one, frequently accompanied by unpleasant consequences. The breakdown, for instance, inflicted by lowering the absorption efficiency of the absorption column can create a situation that the amount of carbon dioxide entrained into the ammonia condenser 6, increases, thus developing ammonium carbamate within the condenser, that is insoluble in water. It begins to settle down in the pipes of the condenser, the passage of heat deteriorates and the temperature in the condenser grows. A disadvantageous consequence of the heat increase in the condenser is the lowering of the ammonia concentration and a decrease of inlet to the absorption column. This fact entails a further decrease of the column's absorption capacity, enlarges losses by virtue of a larger quantity of gaseous NH_3 leakage into the pipes of terminal gases. The insoluble carbamate settles down on the pipes and fittings and clogs them.

By batching the recycled solution and by supplying the raw materials NH_3 and CO_2 , the molar ratio between $\text{NH}_3 : \text{CO}_2 : \text{H}_2\text{O}$ should be preserved equal 4:1:1,1, corresponding to a 60 % conversion of ammonium carbamate to urea. An increase of water ratio, i.e. due to a change of concentration of the recycled solution and its batching, the conversion rate in the reactor decreases, thus detrimentally affecting the procedure. This can result in a smaller concentration of urea in the melt, in a larger quantity of free NH_3 , CO_2 and H_2O in the gaseous phase, a higher load on the absorption column and the NH_3 condenser etc. The productivity of the equipment is thus lowered and a simultaneous increase of losses of raw materials cuts the output, thus directly affecting the entire economics of the process.

The total solution of the control and stabilization problem of the process is a condition for the successful application of

steady-state optimal control systems. Its realization is subject to the utilization of a special processor supplying the algorithm of optimal control, using the mathematical model that controls the quantities of the process by means of setting up the desired values of the relevant regulators.

THE CHOICE OF CONTROL VARIABLES

It is obvious from the technological scheme that the process of urea synthesis is influenced by the following variables:

- a/ flow rate, concentration and temperature of NH_3
- b/ flow rate, concentration of CO_2
- c/ flow rate of the vapour condensate into condenser of NH_3
- d/ temperature in NH_3 condenser.

The temperatures and concentrations of NH_3 and CO_2 practically do not alter, the temperature of the vapour condensate cannot be influenced and the flow rate of NH_3 and CO_2 is in accordance with the molar ratio most advantageous for the process of the synthesis part in the reactor. This molar ratio is detrimentally affected by the change in volume and concentration /contents of H_2O / in the recycling process. The volume and concentration of the recycling course can be controlled by the flow rate of the vapour condensate and by the temperature of condensate NH_3 i.e. by the temperature of the outflowing cooling water. It follows from the abovesaid that from the viewpoint of the optimum control of the urea production process the flow rate of the vapour condensate and the temperature of the cooling water are to be taken into account as the control variables. The flow rate of NH_3 and CO_2 is controlled in a way to preserve to molar ratio of $\text{NH}_3:\text{CO}_2:\text{H}_2\text{O}$ for the most advantageous conversion.

The control scheme for urea synthesis according to the given conception is in Fig. 2.

THE MODEL OF THE PROCESS OF UREA SYNTHESIS

The technological process of urea production can be divided from the point of view of simulation into three parts, namely

the process of urea synthesis, thickening and granulation. There are known linkages between these three parts so that they can be investigated independently.

A complete linear statical and dynamical model of the urea production process was set up on the basis of the analysis of the physical and chemical substance of the processes taking place in the various devices of the manufacturing equipment. It is obvious that the processes /reaction, absorption, condensation/ are nonlinear ones so that the derived linear model holds only for small deviations from stationary equilibrium states.

The block scheme of urea synthesis with partial recycling is shown in Fig. 3. $Y_1 \dots Y_6$ and $X_1 \dots X_6$ are column vectors of input and output quantities of the urea synthesis. The entire mathematical model of the synthesis part is thus determined by six matrix equations that determine the dependencies of the output quantity vectors on the input quantity vectors.

By determining the elements of the transfer matrices /the RE-reactor, the RV-decomposing exchanger, the SV-high pressure separator, AK-absorption column, KC-ammonia condenser, CW-recycling pumps, RN-low pressure decomposing exchanger and SN-low pressure separator/, and by substituting them into the matrix equations valid for the scheme according to Fig. 3, we obtain the concrete mathematical model of urea synthesis. It is advantageous to work with separated transfer matrices. The matrix equations are then set up according to the modified scheme in Fig. 4.

For the output vectors of the Laplace transformations of relative changes of transflux φ , temperature \mathcal{V} , concentrations $\mathcal{X}_1, \mathcal{X}_2, \mathcal{X}_3$, inert gases \bar{x}_2 , water flowing out of the condenser \bar{x}_3 , recycling \bar{v}_4 ,

$$\bar{x}_2 = \begin{bmatrix} \varphi_i \\ \mathcal{V}_i \\ \mathcal{X}_{1i} \\ \mathcal{X}_{2i} \end{bmatrix} ; \quad \bar{x}_3 = \mathcal{V}_{v2} ; \quad \bar{v}_4 = \begin{bmatrix} \varphi_r \\ \mathcal{V}_r \\ \mathcal{X}_{1r} \\ \mathcal{X}_{2r} \end{bmatrix}$$

in dependence on the vectors of relative changes of the cooling water \bar{y}_2 , the vapour condensate \bar{y}_3 , the gases entering the absorption column \bar{u}_2 and the output and revolution of the pump \bar{y}_6

$$\bar{y}_2 = \begin{bmatrix} \varphi_v \\ \nu_v \end{bmatrix}; \quad \bar{y}_3 = \begin{bmatrix} \varphi_k \\ \nu_k \\ \kappa_{1k} \end{bmatrix}; \quad \bar{u}_2 = \begin{bmatrix} \varphi_p \\ \nu_p \\ \kappa_{1p} \\ \kappa_{2p} \end{bmatrix}; \quad \bar{y}_6 = \begin{bmatrix} \nu_{c1} \\ \omega_{o1} \end{bmatrix}$$

the following equations are obtained

$$\bar{x}_2 = [AK1 \cdot KC1 \cdot KC6 \cdot B^{-1} + KC4] \bar{y}_2 + [AK1 \cdot KC1 \cdot KC9 \cdot B^{-1} + KC7] \bar{y}_3 + AK2 \cdot KC1 \cdot B^{-1} \bar{u}_2 \quad (1)$$

$$\bar{x}_3 = [AK1 \cdot KC2 \cdot KC6 \cdot B^{-1} + KC5] \bar{y}_2 + [AK1 \cdot KC2 \cdot KC9 \cdot B^{-1} + KC8] \bar{y}_3 + AK2 \cdot KC2 \cdot B^{-1} \bar{u}_2 \quad (2)$$

$$\bar{v}_4 = AK3 \cdot CW1 \cdot KC6 \cdot B^{-1} \bar{y}_2 + AK3 \cdot CW1 \cdot KC9 \cdot B^{-1} \bar{y}_3 + [AK3 \cdot KC3 \cdot AK2 \cdot B^{-1} + AK4] \bar{u}_2 + CW2 \bar{y}_6 \quad (3)$$

For the remaining circuit of urea synthesis the equation

$$\bar{u}_2 = SV2 \cdot RV2 \bar{y}_4 + SV2 \cdot RV1 \cdot RE \bar{y}_1 + SV2 \cdot RV1 \cdot RE \bar{v}_4 \quad (4)$$

is obtained, further for \bar{x}_4 , \bar{x}_5 , \bar{x}_6 , and the equation for the relative changes of the output product \bar{x}_1 /solution of urea/

$$\begin{aligned} \bar{x}_1 = & Z_1 [I - D_1 + DB_1 + B] [I - D_1]^{-1} \bar{y}_1 + Z_1 D \cdot KC6 \cdot \bar{y}_2 + \\ & + Z_1 D \cdot KC9 \cdot \bar{y}_3 + \{Z_2 + Z_1 [DB_3 + B_4] [I - D_1]^{-1}\} \bar{y}_4 + \\ & + SN1 \cdot RN2 \bar{y}_5 + Z_1 [I - D_1]^{-1} \bar{y}_6 \end{aligned} \quad (5)$$

in which the vectors of relative changes of urea \bar{x}_1 , heated steam \bar{y}_4 and \bar{y}_5 and input raw materials \bar{y}_1 are

$$\bar{x}_1 = \begin{bmatrix} \varphi_m \\ \psi_m \\ \chi_m \end{bmatrix}, \quad \bar{y}_1 = \begin{bmatrix} \varphi_{NH_3} \\ \psi_{NH_3} \\ \chi_{NH_3} \\ \varphi_{CH_2} \\ \psi_{CO_2} \\ \chi_{CO_2} \end{bmatrix}, \quad \bar{y}_4 = \begin{bmatrix} \varphi_{pv} \\ \psi_{pv} \\ \pi_{pv} \end{bmatrix}, \quad \bar{y}_5 = \begin{bmatrix} \varphi_{pn} \\ \psi_{pn} \\ \pi_{pn} \end{bmatrix}$$

and matrices

$$D = AK3 \cdot CW1 [1 - AK1 \cdot KC3]^{-1}; \quad D_1 = D \cdot B_3 \cdot RE - B_2;$$

$$B = 1 - AK1 \cdot KC3;$$

$$B_1 = SV2 \cdot RV1 \cdot RE \cdot 1 \cdot KC3 \cdot AK2;$$

$$B_2 = SV2 \cdot RV1 \cdot RE \cdot CW1 \cdot AK4; \quad B_3 = RV2 \cdot SV2 \cdot KC3 \cdot AK2;$$

$$B_4 = RV2 \cdot SV2 \cdot AK4 \cdot CW1;$$

$$Z_1 = SN1 \cdot RN1 \cdot SV1 \cdot RV1 \cdot RE; \quad Z_2 = SN1 \cdot RN1 \cdot SV1 \cdot RV2$$

The matrix equation (6) is the most essential because it indicates the dependence of the parameter of the manufactured urea on the input quantities. The elements of transfer matrices, i.e. the transference of the separate quantities, were derived in the usual way, for some devices under simplified conditions /e.g. for the condenser of NH_3 /.

In deriving the statical model the dynamical model, already derived, was used as the basis considering the nonlinear properties of the process in the reactor, in the absorption column etc. The model thus derived appeared to be rather sophisticated /also for verification in practice/ and it was necessary to simplify it.

THE CHOICE OF THE PURPOSE FUNCTION AND THE OPTIMIZATION PROCESS

In choosing the purpose function the requirements of the plant and prevailing conditions of operation were taken into account. Two alternatives were considered:

- 1/ To control the process under most advantageous economic conditions;

2/ To control the process from the viewpoint of maximal production from the given raw material adhering to the prescribed quality.

In the first case the purpose function will be the following:

$$Q_1 = a_1 \nu_1 G_M + a_2 \nu_2 G_P - a_3 \nu_3 G_{NH_3} - a_4 \nu_4 G_{CO_2} - a_5 W - R \quad (6)$$

with constraints on G_{NH_3} , G_{CO_2} and temperature T , where

a_j ; $j=1, \dots, 5$ is the price of the unity volume of material and energy

ν_r ; $r=1, \dots, 4$ are quality coefficients

W energy consumption

R steady costs of the process.

The other quantities are obvious from Fig. 2.

In the second case the purpose function is

$$Q_2 = \frac{G_M}{\sum G_{NH_3} + G_{CO_2}} \quad (7)$$

with constraints on G_{NH_3} , G_{CO_2} and T and required quality

$$0.95 \leq \nu_1 \leq 1.0$$

Both in the first and second case it is necessary to satisfy the basic requirement of the most advantageous molar ratio in the reactor, $NH_3 : CO_2 : H_2O = 4:1:1.1$ gained on the basis of many experiments.

The quantities occurring in the purpose functions can be expressed by means of quantities put into the computer. Hence Q is expressed thus

$$Q = f(C, G_{Br}, C_{Br}, G_R, C_R, T_{Ch}, G_1, T_1, G_2, T_2, G_M, C_M, G_P, C_P) \quad (8)$$

where C - molar ratio as the dependence of flow rate NH_3 and CO_2 .

Constraints are the same as in the previous cases.

It follows, however, from the preceding considerations that

$$G_R = f(G_{Br}, C_{Br}, T_{Ch}) ; \quad C_R = f(G_{Br}, C_{Br}) \quad (9)$$

By substituting 9 into 8 we obtain Q as the function

$$Q = f(C, G_{Br}, C_{Br}, T_{Ch}, G_1, T_1, G_2, T_2, G_M, C_M, G_p, C_p) \quad (10)$$

If the derivatives of this function according to the control variables are put equal to zero, i.e.

$$\frac{\partial Q}{\partial G_{Br}} = 0 ; \quad \frac{\partial Q}{\partial T_{Ch}} = 0 \quad (11)$$

we obtain the so called optimizing equations, from which the optimal values of the control variables $G_{Br \text{ opt}}$ and $T_{Ch \text{ opt}}$ are calculated. The optimal G_{NH_3} and G_{CO_2} are then determined according to the amount and composition of the recycling on the basis of the required molar ratio for the most advantageous conversion.

The scheme of the optimal control of urea production is in Fig. 2 and Fig. 5 shows the course of logical functions carried out by the processor.

CONCLUSION

The suggested control system of urea synthesis along with the optimization algorithm was experimentally verified on the hybrid computer. Various modes of operation were simulated on the basis of quantity values taken directly from the production process. By the application of the optimization algorithm the optimal mode was found for criteria according to equations (6) and (7). The results attained from the solution on the hybrid computer were re-applied in operation to compare the feasibility of the suggested optimal control system with the present state.

The results of these experiments prove that the suggested sys-

tem of control meets the conditions of adhering to the most advantageous conversion in the reactor both as to the economic effect and to that of yield. They have also shown that a more essential effect could be achieved by surmounting certain limitations /mainly that of C_{NH_3} concentration in recycling/ this must be low with regard to the function of pumps of the applied design.

The optimal control of this process requires a small, relatively simple /cheap/ processor to secure the rentability of introducing the optimal control of this process /which is technologically not most suitably arranged - a prototype equipment/.

More detailed data are not given, they are the property of the enterprise.

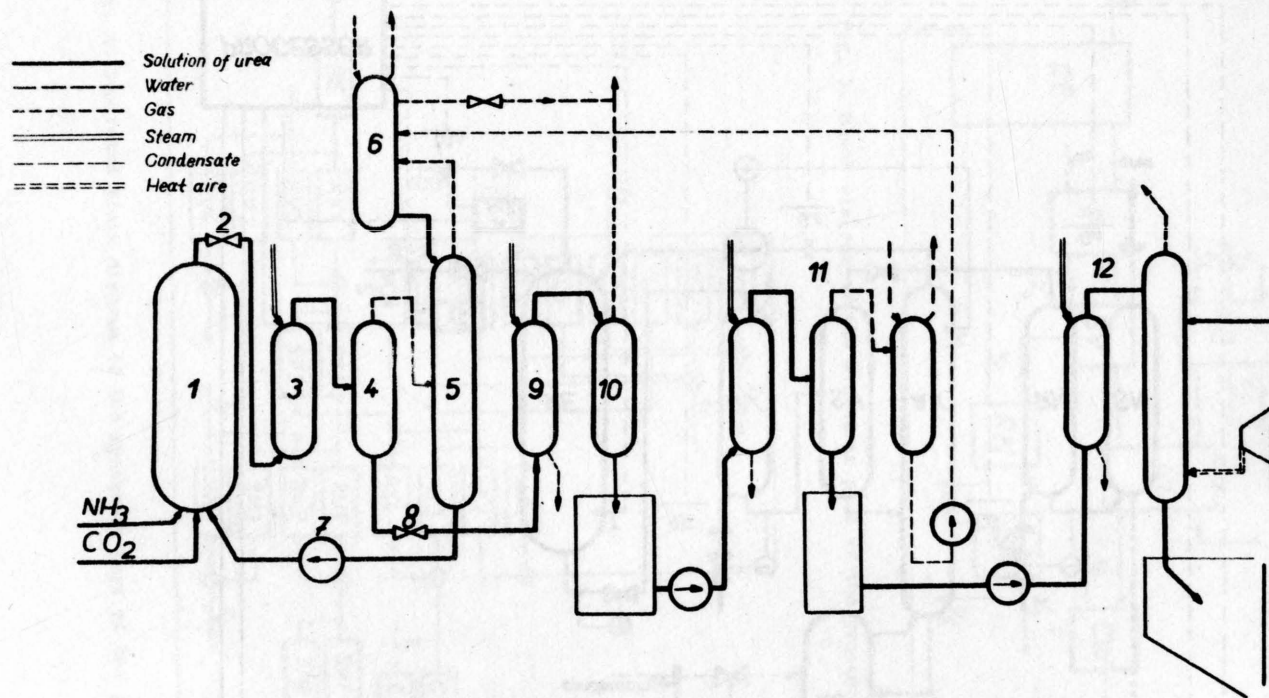


Fig. 1. Technological diagram of the urea production process

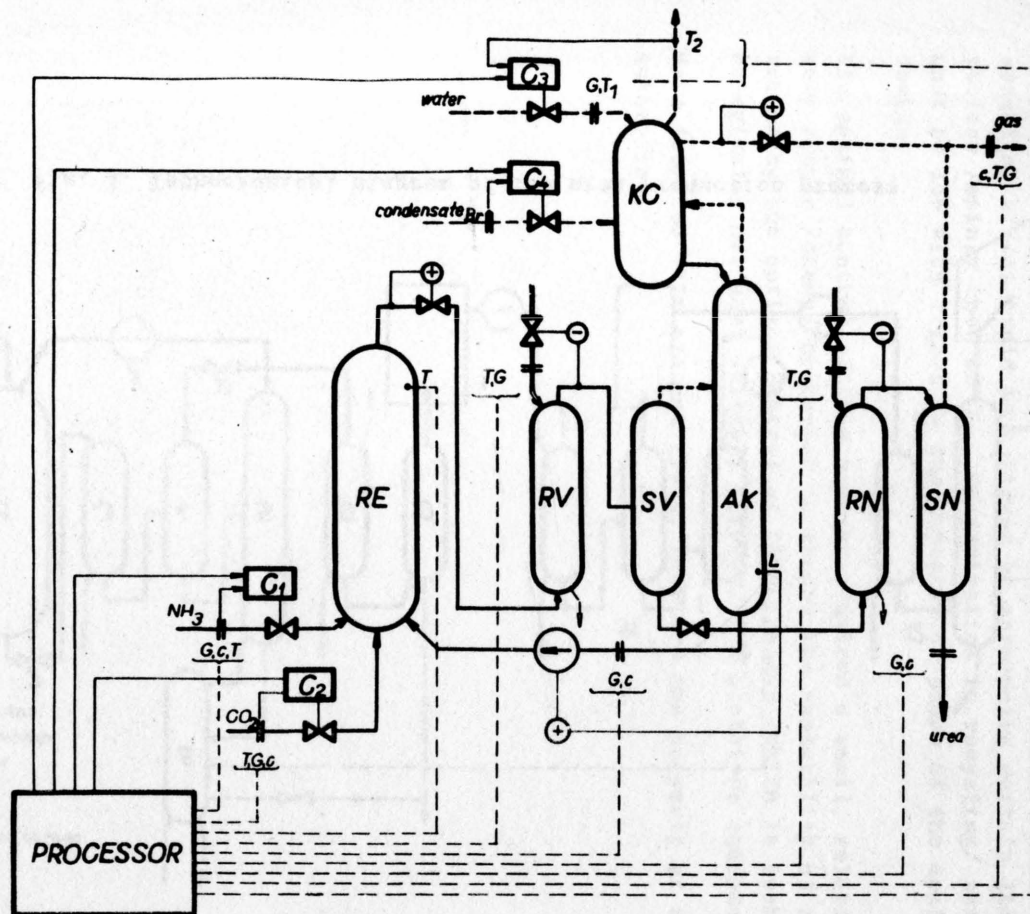


Fig. 2. Block diagram of the control process

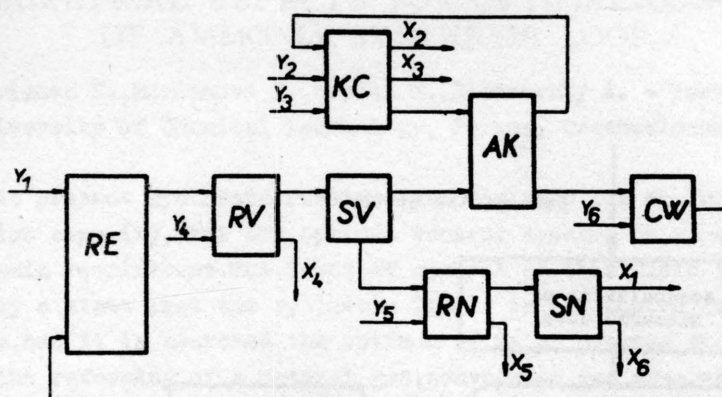


Fig. 3. Block diagram of the synthesis part of the process

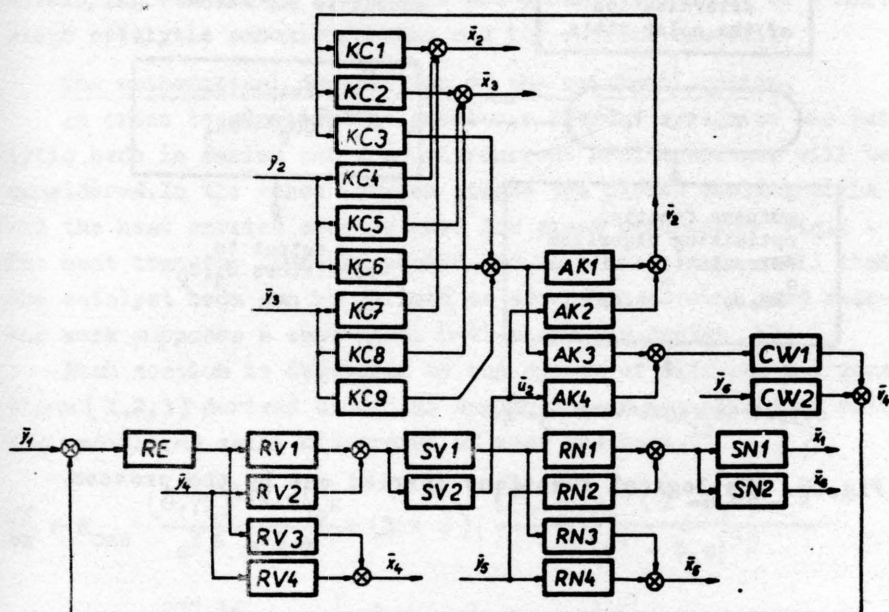


Fig. 4. Separated block diagram of the synthesis part of the process

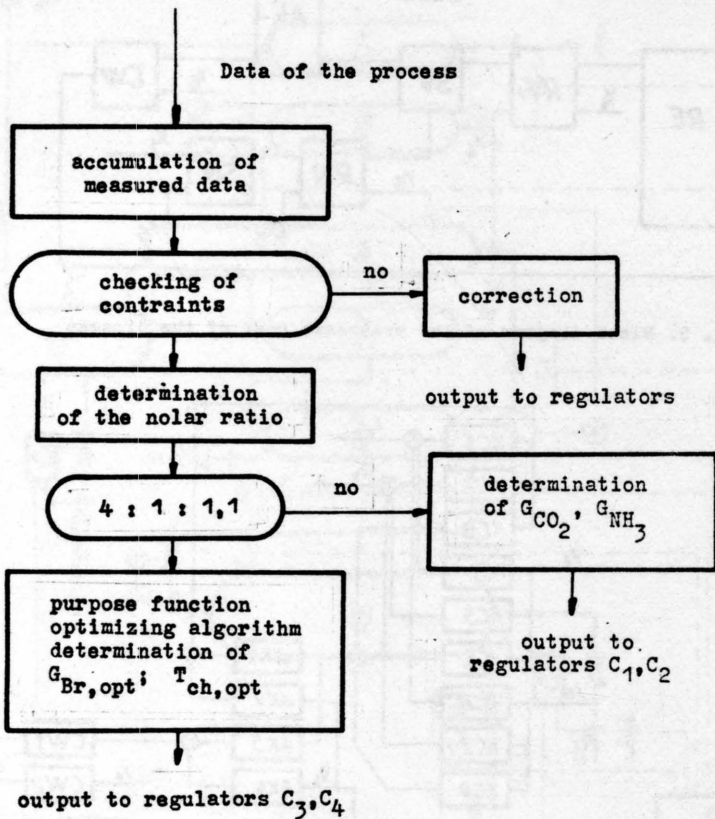


Fig. 5. The logical functions carried out by the process

THEORETICAL ASPECTS FOR OPTIMAL CONTROL OF AMMONIA SYNTHESIS LOOP

Burianec Z., Burianová J., Hruška M., Sichrovský A. - Technical University of Chemical technology, Prague, Czechoslovakia.

At present synthesis reactors are designed for so large production capacity, that the optimal control appears as a necessary economic requirement. The level of control in this field is defined by a state that the synthesis itself is not controlled at optimum, but it is searched the optimum of major process steps including the reforming of a natural gas, conversion, gas absorption, compression and the synthesis². The optimal computer control of a synthesis reactor only is the object of theoretical considerations¹⁴. The purpose of this paper is to show the possibility of developing a model of the static and dynamic behaviour of a multi-stage catalytic ammonia reactor and its optimal control.

The mathematical description of the catalyst section.

In order to simplify the problem, a reactor system of two catalytic beds in series and a countercurrent heat exchanger will be considered. In the space between stages are placed cooling coils and the heat carried away is used for steam production Fig.1. The heat transfer from the packed bed to a wall is so small that the catalyst beds can be defined as adiabatic ones. A good reactor work supposes a convenient heat-exchanger design E2.

Each section is described by the system of differential equations (1,2,3) derived under the assumption of gas plug flow without radial and axial dispersion of mass and heat.¹²

$$\frac{df}{dz} = K_{act} \frac{(0,75)^{1,5} 290k}{a^{3\beta} p^{\beta} G} (1+z) \frac{L^2(1-b_1z)^3(1-b_2z) - z^2}{z^{2\alpha}(1-b_1z)^{3\beta}} \quad (1)$$

$$k = k_{450} \cdot \frac{273,16}{T} \cdot \exp \left[\frac{A}{R} \left(-\frac{1}{273,16} - \frac{1}{T} \right) \right]$$

where τ, λ, L^2 are complex functions of composition, mass velocity, temperature and pressure.

$$\frac{dT}{dz} = \tau \frac{df}{dz} - \lambda_1(T - T_s) \quad (2)$$

$$\frac{dT}{dx} = -\lambda_2(T - T_s) \quad (3)$$

This system of equations (1,2,3) must be solved numerically where the initial conditions have to be evaluated iteratively.

This reactor model can be used for on-line optimisation calculations but its mathematical complexity presents formidable difficulties from the point of view of a computer time.

There are two methods of simplifying this problem. The first one is to modify the system of differential equations (1,2,3) in a simpler form (Model type I), the other one is to use a multiple stepwise regression technique on the simulation results to yield algebraic expressions (Model type II) from the differential equations (1,2,3).

Approximative steady-state model type I.

The general-purpose applicability of this mode of formulation has some advantages. Further, the limiting conditions appear as a result of the numerical solution. The simplification can be attained by substitution of $\tau(z, T, P)$ and $\lambda(z, T, P, G)$ by their mean values $\bar{\tau}, \bar{\lambda}$ corresponding to a defined working range. This can be carried out by using algebraic regression expressions of physical and chemical variables (C_p , viscosity, heat conductivity) as a function of temperature, pressure and composition³.

Further, more significant simplification can be attained by substitution of a complicated mathematical form on the right-hand side of the equation (1) by means of an empirical formula³

$$\begin{aligned} \frac{df}{dx} = & K_{00} + K_{01} \cdot T + K_{02} \cdot T^2 + K_{03} \cdot T^3 + (K_{10} + K_{11} \cdot T + K_{12} \cdot T^2 + \\ & + K_{13} \cdot T^3) f + (K_{20} + K_{21} \cdot T + K_{22} \cdot T^2 + K_{23} \cdot T^3) f^2 \end{aligned} \quad (4)$$

This formula (4) can be employed only in a limited and defined range of temperature and conversion.

The profiles of temperature and ammonia mole fraction z within the catalyst section computed on the principle of above-mentioned approximation, coincide with the profiles obtained from the solution of the system of equations (1,2,3). The error is not greater than $+3^\circ\text{C}$ and $1\% z$.

On the other hand, we can use various simple quadratic polynomials as empirical formula in a so simple form that the solution of the system of simplified equations (1,2,3) can be easily carried out on

an analogue computer. In this case these polynoms can be used only in a more narrow range of temperature and conversion.

Approximative steady-state model typ II.

By the use of this model we can characterise each catalyst section as a multivariable controlled system, where the disturbing and measured variable is the ammonia mole fraction z_1 , the other disturbing variable, whose value cannot be measured directly, is the catalyst activity; the manipulated variables are pressure, temperature and flow rate. The controlled variable is the conversion ammonia mole fraction at the outlet of the section and the variable which should be optimised is the total net profit per time.

One cannot practically attain a sufficient number of plant data to obtain corresponding relationship of regression analysis. It seems to be convenient to adjust the exact or approximation model to boundary conditions and then to yield algebraic expressions by using a multiple regression technique from a set of computer results.

We will consider in this paper two catalytic sections with following data:

Table 1.

	Length [mm]	Cross-sect. area [m ²]	k ₄₅₀	H ₂ /N ₂	% inerts	Pressure [atm]
Catalyst bed 1	2000	0,5	1600	3	5	200
bed 2	1000	0,5	1600	3	5	200

By the use of regression analysis we obtain the results expressed in a form of equations (5-8) and shown in Fig. 2 - 5.

Catalyst bed B1:

$$z_1 = -4,754 \cdot 10^{-1} + 3,680 \cdot z_1 + 1,966 \cdot 10^{-3} \cdot T_1 + 2,611 \cdot 10^{-6} \cdot G + \\ + 21,62 \cdot z_1^2 + 3,976 \cdot 10^{-8} \cdot T_1^2 + 2,895 \cdot 10^{-12} \cdot G^2 - 1,859 \cdot 10^{-2} \cdot z_1 \cdot T_1 + \\ + 2,428 \cdot 10^{-5} \cdot z_1 \cdot G - 1,371 \cdot 10^{-8} \cdot T_1 \cdot G \quad (5)$$

Boundary conditions and working range:

$$0,015 \leq z_1 \leq 0,045, \quad 20000 \leq G \leq 70000, \quad 350 \leq T_1 \leq T_{1\max}$$

$$T_{1\max} = 2,702 \cdot 10^2 + 2,415 \cdot 10^3 \cdot z_1 + 1,577 \cdot 10^{-3} \cdot G - 1,219 \cdot 10^4 \cdot z_1^2 +$$

$$+ 1,608.10^{-9}.G^2 - 6,706.10^{-3}.z_1.G \quad (6)$$

The dependence of the output ammonia mole fraction z_1^1 of the first catalyst bed on the values of T_1, G for $z_1 = 0,035$ according to equation(5) is plotted in Fig.2. The boundary conditions and working range according to equation (6) is plotted in Fig. 3.

Catalyst section B2:

$$\begin{aligned} z_2^1 = & -2,752.10^{-1} + 1,510.z + 8,321.10^{-4}.T_2 + 1,724.10^{-6}.G + \\ & + 7,865.z_2^2 + 8,307.10^{-7}.T_2^2 + 1,230.10^{-11}.G^2 - \\ & - 6,998.10^{-3}.z_2.T_2 + 1,172.10^{-5}.z_2.G - 1,042.10^{-8}.T_2.G \end{aligned} \quad (7)$$

Boundary conditions and working range:

$$0,08 \leq z_2 \leq 0,13, \quad 20000 \leq G \leq 70000, \quad 450 \leq T_2 \leq T_{2max}$$

$$\begin{aligned} T_{2max} = & 2,549.10^2 + 1,021.10^3.z_2 + 6,270.10^{-3}.G - 3,441.10^3.z_2^2 - \\ & - 6,401.10^{-8}.G^2 + 5,037.10^{-3}.z_2.G \end{aligned} \quad (8)$$

The dependence of the output ammonia mole fraction z_2^1 of the second catalyst bed B2 on the values of T_2, G for $z_2 = 0,105$ according to equation(7) is plotted in Fig. 4 . The boundary conditions and working range according to equation(8) is plotted in Fig.5.

From previous results we can conclude that in the range of low ammonia mole fraction the reverse reaction of ammonia decomposition does not take place and there is not local maximum in multidimensional space $z^1 = z^1(z, T, G)$.

It is true that the reaction rate is governed also by the catalyst activity and the pressure. In this case the equations (5-8) should be more complicated. Generally speaking, the effect of a lower catalyst activity can be eliminated by the increase of the pressure. For example, if the catalyst activity is reduced to 50%, one can obtain approximatively the same output conversions at a pressure 250 atm, as at full activity of the catalyst and working pressure 200 atm.

Optimal steady-state control.

The background of the optimal control is to determine the values of T_1, T_2, G, P so that the plant could be held at its opti-

imum conditions, in our case, the profit per unit time is maximised. We will classify the optimal control of the ammonia synthesis reactor as a multistage decision process developed in this way in a form applicable to the design and to the optimal control of chemical reactors by Aris¹.

Simplifying assumptions can be made in assuming both catalyst activity and pressure constant. Further, the temperatures T_1, T_2 can be adjusted without limitations and the heat carried away from the heat exchanger is used either for steam production, or for adjusting the desired value of temperature T_2 - the inlet temperature to the section B2. The heat generated in the reactor is used for the preheating of fresh synthesis gas.

New functions (9)(10) are formed by making use of equations (5) and (7):

$$z_1' = z_1'(z_1, T_1, G) \quad (9)$$

$$z_2' = z_2'(z_2, T_2, G) \quad (10)$$

Let us define $W = G.S$ [kg/hour], where W is the total mass flow and V_1 is the cost of the produced ammonia, then the profit per unit time is defined by

$$r_1 = (z_1'(z_1, T_1, G) - z_1) \cdot W \cdot V_1 \quad (11)$$

The equation (12) shows the expenses per unit time for the circulation of the gas mixture together with the expenses per unit time for the separation of produced ammonia.

$$v_{\text{sep}} = v_{\text{sep}}(W, z_2') \quad (12)$$

The expenses per unit time for fresh synthesis gas depends on the working pressure and the amount of produced ammonia. (13)

$$v_m = v_m(W, \Delta z, P), \Delta z = z_j' - z_j, j = 1, 2 \quad (13)$$

The profit per unit time for produced steam is given by

$$v_v = v_v(T) = W \cdot C_p \cdot (T_1' - T_2) \cdot q \cdot V_2 \quad (14)$$

where q is the ratio coefficient between the heat evolved and the quantity of the steam and its quality, V_2 is the cost of the steam.

By making use of equations (9 - 14) we can define the objective function $R(z_1, z_2, T_1, T_2, W)$

$$R(z_1, z_2, T_1, T_2, W) = \text{Max} \left\{ \left[\left(z_1' (z_1, T_1, G) - z_1 \right) \cdot W \cdot V_1 + \right. \right. \\ \left. \left. + W \cdot C_p \cdot (T_1' - T_2) \cdot q \cdot V_2 - v_m(W, \Delta z, P) + \text{Max} \left\{ \left(z_2' (z_2, T_2, G) - \right. \right. \right. \right. \\ \left. \left. \left. - z_2 \right) \cdot W \cdot V_1 - v_m(W, \Delta z, P) \right\} \right] ; \left[-v_{sep} = v_{sep}(W, z_2') \right] \right\} \quad (15)$$

Equation (15) is the basic form of the objective function, which can be used to optimal steady-state control of ammonia synthesis reactor. The problem of the control from the point of view of the total catalyst life¹³ is not mentioned in this paper.

To illustrate some numerical results the tables 2,3 were compiled, where the profit per unit time for various operating conditions inlet temperatures, conversions, flow-rates of both catalyst sections is shown. The profit from the steam production is not included here because the quantity of produced steam depends upon the control strategy. For the purposes of the approximative estimation of the optimal control we should need other two tables, where output ammonia mole fractions and temperatures are shown. These tables are here not published. Nevertheless, the tables 2,3 are satisfying for the estimation of the dependence of the profit per unit time upon the operating conditions.

Table 2. Profit per unit time [Kčs/hour] for bed 1.

z	0,015			0,025			0,035			0,045		
G.10 ⁻⁴	3	5	7	3	5	7	3	5	7	3	5	7
T ₁												
350	1710	1800	1790	1205	1350	1160	920	975	935	780	975	915
370	-	2225	2245	1620	1700	1490	1215	1350	1260	935	1225	1060
390	-	-	2735	-	1910	1840	-	1630	1590	-	1305	1340
410	-	-	-	-	-	2410	-	2025	1990	-	1340	1635
430	-	-	-	-	-	-	-	-	1570	-	-	2030

In both tables 2,3 are used the same values of the cost and expenses: The cost of the ammonia is 2 Kčs per kg, the cost of fresh synthesis mixture is 1 Kčs per kg, the expenses per unit time for the circulating gas mixture ~~xxx~~ including the separation of ammonia are 30 Kčs per 10000 kg/hour of the circulating gas mixture.

Table 3. Profit per unit time [Kčs/hour] for bed 2.

z	0,08			0,105			0,13		
G.10 ⁻⁴	3	5	7	3	5	7	3	5	7
T ₂									
410	415	395	315	-	-	-	-	-	-
430	585	500	455	345	350	280	-	-	-
450	735	625	630	465	400	350	300	200	75
470	-	850	840	600	545	455	405	325	180
490	-	-	-	-	675	630	510	450	275
510	-	-	-	-	-	-	-	-	390

Dynamic model of an ammonia synthesis reactor.

To realise the above-mentioned control algorithm, it is necessary to provide the actual production equipment with either the classical feedback control loops stabilizing single parameters or the direct digital control. Then the computed optimal values T_1 , T_2 , G will determine the corresponding controller settings. The most difficult problem is the analysis of control system dynamics.

A theoretical design for operation of an ammonia reactor in unsteady regime is a difficult problem because the reactor system is nonlinear and even in the simplest case it is necessary to work with the system of quasilinear partial-differential equations

$$\begin{aligned} \frac{\partial c}{\partial t} + v \frac{\partial c}{\partial x} &= r(c, T) \\ \frac{\partial T}{\partial t} + v \frac{\partial T}{\partial x} &= g(c, T), \end{aligned} \quad (16)$$

where r, g are generally nonlinear functions. If it is not possible to neglect the influence of axial mass and heat dispersion, the right-hand sides of the equations (16) will be extended of the terms involving the second derivatives of dependent variables after x .

The solution of the system (16), completed by a set of initial and boundary conditions, can be realized on an analogue computer using the method of cyclical approximations described by Gilles⁸. The principle of this method is based on the well-known method of straight lines when one divides a space coordinate x from the interval $\langle 0, 1 \rangle$ in n subintervals, so that the system (16) will

be approximated by the equivalent set of equations (17)

$$\begin{aligned} -\frac{dc_i}{dt} &= \frac{vn}{l} (c_i - c_{i-1}) - r(c_i, T_i) \\ -\frac{dT_i}{dt} &= \frac{vn}{l} (T_i - T_{i-1}) - g(c_i, T_i). \end{aligned} \quad (17)$$

$i = 1, 2, 3, \dots, n.$

Then the method of cyclical approximations consists of dividing the computing network of the system (17) into n integrators for each dependent variable equivalent the left-hand side of the system (17) and a central block realizing generally nonlinear algebraic operations equivalent the right-hand side of the system (17). The block of algebraic operations is cyclically switched to the singular integrator sections. Thus each integrator calculates the corresponding integral after $1/n$ of the full computing time only, in the mean time it works in a memory state. The calculation accuracy depends on the choice of the value n which is limited by technical feasibility of switching mechanism and the capacity of the computer used. Let us define the general solution of the system (16) as $S(c, T)$ and the solution of the equivalent system (17) as $S_n(c, T)$, and then

$$S(c, T) = \lim_{n \rightarrow \infty} S_n(c, T). \quad (18)$$

It is possible to prove the validity of the relation (19) for some finite n

$$S_n(c, T) = S(c, T, D), \quad (19)$$

where the right-hand side of the equation (19) signifies symbolically the solution of the system (16) the equations of which contain the terms on the right-hand side involving the influence of axial dispersion of mass and heat. One may make use of this fact in modelling above-mentioned system by the method of cyclical approximations.

Since the section number n is not only a function of diffusivity D as follows from the relation (19) but it depends also on the choice of the time scale $\kappa_t = t/t_m$ (t_m is machine time unit) it is necessary to select for a given value D and

the constant n which is determined by the construction of the switching equipment, the time scale so that the relation (20) is fulfilled

$$k_t = f(n, D), \quad (20)$$

while the system is simulated as if it were described by a first-order system only. Owing to a limiting extend of this information it is not possible to describe in detail the derivation of the function f and its expression in the variables n and D , this matter will be discussed while reading the paper.

The analysis of the system (16) shows that an input change of a single variable e.g. $T(0, t)$ affects profiles of the second variable $c(x, t)$ along the whole interval $(0, l)$. There exists a possibility of smoothing the disturbances affecting the input $c(0, t)$ by some suitable function of the input variable $T(0, t)$ so that e.g. the output value $c(l, t)$ may be held at a given constant value. For this reason it is useful to introduce the expression "feedback model" for a variable having to fulfill the function of a control variable. In this case the feedback model is defined for the variable $T(x, t)$ by the equation

$$-\frac{dT_{i-1}}{dt} = \frac{vn}{l} (T_i - T_{i-1}) + g(c_{i-1}, T_{i-1}) \quad (21)$$

$$i = 1, 2, 3, \dots, n.$$

It is possible to characterize the resulting effect in such a defined channel so that the transfer of the information on a steady state is realized inversely with regard to the orientation of the space coordinate x .

The whole adjustable system is built up after the block scheme in Fig.6 where the analogue model with the feedback-defined channel of the adjustable variable T represents the controller function. A disturbance of the input variable $c(0, t)$ is transformed to a corresponding electric signal $\bar{c}(0, t_m)$ which acts as the input of the analogue model. This model calculates now the value of the correcting variable $T(0, t)$ in a short time. Assuming that the ratio k_t was chosen sufficiently large it is possible to consider the steady-states of the variables $\bar{c}(l_m, t_m)$ and

$\bar{T}(0, t_m)$ like the instant states of the corresponding original variables. The adjustable process itself will pass through according to this assumption at least one order quicker than with usual feedback control features. In Fig.7 is shown the time behaviour of both the variables $T(0, t)$ and $c(1, t)$ after a step change of the input variable $c(0, t)$ if the ratio of the time coordinates t/t_m is 10.

The next approach to this problem consists of using the experimental method when dynamic characteristics are determined from measured data. The classical methods of the dynamic identification - the methods of the step response and the frequency response are not convenient for identification of industrial equipments ⁷, the methods of dynamical statistics are more suitable. One of these methods makes use of the system response to pseudorandom binary signal /PRBS/ where from that response the impulse characteristic may be determined ^{5,9}, this method has been applied in two industrial cases ^{6,10}.

Brian et al. ⁴ have simulated the dynamic behaviour of one reactor catalyst bed. The model has assumed the heat removal from the bed, the nonlinear differential equations has been linearized before the solution. The calculated step responses have been approximated by means of the first-order transfer function with a time lag. It may be expected that even a multibed reactor will have the similar response, derived under above-mentioned approximation.

A five-bed Fauser-Montecatini industrial reactor was chosen for the determination of dynamic behaviour where the transfer between the circulation rate of gas mixture and the output ammonia mole fraction were traced. The below-mentioned result is a part of the work of one of the authors ¹¹. The identification was realized by PRBS with the period $N = 63$ and the bit interval $t = 1$ min. The signal amplitude was 1,75 % of the nominal value of the mass flow. The measuring consisted of the five-multiple application of PRBS on the reactor input, the resulting averaged impulse characteristic is shown in Fig.8. By integrating this characteristic, the step response in Fig.9 was obtained.

The dynamic properties of a single catalytic bed can be ap-

proximated after existing experimental measurements on industrial reactors by the transfer functions

$$F(p)_{ij} = \frac{k_{ij}}{\tau_p + 1} \exp(-\tau_d p) \quad (22)$$

$$i = 1, 2, 3$$

$$j = 1, 2,$$

where k_{ij} is the system gain for the singular input variables /Laplace transform/ $T_j(p)$, $z_j(p)$, $G(p)$ in the region of the corresponding steady states T_j^0 , z_j^0 , G^0 . The conversion at the end of one catalyst section will be the Laplace transform $z_j(p)$. It is necessary to obtain the time constants τ , τ_d from experimental results since they are the function of a reactor construction and working conditions.

The gains of the transfer functions may be estimated by the linearisation of the static model equations (5) and (7)

$$k_{1j} = \left. \frac{\partial z_j^1(z_j, T_j, G)}{\partial z_j} \right|_{T_j^0, z_j^0, G^0} \quad j = 1, 2 \quad (23)$$

$$k_{2j} = \left. \frac{\partial z_j^1(z_j, T_j, G)}{\partial z_j} \right|_{T_j^0, z_j^0, G^0} \quad j = 1, 2 \quad (24)$$

$$k_{3j} = \left. \frac{\partial z_j^1(z_j, T_j, G)}{\partial z_j} \right|_{T_j^0, z_j^0, G^0} \quad j = 1, 2. \quad (25)$$

Conclusion.

There have been worked out two models of the catalyst beds of ammonia synthesis reactor. These models can be used as a basis of optimal control algorithm by means of the method of dynamic programming. In the other part of this paper there have been derived theoretical and experimental models /dynamic/ which may be applied to the analysis of feedback control loops.

Symbols.

a	... hydrogen mole fraction in completely synthesis gas mixture
A	... activation energy for ammonia decomposition [kcal/gmole]
b _{1,2}	... constants
c	... concentration
D	... diffusion coefficient [m^2/h]
e _p	... specific heat of gas [kcal/kg °C]
f = f(z)	... fractional conversion
g	... general function of reaction rate
G	... mass velocity [$\text{kg}/\text{m}^2\text{h}$]
h(t)	... response to unit impulse
k _t	... time scale ratio
k ₄₅₀	... reaction rate constant at 450°C [$\text{atm}^\beta \text{h}^{-1}$]
K _{act}	... activity coefficient
l	... length of catalyst bed [m]
L ²	... function of ammonia equilibrium mole fraction
n	... number of subintervals
P	... gas pressure
q	... ratio coefficient
r	... general function of reaction rate, gain per unit time [Kčs/h]
R	... gas constant, objective function
S	... cross section of the catalyst bed [m^2]
t	... time [h]
T	... temperature
u(t)	... unit function response
v	... gas flow velocity [m/h]
V	... cost of the material [Kčs/kg]
v _{sep}	... cost per unit time for the separation [Kčs/h]
v _m	... cost per unit time for the fresh synth. mixture [Kčs/h]
W	... mass flow [kg/h]
x	... axial reactor coordinate [m]
z	... ammonia mole fraction
α, β	... constants
λ	... cooling constant [m^{-1}]

- ρ_0 ... gas density [kg/m^3]
 τ ... adiabatic temperature increase [$^{\circ}\text{C}$], time-constant [h].

Bibliography.

- 1 Aris R.: The optimal design of chemical reactors. A study in dynamic programming. New York, Academic press 1961.
- 2 Bozeman H.C.: The Oil and Gas J., 1960, Nov. 14, No. 46.
- 3 Burianec Z., Burianová J., Macháček L.: A research study TUCHT, Prague, 1967.
- 4 Brian P.L.T., Baddour R.F., Eymery J.P.: Chem. Eng. Sci. 1965, 20, 297.
- 5 Briggs P.A.N., Godfrey K.R., Hammond P.H.: IFAC Symp. on ident. autom. contr. syst. Paper 3.10, Prague 1967.
- 6 Corran E.R., Cummings J.D., Hopkinson A.: AEEW Report 373, Winfrith 1964.
- 7 Eykhoff P., van der Grinten P.M.L., Kwakernaak H., Veltman B.P.: Survey, 3-rd Congress IFAC, London 1966.
- 8 Gilles E.D.: Das dynamische Verhalten und die Regelung chemischer Rohrreaktoren. Ph.D. Thesis, Technische Hochschule, Darmstadt 1963.
- 9 Hazlerigg A.D.G.: System identification by cross-correlation using a class of binary signals. Ph.D. Thesis, University of Nottingham, 1965.
- 10 Hazlerigg A.D.G., Noton A.R.M.: Proc. IEE, 1965, 112, 2385.
- 11 Hruška M.: Problémy použití pseudonáhodných binárních signálů k identifikaci dynamických vlastností. Ph.D. Thesis, Techn. University of Chem. Technology, Prague, 1968.
- 12 Kjaer J.: Measurement and calculation of temperature and conversion in fixed-bed catalytic reactors. Jul. Gjellerups Forlag, Copenhagen, 1958.
- 13 Roberts M.S.: Dynamic programming in chem. engineering and process control. Academic press 1964, London.
- 14 Shah M.J.: Ind. Eng. Chem. 1967, 59, 72.

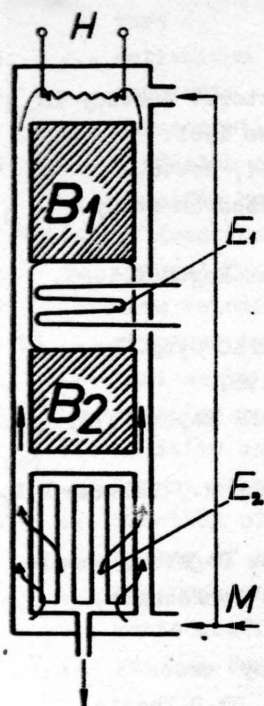


Fig. 1.

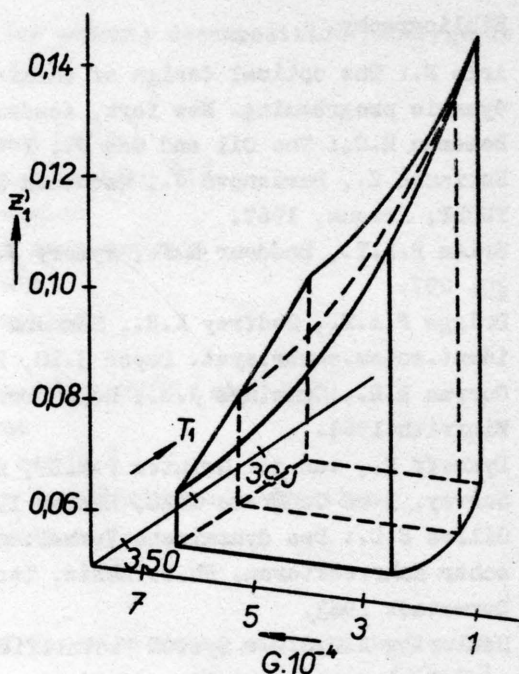


Fig. 2

- Fig.1.** Schematic view of the ammonia synthesis reactor. Catalyst beds B_1 , B_2 ; heat exchangers E_1 , E_2 ; direction of mass flow M ; electrical heating H .
- Fig.2.** The dependence of the output ammonia mole fraction z_1' of the first catalyst bed on the values of T_1 , G for the input ammonia mole fraction $z_1 = 0,035$.

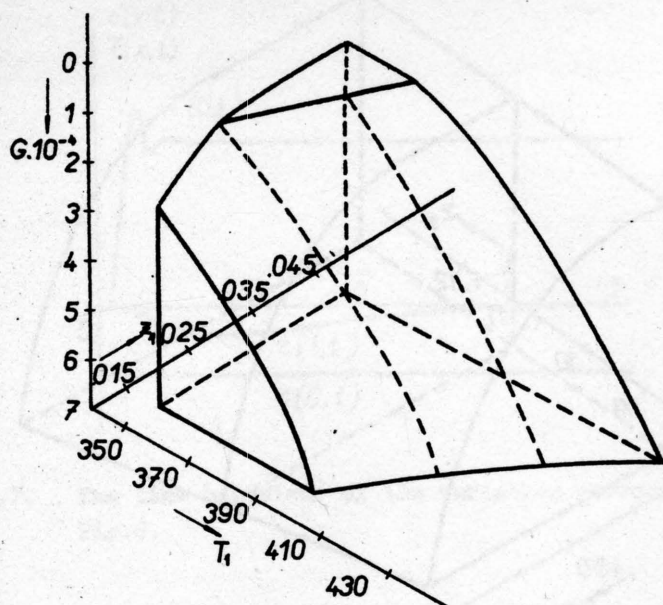


Fig.3. the working range and boundary conditions of the first catalyst bed.

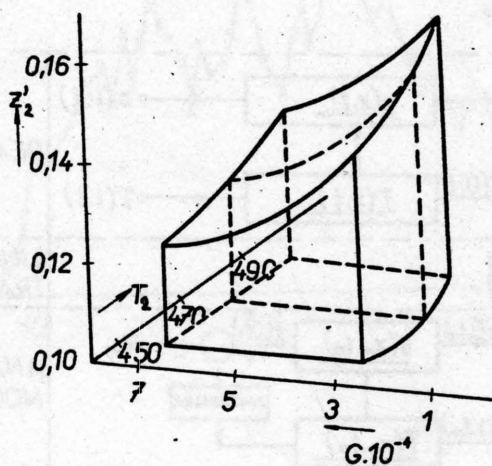


Fig.4. The dependence of the output ammonia mole fraction z_2' of the second catalyst bed on the values of T_2 , G for the input ammonia mole fraction $z_2 = 0.105$.

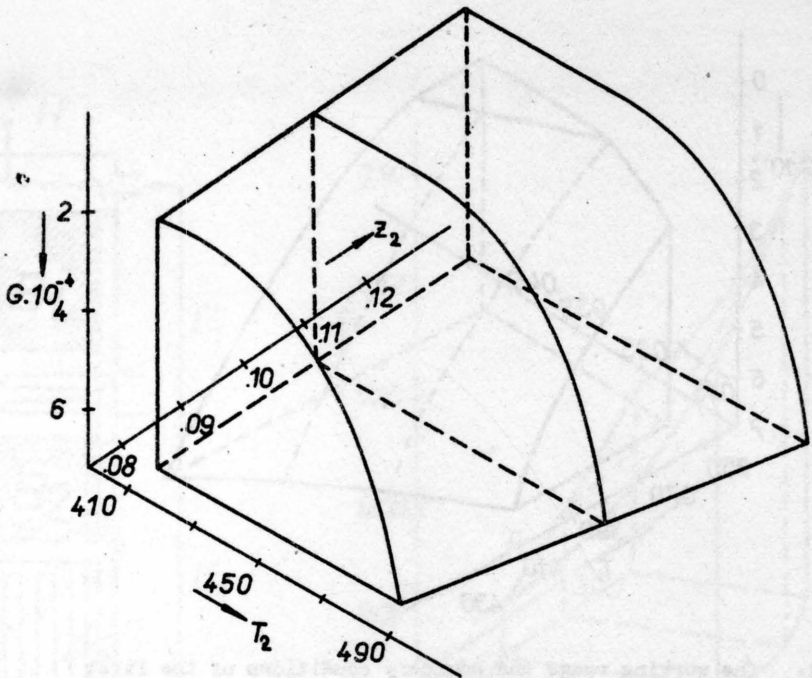


Fig.5. The working range and boundary conditions of the second catalyst bed.

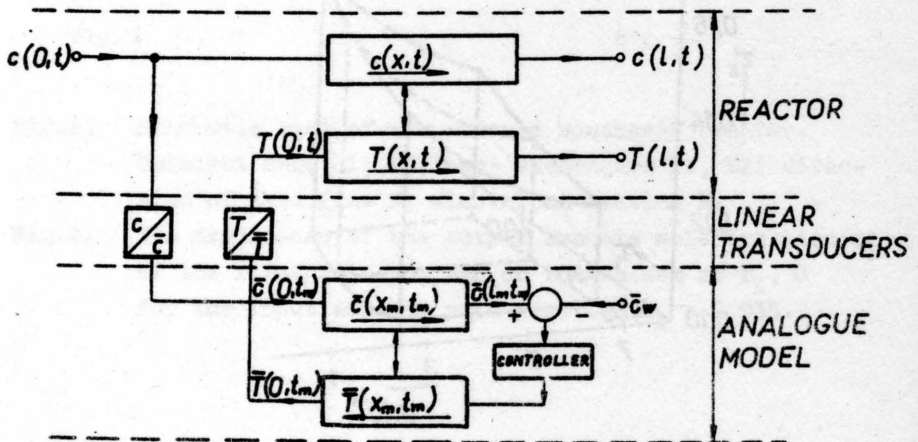


Fig.6. Schematic diagram of the reactor control system.

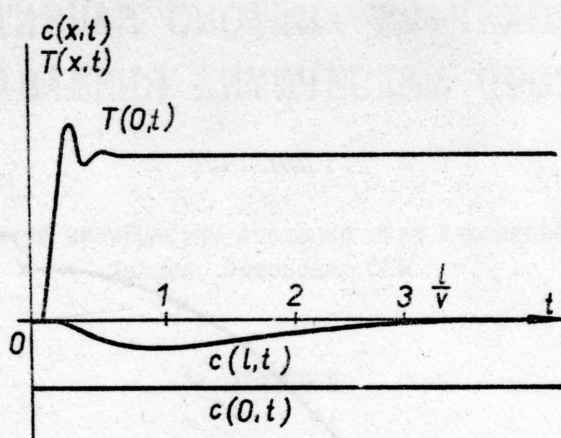


Fig.7. The time behaviour of the variables corresponding to Fig.6.

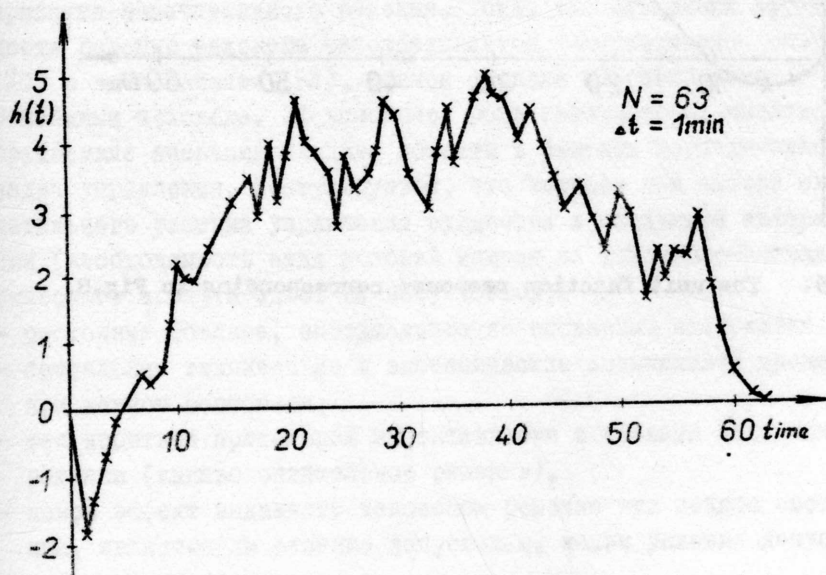


Fig.8. The averaged impulse characteristic for the Fauser-Montecatini reactor.

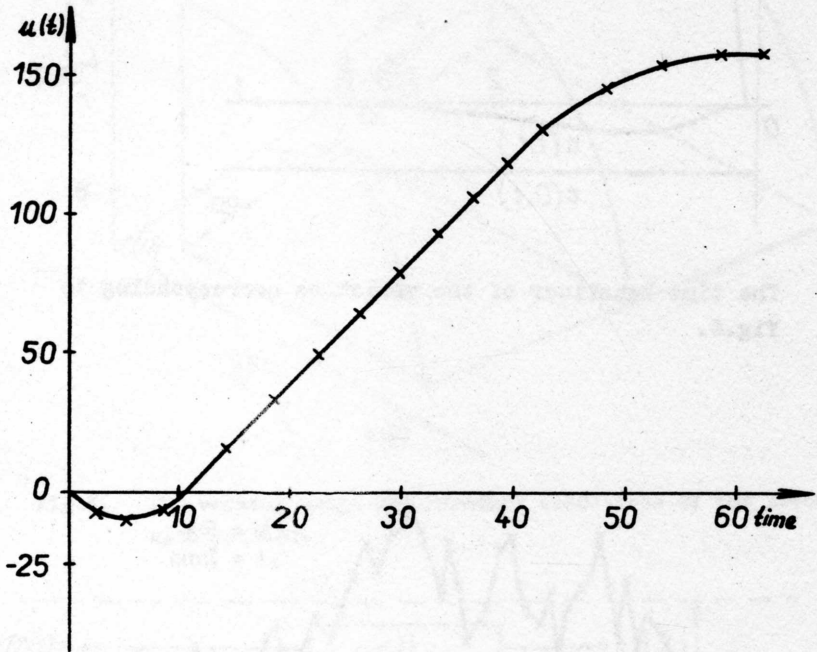


Fig.9. The unit function response corresponding to Fig.8.

АДАПТИВНАЯ СИСТЕМА ВМ-ЧЕЛОВЕК ДЛЯ УПРАВЛЕНИЯ ХИМИЧЕСКИМ ПРОЦЕССОМ

Р.Р.ТАВАСТ

Институт кибернетики Академии наук Эстонской ССР
Таллин, Эстонская ССР

I. Введение

Системы оптимизации, замкнутые через человека, рассматриваются обычно лишь как этап на пути к созданию полностью автоматической системы. В то же время в случаях: высокой ответственности решений (взрывоопасность, высокая цена перерабатываемых материалов), или существенного влияния неформализуемых факторов, человек должен оставаться в системе управления как звено принятия окончательного решения. Тогда для повышения эффективности решений человека разрабатывается информационная система (ИС) с вычислителем (ВМ), причем функции ИС согласуются с требованиями человека. ВМ выполняет роль информатора, выполняя трудоемкие операции анализа объекта и решения формализованных задач управления. Постулируется, что человек при выборе окончательного решения управления нуждается в следующей информации (необходимость этих условий исходя из инженерно-психологического аспекта здесь не обсуждается):

- состояние объекта, определяемое по косвенным измерениям,
- предельные технические и экономические возможности процесса при данном состоянии,
- как добиться предельной эффективности используя допустимые решения (каково оптимальное решение),
- каков эффект заданного человеком решения при данном состоянии, является ли решение допустимым, какие условия допустимости нарушаются.

Таким образом, ИС должна идентифицировать объект в условиях помех, решать задачи оптимизации с различными критериями и условиями и имитировать работу объекта. Поэтому при разработке

алгоритмов ИС должны рассматриваться стохастические задачи управления с сепаративной оценкой параметров модели с последующей оптимизацией.

В работе дается постановка задачи управления для типичного процесса химической технологии и способ ее решения. Приводится конкретный пример применения методики для управления непрерывным каталитическим процессом производства формалина из метанола.

2. Описание проблемной ситуации, стоящей перед системой.

Объект управления функционирует непрерывно на интервале времени $[0, T]$. Объект имеет векторные управляемый $U = (u_1, \dots, u_n)'$ и неуправляемый $V = (v_1, \dots, v_s)'$ входы ($'$ - знак транспонирования), значения компонент которых известны точно. Компоненты векторного выхода $\bar{Y} = (y_1, \dots, y_m)'$ измеряются в дискретные моменты времени $n = 1, 2, \dots, N$ с погрешностями ε_{y_j} . Измеряемыми величинами являются

$$z_{y_j} = \bar{y}_j + \varepsilon_{y_j}, \quad j = 1, \dots, m. \quad (I)$$

Управляющей системе известно в любой момент времени n :

- 1) $U(n), V(n), z_{y_j}(n), j = 1, \dots, m$,
- 2) гипотетическая модель объекта с неизвестным вектором параметров

$$y_j = f_j(U, V, \hat{\theta}_n, n), \quad j = 1, \dots, m, \quad (2)$$

- 3) некоторые сведения о внешней среде (спрос на продукт, цены, опыт других аналогичных производств, плановые задания и т.д.) которые изменяются. Обозначим эти сведения через S . От S зависит выбор критерия оптимизации и (частично) выбор допустимой области управлений,
- 4) конечный набор критериев управления w_1, \dots, w_ℓ ,
- 5) часть компонент векторов технических ограничений, входящих в определение допустимой области управлений.

Задача системы ВМ-человек заключается в выборе управления (решения) в соответствии с изменяющимися характеристиками объекта и изменением внешней ситуации S . При фиксированном

С решением управляющей системы заключается в выборе точки U^* из множества Γ_U , евклидова пространства E^n при условии минимума выбранной цели I .

Допустимое множество Γ_U определяется в виде вероятностных условий

$$\Gamma_U = \{U: \mathcal{P}[G(\bar{Y}, U, V, \underline{G}, \bar{G}) \leq 0] \geq \gamma_G\} \quad (3)$$

$\mathcal{P}[A]$ - вероятность события A , γ_G - положительная константа, $0,5 \leq \gamma_G \leq 1$. $1 - \gamma_G$ представляет субъективную допустимую вероятность нарушения требования $G \leq 0$. $G(\bar{Y}, U, V, \underline{G}, \bar{G}) \leq 0$ означает сокращенную запись системы неравенств

$$\begin{aligned} \underline{g}_i &\leq g_i(\bar{Y}, U) \leq \bar{g}_i \\ \underline{g}_p &\leq g_p(\bar{Y}, U) \leq \bar{g}_p \end{aligned} \quad (4)$$

где часть компонентов $\underline{G} = (\underline{g}_1, \dots, \underline{g}_p)'$, $\bar{G} = (\bar{g}_1, \dots, \bar{g}_p)'$ задано, часть определяется человеком на основе S , учитывая γ_G . Каждая функция цели есть математическое ожидание критерия на единичном шаге

$$J_i = E w_i(\bar{Y}, U), \quad i = 1, \dots, \ell \quad (5)$$

В каждой ситуации S человек имеет некоторую свободу выбора критерия w_i и ограничений Γ_U (в пределах технических и экономических допусков). Эту свободу он использует для максимизации некоторой интуитивной функции полезности. Формулировка w_i и Γ_U с учетом S - первая задача человека в системе управления. ИС содержит адаптивную модель объекта, которая используется человеком для безопасных и быстрых опытов с целью выбора окончательного решения U_K : 1) Определение

$U_j^*, j = 1, \dots, \alpha \leq \ell: J_j(U^*) = \min_{U \in \Gamma_U}$ для различных w_j , Γ_U при заданном состоянии объекта (модели). В качестве окончательного выбора человек может выбрать $U_K = U_j^*$ соответствующее цели J_j или компромиссное между несколькими целями решение.

2) Решение U_k может быть испытано на ИС до реализации на объекте.

Таким образом управляющая система ИС-человек адаптируется к изменениям внешних условий через человека и к изменениям объекта - через ИС (рис. 1). В процессе принятия окончательного решения человек многократно использует ИС.

3. Структура модели объекта в ИС

Рассматривается объект с распределенными параметрами, состояние которого в статическом режиме характеризуется распределением некоторых физических величин (температур, концентраций веществ, давлений и т.д.) $Q = (q_1, \dots, q_t)'$ по пространственной координате η . Информация о состоянии $Q(\eta)$ может быть получена в результате наблюдения последовательности случайных величин $z_{y_j}(n)$, которые генерируются следующим образом

$$z_{y_j}(n) = \bar{y}_j(n) + \varepsilon_{y_j}(n) = h_j(Q(\eta_1, \dots, \eta_s)) + \varepsilon_{y_j}(n), \quad j=1, \dots, m, \quad (6)$$

где η_1, \dots, η_s - фиксированные пространственные точки в пределах объекта, h_j - известные функции от состояния Q , $\varepsilon_y(n) = (\varepsilon_{y_1}(n), \dots, \varepsilon_{y_m}(n))'$ - последовательность независимых случайных векторов с одинаковыми многомерными нормальными распределениями $N(0, \Sigma)$ для любого n .

Объект не имеет памяти в том смысле, что переходные процессы в объекте затухают за время, несоизмеримо меньшее времени Δt .

Имеется ряд гипотез о закономерностях механизма процессов в объекте, которые формализуются в виде оператора

$$D(Q(\eta), U, V, \bar{\theta}) = 0 \quad (7)$$

Оператор D может содержать производные по пространственной координате $\partial q_i / \partial \eta$, $i = 1, \dots, t$ и вектор неизвестных параметров $\bar{\theta} = (\bar{\theta}_1, \dots, \bar{\theta}_p)$, но не содержит производных по времени (уравнения стационарного режима теплопередачи

диффузии, химической кинетики и т.д.) Выражение (7) совместно с граничными условиями,

$$B(Q, \eta_g), U, V) = 0, \quad (8)$$

где η_g - координаты пространственной границы объекта, определяющей решение

$$q_k = \varphi_k(\eta, U, V, \bar{\theta}), \quad k = 1, \dots, t \quad (9)$$

при фиксированных $U, V, \bar{\theta}$. Подставляя (9) в известные функции h_j получаем гипотетический статический оператор объекта в виде модели

$$y_j = f_j(U, V, \bar{\theta}), \quad j = 1, \dots, m. \quad (10)$$

Функции (10) лишь в редких случаях могут быть получены в явной форме, во всех практических случаях требуется численное решение (7), (8).

Параметры $\bar{\theta}$ в (9) имеют определенный физический смысл, например, коэффициентов теплопроводности, диффузии, гидравлического сопротивления, скоростей химических реакций и т.д. Некоторые из них могут по их смыслу медленно (часто монотонно) изменяться во времени. Если по созданию моделей (7), (8) для процессов химической технологии имеется обширная литература (отсылаем, например, к [3]), то конструировать модели медленного дрейфа параметров объектов на основе изучения механизма явления удается редко. Здесь применяем формальные модели, наиболее удобные с точки зрения их применения в ИС. Предполагается, что изменение параметров безынерционно

$$\bar{\theta} = C(n, \theta), \quad (II)$$

где θ - p - вектор неизвестных параметров. Простые частные случаи (II)

$$\bar{\theta}(n) = \theta \quad (12)$$

$$\bar{\theta}(n) = H \begin{pmatrix} 1 \\ n \end{pmatrix}, \quad H - (p \times 2) \text{ матрица неизвестных параметров} \quad (13)$$

Могут быть известны ρ -векторы \bar{a}_1, \bar{a}_2 в неравенствах $\bar{a}_1 \leq \theta \leq \bar{a}_2$. Учитывая (II) и (10), имеем модель объекта

$$y_j = f_j(U, V, \theta, n), \quad j = 1, \dots, m. \quad (I4)$$

4. Оценка параметров модели с многомерным выходом

Рассогласование между j -тым выходом объекта и соответствующим выходом модели для фиксированных U, V, θ, n равняется

$$\varepsilon_j(n) = z_{y_j}(n) - f_j(U, V, \theta, n), \quad j = 1, \dots, m, \quad n = 1, \dots, N \quad (I5)$$

В начальный период оценки имеется N_1 опытов (N_1 совокупностей векторов U, V, z_j, n). Введем следующие обозначения

$$\begin{aligned} X &= (U', V', n)', \\ Z &= (z_{y_1}(1), \dots, z_{y_m}(N_1))', \\ \varepsilon_j &= (\varepsilon_j(1), \dots, \varepsilon_j(N_1))', \\ F_j &= (f_j(X(1), \theta), \dots, f_j(X(N_1), \theta))', \\ Z &= (Z_1', \dots, Z_m')', \\ \varepsilon &= (\varepsilon_1', \dots, \varepsilon_m')', \\ F &= (F_1', \dots, F_m')', \end{aligned} \quad (I6)$$

тогда получим более компактно

$$\varepsilon = Z - F(\theta) \quad (I7)$$

и приходим к проблеме нелинейной симультианной (векторный выход \bar{Y}) оценки вектора параметров θ . Один и тот же вектор X входит во все функции $f_j, j = 1, \dots, m$; одна компонента вектора θ может входить во все функции f_j .

Будем искать марковскую оценку $\hat{\theta}$ вектора параметров θ , минимизирующую квадратичную форму

$$\Phi_{N_1}(\theta, \Omega) = [Z - F(\theta)]^T \hat{\Omega}^{-1} [Z - F(\theta)], \quad (18)$$

где $\hat{\Omega}$ - оценка неизвестной ковариационной матрицы Ω рас-
согласований ε .

Рассмотрим возможности получения оценки $\hat{\Omega}$ на N_1 опы-
тах. Согласно предположениям, сделанным ранее, Ω имеет
следующую структуру. $\varepsilon_j(n)$ независимо и одинаково распре-
деленные случайные векторы с нулевым математическим ожиданием
и ковариационной матрицей $E(\varepsilon_j \varepsilon_j^T) = \sigma_{jj} I$, $E(\varepsilon_j \varepsilon_k^T) = \sigma_{jk} I$,
 σ_{jk} , $j, k = 1, \dots, m$ - элементы матрицы Σ

где I - $N_1 \times N_1$ единичные матрицы, т.е. предполагается,
что рассогласования различных выходов в один и тот же мо-
мент коррелированы. Ковариационная матрица случайного векто-
ра ε согласно определениям (16) будет

$$\Omega = \Sigma \otimes I \quad (19)$$

\otimes - обозначает операцию прямого произведения матриц.

Обозначим оценку вектора параметров полученную из условия
минимума функции $\Phi_{N_1}(\theta, \hat{\Omega}^i)$ через $\hat{\theta}_{N_1}(\hat{\Omega}^i)$. Тогда
можно рассмотреть следующий итерационный процесс.

1. начальная оценка $\hat{\Omega}^0$ равна $\hat{\Omega}^0 = \hat{\Sigma} \otimes I$,
2. минимизация $\Phi_{N_1}(\theta, \hat{\Omega}^0)$, получение $\hat{\theta}_{N_1}(\hat{\Omega}^0)$,
3. вычисление оценки элементов $\hat{\Omega}^1$

$$\hat{\sigma}_{jk} = \frac{\hat{\varepsilon}_j^T \hat{\varepsilon}_k}{N_1}, \quad \hat{\varepsilon}_j = (\hat{\varepsilon}_j(1), \dots, \hat{\varepsilon}_j(N_1))^T, \quad (20)$$

$$\hat{\varepsilon}_j(n) = z_{y_j}(n) - f_j(\theta_{N_1}(\hat{\Omega}^1), x(n)),$$

4. повторение 1.

Эта процедура требует на каждом шаге итерации обращения
 $N_1 m \times N_1 m$ матрицы. Следующий метод этого не требует.
Учитывая сложное переплетение случайных независимых факторов
в образовании ошибки сделаем предположение о нормальности рас-
пределения каждого $\varepsilon_j(n)$. Тогда оценка наименьших квад-
ратов $\hat{\theta}^{(j)}$ сделанная для j -того уравнения (13)

будет состоятельной. В / I / показывается, что если элементы $\hat{\Omega}$ вычисляются как в (20), где $\hat{\varepsilon}_j(n) = z_{y_j}(n) - f(\hat{\theta}^{(j)}, x(n))$ то полученная таким образом $\hat{\Omega}$ сходится по вероятности к Ω . Тогда $\hat{\Omega}$ нужно обращать лишь один раз при подстановке в (18) для вычисления симультанной оценки $\hat{\theta}_{N_1}$, которая также будет состоятельной.

Для минимизации $\Phi_{N_1}(\theta, \Omega)$ целесообразно применение алгоритма нелокального поиска минимума. Таким алгоритмом является RU [7], который кратко будет описан ниже в п. 5.

Обычно N_1 невелико и при поступлении текущих данных $x(n), z_{y_j}(n), j=1, \dots, m, n=N_1+1, N_1+2, \dots$ должны вычисляться текущие оценки $\hat{\theta}_n, \hat{\theta}_{n+1}, \dots$

Естественно применять для этой цели схемы стохастической аппроксимации [4], [5], [6].

Рассмотрим рекуррентную схему определения оценки $\hat{\theta}_n(\hat{\Omega})$, близкой к θ в смысле (18) при увеличении $n, n+1, \dots$ для случая векторного выхода объекта \bar{Y} . Функция потерь на единичном шаге будет

$$\zeta = \varepsilon' \hat{\Sigma} \varepsilon \quad (21)$$

где ε соответствует определению (16) при $N_1=1$. Градиент ζ равняется

$$\nabla \zeta = \left(\frac{\partial \zeta}{\partial \theta} \right)' = -2 \left(\frac{\partial F}{\partial \theta} \right)' \hat{\Sigma} \varepsilon, \quad (22)$$

где $\frac{\partial F}{\partial \theta} - m \times p$ - матрица. Введем $p \times m$ - матрицу

$$K(n) = \frac{1}{\sum_{k=1}^n \left\| \left(\frac{\partial F}{\partial \theta} \right)_{\hat{\theta}_k} \right\|^2} \left(\frac{\partial F}{\partial \theta} \right)'_{\hat{\theta}_n} \hat{\Sigma} \varepsilon. \quad (23)$$

Тогда последовательная схема оценки

$$\hat{\theta}_{n+1} = [\hat{\theta}_n + K(n) \varepsilon(n)] \bar{a}_1^{-1}, \quad (24)$$

где обозначено

$$[\hat{\theta}]_{\bar{a}_1}^{\bar{a}_2} = \begin{cases} \bar{a}_2, & \text{если } \hat{\theta} \geq \bar{a}_2 \\ \hat{\theta}, & \text{если } \bar{a}_1 < \hat{\theta} < \bar{a}_2 \\ \bar{a}_1, & \text{если } \hat{\theta} \leq \bar{a}_1 \end{cases} \quad (25)$$

$\|P\|^2 = \lambda_{\max}$ - норма прямоугольной матрицы P ,
 λ_{\max} - максимальное собственное значение матрицы $P'P$,
 \bar{a}_1, \bar{a}_2 - заданные P - векторы, удовлетворяет условиям теоремы 6.4 / 5 / и $\hat{G}(\hat{\theta} - \theta) \rightarrow 0$ при $n \rightarrow \infty$. Могут применяться как детерминированная матрица $K(n, \hat{\theta}_n)$ так и "адаптивная" матрица $K(n, \hat{\theta}_n)$.

5. Решение статической задачи оптимизации

Вместо стохастической задачи (3), (5) ИС находит некоторое ее приближенное решение. При построении точного детерминированного эквивалента задачи нелинейного программирования с совокупностью вероятностных ограничений возникают пока нерешенные проблемы. Здесь предполагается, что человек способен задать \underline{G}, \bar{G} так, что получаемая система неравенств $(\Gamma_U)_d$ удовлетворится с вероятностью, близкой к γ_0 . Соответствующая детерминированная задача программирования формулируется в виде условий для определения U^*

$$J = w(U^*, \gamma(U^*, \bar{V}, \hat{\theta}_n, n)) = \min_{U \in (\Gamma_U)_d}, \quad (26)$$

$$(\Gamma_U)_d = \{U : \underline{G} \leq G(U^*, \bar{V}, \hat{\theta}_n, n) \leq \bar{G}\}. \quad (27)$$

Сведем (26), (27) к нахождению безусловного минимума следующей функции

$$\bar{J} = J + \chi \Pi(G, \underline{G}, \bar{G}), \quad (28)$$

где

$$\Pi = \sum_{i=1}^p \underline{q}_i - \bar{q}_i + |q_i - \underline{q}_i| + |q_i - \bar{q}_i|, \quad (29)$$

χ - достаточно большое число.

Для минимизации (28) применяется алгоритм Ru [7] использующий лишь значения минимизирующей функции в дискретных точках сетки независимых переменных (функция (28) - не дифференцируема). Поиск ведется в постепенно сужающейся области с постепенно уменьшающимся шагом.

Блок-схема ИС в целом и ее связи с человеком приведена на рис. 2. Для начальной оценки на всех этапах, где требуется минимизация функции (при начальной оценке параметров, при минимизации (28)) применяется Ru . Последовательная оценка согласно (24) исходя из начальной оценки $\hat{\theta}_{N_1}$ при постоянном \sum ведется для измеренных значений $\chi(n)$. Получаемые оценки $\hat{\theta}_n$ и измеренные $V(n)$ используются в модели для определения оптимального режима U^* согласно заданным $\omega, (\Gamma_v)_d$ и для вычисления выходов модели Y_k для задаваемых человеком входов U_k .

6. Система управления процессом производства формалина

Процесс производства формалина как объект управления. Управляемый объект состоит из ряда аппаратов (рис. 3), в которых в непрерывном потоке протекает процесс фазового и химического превращения жидких и газообразных веществ. Метиловый спирт разбавляется водой и подогревается (аппарат I), смесь испаряется и смешивается с кислородом воздуха (2), пар перегревается (3) и поступает в контактный аппарат (5). Получаемый "контактный газ" идет в систему поглощения, где $q_{(2)}, q_{(3)}$ поглощается в воде - получается готовый продукт формалин, а газ состоящий из $q_{(4)}, q_{(5)}, q_{(6)}, q_{(8)}$ выбрасывается.^{х)} Процессы

х) Вещества обозначаются через $q_{(i)}$: $q_{(1)} - O_2$, $q_{(2)} - CH_2O$, $q_{(3)} - CH_3OH$, $q_{(4)} - CO_2$, $q_{(5)} - CO$, $q_{(6)} - H_2$, $q_{(7)} - H_2O$, $q_{(8)} - N_2$.

в аппаратах управляемы заданиями регуляторов расхода воздуха (u_1), соотношения вода-метанол (u_2), температуры контакта (u_3) и температуры перегрева (u_4). Процесс поглощения считается неуправляемым. Выходы систем регулирования z_{u_i} , $i = 1, 2, 3, 4$, а также температура и давление поступающего воздуха z_{v_1}, z_{v_2} непрерывно измеряются и фильтруются, погрешностью фильтрации пренебрегаем: $z_{u_i} = u_i$, $z_{v_1} = v_1$, $z_{v_2} = v_2$. В дискретные моменты времени $n = 1, 2, \dots, N$ измеряются состав контактного газа и готового продукта, интегральные расходы формалина и метанола.

Необходимость управления. Технолог цеха формалина выбирает и устанавливает режим в сложных изменяющихся условиях. Первое решение о режиме технолог при выведении агрегата на режим после пуска: это решение зависит от способа приготовления катализатора, количества массы катализатора, планового задания, требований на качество продукта, наличия сырья, наличия спроса, времени года, состояния системы поглощения, т.е. от условий ведения процесса. Агрегат будучи выведенный на режим может при этом работать до изменения условий вызываемых: 1) Изменением активности катализатора в результате старения, 2) Изменением требований к продукту, 3) Изменением целей управления по экономическим соображениям, 4) Изменением гидравлического сопротивления газового тракта агрегата, 5) Изменением свойств катализатора при кратковременных остановках агрегата.

Цели управления. Допустимым называем режим (решение)

$U = (u_1, \dots, u_n)$, при котором не возникает взрывоопасной смеси, выполняются требования на качество и количество и себестоимость продукта. В зависимости от экономической ситуации из множества допустимых режимов выбирается в каждом состоянии объекта оптимальный режим по одному из следующих целей: 1) максимальная средняя производительность, 2) минимальная средняя себестоимость продукта, 3) максимальный средний доход, 4) минимальный средний процент метанола в формалине.

Оператор ставится в каждом случае изменения условий в проблемную ситуацию. В случаях 1, 5 оператор может вообще не заметить изменения ситуации, не говоря об оптимальном решении.

Интуиция и опыт позволяют оператору процесс в среднем вести удовлетворительно, но далеко не оптимально. Если при изменении условий предыдущий режим оказался допустимым, технолог старается не принимать нового, хотя и может быть более эффективного решения, поэтому на практике часто применяются малоэффективные режимы. Это связано с одной стороны неточным знанием допустимой области решений, с другой - незнанием наилучших с различных точек зрения допустимых решений в изменяющихся ситуациях. Информационная система призвана повысить эффективность решений, принимаемых человеком путем дополнения человеческой "концептуальной" модели объекта количественными оценками о состоянии процесса и эффекте различных режимов.

Модель процесса. Центральную часть в описании занимает модель процессов в контактном аппарате. Процесс контактного превращения метанола в присутствии кислорода и паров воды в формальдегид идет по гетерогенному окислительно-дегидрогенизационному механизму в неподвижном изотермичном слое частиц пемзосеребряного катализатора. Основные реакции сопровождаются параллельными и последовательными побочными реакциями, часть которых идет гомогенно. В уравнениях кинетики учитывается факт, что в промышленном процессе скорости гетерогенных реакций лимитируются скоростью массопередачи от потока реагентов к поверхности частиц катализатора, поэтому скорости реакций зависят от гидродинамических условий в слое. Учитывается существенный распад продукта в подконтактном холодильнике в неравномерном поле температуры. Остальные части агрегата описываются уравнениями материального баланса.

Благодаря автотермичности контактного процесса температура в слое определяется параметрами исходной смеси и скоростями реакции. Последние в свою очередь зависят от температуры. Поэтому выход модели Y для фиксированных $U, V, \hat{\theta}_n, \rho$ и определяется итерациями. Структура модели правильно отражает важные качественные свойства объекта (наличие устойчивых точек, направление градиентов выходов по входам и параметрам). Идентификацией достигается минимизация среднего рассогласования объекта и модели.

Идентификация. При каждом новом катализаторе происходит смещение оценок параметров. Поэтому делается начальная оценка $\hat{\theta}_{N_1}$ и $\hat{\Omega}$ на N_1 первых опытах. Согласно п. 4. Оцениваются коэффициенты $\theta_1, \dots, \theta_5$ в предэкспонентах скоростей реакций. Поступающие в дальнейшем группы $X(n), Z_v(n), n = N_1+1, N_1+2, \dots$ обрабатываются рекурсивно согласно (24) для получения $\hat{\theta}_n, \hat{\theta}_{n+1}, \dots$, которые рассматриваются фиксированными при остальной работе ИС.

Решение статических (одношаговых) задач определения оптимальных решений. Допустимая область $(\Gamma_U)_d$ определена следующими условиями при

- 1) $\underline{q}_U \leq U \leq \bar{q}_U$ $\underline{q}_U, \bar{q}_U$ - 4х мерные векторы технических ограничений,
- 2) $\underline{q}_2 \leq q_2(U, Y(U, V, \hat{\theta}_n, n))$ - условие взрывобезопасности,
- 3) $q_3(U, Y(U, V, \hat{\theta}_n, n)) \leq \bar{q}_3$ - условие нормальной работы поглощения,
- 4) $\underline{q}_4 \leq q_4(U, Y(U, V, \hat{\theta}_n, n)) \leq \bar{q}_4$ - условие требований на качество формалина,
- 5) $\underline{q}_5 \leq q_5(U, Y(U, V, \hat{\theta}_n, n))$ - условие заданной средней производительности,
- 6) $\underline{q}_6 \leq q_6(U, Y(U, V, \hat{\theta}_n, n)) \leq \bar{q}_6$ - условие заданной себестоимости.

Здесь q_2 - концентрация $a_{(3)}$ в парах перед контактным аппаратом, q_3 - объемная скорость веществ через слой катализатора, q_4 - содержание метанола в продукте, q_5 - производительность агрегата, q_6 - себестоимость продукта.

Если решаются задачи 1, 2, 3, 4 (см. цели управления), то: задача 1 - $q_5(U, Y(U, V, \hat{\theta}_n, n)) = \min$ условие 5) снимается

задача 2 $q_6(U, Y(U, V, \hat{\theta}_n, n)) = \min$ -" 6) -"

задача 3 $-q_7 = q_5(\lambda_1 q_6 + \lambda_2) = \min$ при условиях 1) - 6)

задача 4 $q_4(u, v(u, v, \hat{\theta}_n, n)) = \min$ условие 4) снимается

q_7 - чистый доход производства,

λ_1, λ_2 - стоимости в выражении дохода.

Техническая реализация системы управления. Изменение условий ведения процесса происходит двояко: катализатор теряет активность непрерывно за два месяца, а изменение внешних условий 5 возникает скачкообразно. Средний период между изменениями режима по различным причинам на одном производстве до внедрения системы равнялся 67 часам. Поэтому вычисления в реальном масштабе времени могут в данном случае вестись "off-line". Темп поступления $X(n), Z_1(n)$ низок - 16 чисел в 2 часа для одного агрегата. Данные за сутки перфорируются на телетайпе цеха и пересылаются в вычислительный центр с указанием номера агрегата. $X(n), Z_1(n)$ есть базовая информация B_1 , передаваемая регулярно. В зависимости от кода режима вычислений (передается каждый раз при B_1) могут проводиться следующие вычисления:

1. Вычисление среднесуточных экономических и технических показателей. Результат (как и других видов вычислений) выводится на выходной перфторатор ВМ в коде M2 и передается на телетайп цеха (рис.4) под названием "сводка режимов агрегата № ...".

2. Начальная идентификация - определение $\hat{\theta}_n$ и $\hat{\Omega}$ на N_1 делается снова для каждой новой загрузки катализатора.

3. Идентификация параметров модели объекта делается автоматически каждый раз при поступлении B_1 . Результат выводится под названием "состояние процесса" (рис.4) (В тексте не был описан способ определения характеристик системы поглощения).

4. Вычисление выходов модели y_k для заданных u_k (вероятных выходов объекта) при данном состоянии. Возможностью узнать вероятный результат решений до его реализации на объ-

екте человек пользуется охотно. Группа задаваемых режимов перфорируется в виде массива B_2 после B_1 . Результат выводится под названием "испытание заданных режимов" (рис. 5).

5. Вычисления оптимального режима. Для этого задаются в виде B_3 номера задач, верхние и нижние допустимые значения ограничений \underline{G} , \bar{G} для каждой задачи. Результат выводится под названием "оптимальные режимы" с указанием критерия. Выводится также ожидаемая эффективность оптимальных режимов - "ожидаемые показатели" (рис. 6). B_3 является результатом формализации 5 и передается при изменении внешней ситуации ведения процесса.

Реализованный в универсальной ВМ алгоритм служит для управления несколькими независимых агрегатов производства формалина.

Л и т е р а т у р а

1. Beauchamp J.J., Cornell R.G. Simultaneous nonlinear estimation. Technometrics, V. 8, № 2, May, 1966.
2. Андерсон Т. Введение в многомерный статистический анализ. М. 1963.
3. Арис Р. Анализ процессов в химических реакторах. Л. 1967.
4. Цыпкин Я.Э. Адаптация, обучение и самообучение в автоматических системах. Автоматика и телемеханика, т. XXVII, № I, 1966.
5. Albert A.E., Gardner L.A., Stochastic approximation and nonlinear regression. MIT Press, Cambridge, Mass., 1967.
6. Zhivoglyadov V.P., Kaipov V.Kh. Identification of distributed parameter plants in the presence of noises. Prepr. of the IFAC symp. Identification in automatic control systems, Prague, 1967.
7. Руубель Х.В. Поиск точки минимума функции, в сб. программы для ЦВМ "Минск-2", вып. 7 (в печати).

Таваст рауль Романович, мл. научн. сотр. Института кибернетики Академии Наук Эстонской ССР. Служ адрес Эстонская ССР, Таллин бульвар Ленина 10, телеф. 605-783.

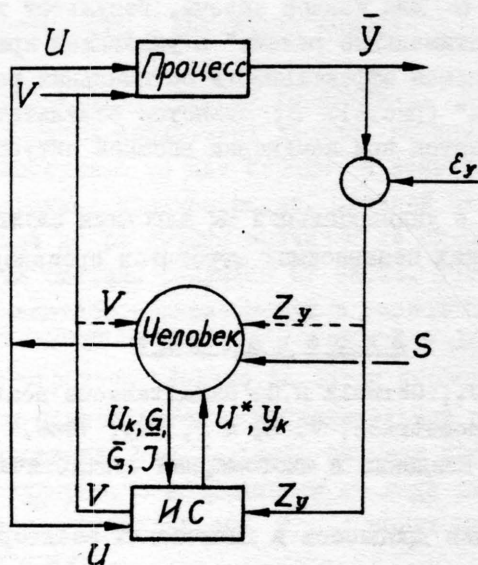


Рис. 1

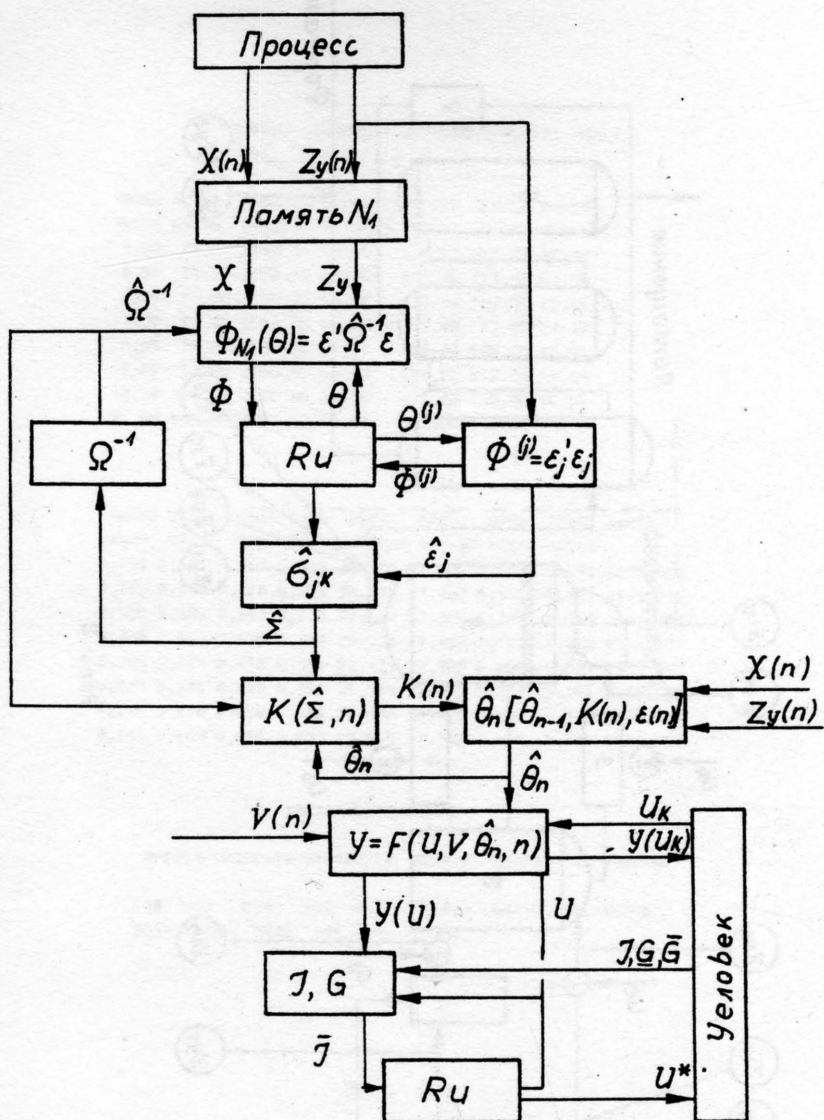


Рис. 2

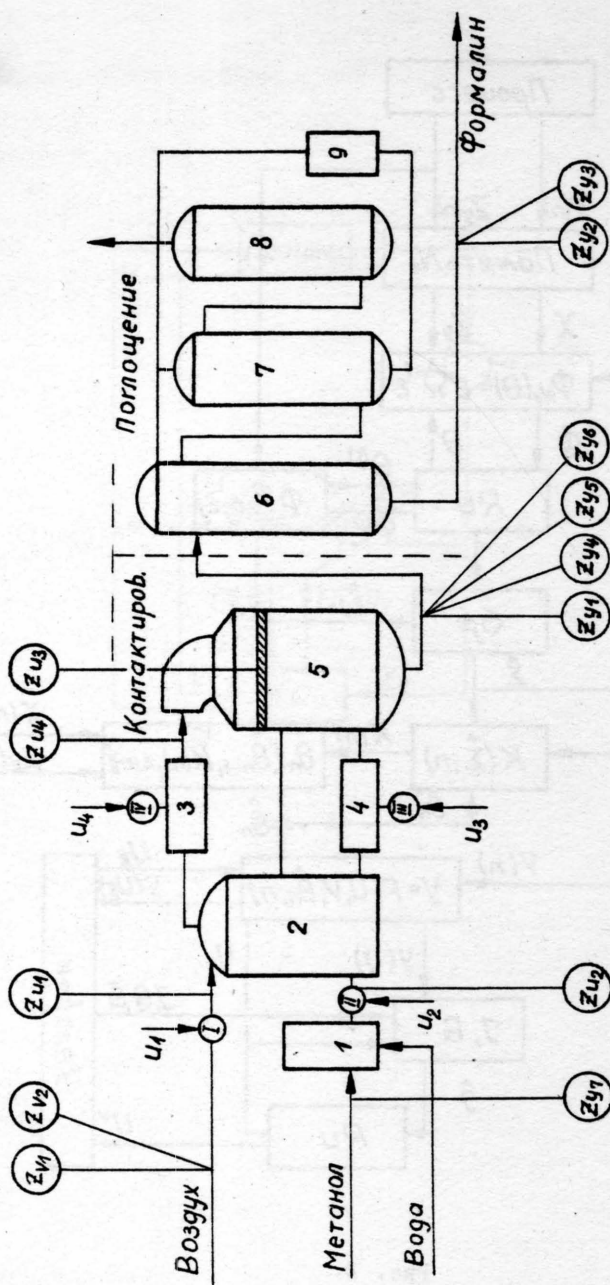


Рис. 3

СВОДНА РЕЖИМОВ И ВЫХОДОВ АГРЕГАТА НОМЕР

2

ЧИСЛО МЕСЯЦ	НОМЕР СМЕНЫ	РАСХОД ВОЗДУХА	КОНЦ МЕТАНОЛ	ТЕМПЕР КОНТАК	ТЕМПЕР ПЕРЕГР	РАСХОД МЕТАНОЛ
4,09	82,00	2050,00	63,40	695,00	112,00	17,42
5,09	85,00	2050,00	63,70	695,00	113,00	17,38
6,09	88,00	2050,00	63,30	695,00	112,00	17,66
7,09	91,00	2050,00	63,60	694,00	113,00	17,32
8,09	94,00	2050,00	63,50	695,00	111,00	16,59
9,09	97,00	2050,00	63,50	694,00	110,00	17,04
10,09	100,00	2050,00	63,50	695,00	110,00	16,08
11,09	103,00	2050,00	63,90	694,00	110,00	14,92

ВЫХОД ФОРМ	СЕЛЕК ТИВН	ОБЩАЯ КОНВ	РАСХ КОЭФ	ВЫРАБ ФОР-НА	ПРОЦ ФОР-ДА	ПРОЦ МЕТАН	ЭКОН МЕТАН	ДОХОД
0,756	0,883	0,856	0,523	30,387	37,400	6,600	-0,091	2513,010
0,755	0,879	0,860	0,523	30,293	37,400	6,400	-0,105	2503,836
0,755	0,885	0,853	0,525	30,674	37,500	6,700	-0,159	2529,996
0,748	0,883	0,846	0,529	29,864	37,400	7,100	-0,269	2451,801
0,744	0,874	0,852	0,531	28,477	37,400	6,800	-0,323	2331,244
0,747	0,873	0,855	0,529	29,384	37,400	7,300	-0,266	2412,255
0,745	0,870	0,856	0,526	27,888	37,100	7,200	-0,173	2297,420
0,740	0,864	0,856	0,533	25,554	37,300	7,100	-0,326	2088,409

СОСТОЯНИЕ ПРОЦЕССА

ПРЕДЪЭКСПОНЕНТЫ СКОРОСТЕЙ ПОТЕРИ СТЕПЕНИ ПОГЛОЩЕНИЯ

К00	К10	К20	К30	К40	ТЕПЛА	ФОРМ-ДА МЕТАНОЛА
3037	4309	2476	185	593	55000	

1,000 0,917

Рис. 4

ИСПЫТАНИЕ ЗАДАНЫХ РЕЖИМОВ

1, 2050,0	63,0	695,0	113,0					
2, 2050,0	63,5	695,0	114,0					
3, 2100,0	64,0	695,0	110,0					
	1	2	3	0	0	0	0	0
ВЫРАБОТКА								
	31,0	31,0	32,7	0,0	0,0	0,0	0,0	0,0
РАСХ КОЗ								
	0,512	0,517	0,609	0,000	0,000	0,000	0,000	0,000
ДОХОД								
	2597	2582	2422	0	0	0	0	0
СОДЕРЖ МЕТАН								
	6,4	6,8	16,6	0,0	0,0	0,0	0,0	0,0
СОДЕРЖ ФОРМ								
	49,2	49,1	40,6	0,0	0,0	0,0	0,0	0,0
ЭКОНОМИЯ								
	0,24	0,09	-2,90	0,00	0,00	0,00	0,00	0,00
ВЫХОД ФОРМ								
	0,767	0,760	0,645	0,000	0,000	0,000	0,000	0,000
СЕЛЕКТИВН								
	0,887	0,887	0,314	0,000	0,000	0,000	0,000	0,000
ГАЗО O2								
	0,20	0,20	0,24	0,00	0,00	0,00	0,00	0,00
ВЫИ CO2								
	3,92	3,92	4,02	0,00	0,00	0,00	0,00	0,00
АНА CO								
	1,60	1,60	0,30	0,00	0,00	0,00	0,00	0,00
ЛИЗ H2								
	18,0	18,0	17,1	0,0	0,0	0,0	0,0	0,0
КОНИ O2								
	0,096	0,096	0,087	0,000	0,000	0,000	0,000	0,000
КОНИ СН3ОН								
	0,266	0,269	0,294	0,000	0,000	0,000	0,000	0,000

Рис. 5

РЕКОМЕНДУЕМЫЕ РЕЖИМЫ

1 МАКС ВЫРАБОТКА	2050,0	61,0	692,0	129,0
2 МИН РАСХ КОЗ	2050,0	63,5	712,0	125,0
3 МАКС ДОХОД	2050,0	61,5	696,0	120,0
4 МИН СОДЕРЖ МЕТ	2050,0	64,0	718,0	115,0

РЕЗУЛЬТАТ ОПТИМАЛЬНЫХ РЕЖИМОВ

	1	2	3	4	0	0	0	0
ВЫРАБОТКА	31,1	30,4	31,0	30,1	0,0	0,0	0,0	0,0
РАСХ КОЗ	0,519	0,506	0,508	0,491	0,000	0,000	0,000	0,000
ДОХОД	2587	2568	2612	2587	0	0	0	0
СОДЕРЖ МЕТАН	7,2	5,0	6,0	3,2	0,0	0,0	0,0	0,0
СОДЕРЖ ФОРМ	46,6	51,2	48,4	53,9	0,0	0,0	0,0	0,0
ЭКОНОМИЯ	0,02	0,43	0,39	0,88	0,00	0,00	0,00	0,00
РЫХОД ФОРМ	0,757	0,777	0,774	0,801	0,000	0,000	0,000	0,000
СЕЛЕКТИВН	0,891	0,870	0,887	0,861	0,000	0,000	0,000	0,000
ГАЗО О2	0,21	0,19	0,20	0,19	0,00	0,00	0,00	0,00
УСЛ СО2	3,93	3,86	3,92	3,82	0,00	0,00	0,00	0,00
АНА СО	1,41	2,37	1,60	2,80	0,00	0,00	0,00	0,00
ЛИЗ Н2	17,8	18,5	18,0	18,8	0,0	0,0	0,0	0,0
КОИО О2	0,093	0,098	0,095	0,101	0,000	0,000	0,000	0,000
КОИО СН3ОН	0,262	0,264	0,260	0,260	0,000	0,000	0,000	0,000

Рис. 6

